NASA/CR—2005-213328

Large Engine Technology Program: Task 22—Variable Geometry Concepts for Rich-Quench-Lean Combustors

J.M. Cohen and F.C. Padget
United Technologies Research Center, East Hartford, Connecticut

D. Kwoka, Q. Wang, and R.P. Lohmann
Pratt & Whitney, West Palm Beach, Florida

February 2005

The NASA STI Program Office . . . in Profile

Since its founding, NASA has been dedicated to the advancement of aeronautics and space science. The NASA Scientific and Technical Information (STI) Program Office plays a key part in helping NASA maintain this important role.

The NASA STI Program Office is operated by Langley Research Center, the Lead Center for NASA's scientific and technical information. The NASA STI Program Office provides access to the NASA STI Database, the largest collection of aeronautical and space science STI in the world. The Program Office is also NASA's institutional mechanism for disseminating the results of its research and development activities. These results are published by NASA in the NASA STI Report Series, which includes the following report types:

- TECHNICAL PUBLICATION. Reports of completed research or a major significant phase of research that present the results of NASA programs and include extensive data or theoretical analysis. Includes compilations of significant scientific and technical data and information deemed to be of continuing reference value. NASA's counterpart of peer-reviewed formal professional papers but has less stringent limitations on manuscript length and extent of graphic presentations.

- TECHNICAL MEMORANDUM. Scientific and technical findings that are preliminary or of specialized interest, e.g., quick release reports, working papers, and bibliographies that contain minimal annotation. Does not contain extensive analysis.

- CONTRACTOR REPORT. Scientific and technical findings by NASA-sponsored contractors and grantees.

- CONFERENCE PUBLICATION. Collected papers from scientific and technical conferences, symposia, seminars, or other meetings sponsored or cosponsored by NASA.

- SPECIAL PUBLICATION. Scientific, technical, or historical information from NASA programs, projects, and missions, often concerned with subjects having substantial public interest.

- TECHNICAL TRANSLATION. English-language translations of foreign scientific and technical material pertinent to NASA's mission.

Specialized services that complement the STI Program Office's diverse offerings include creating custom thesauri, building customized databases, organizing and publishing research results . . . even providing videos.

For more information about the NASA STI Program Office, see the following:

- Access the NASA STI Program Home Page at ***http://www.sti.nasa.gov***

- E-mail your question via the Internet to help@sti.nasa.gov

- Fax your question to the NASA Access Help Desk at 301–621–0134

- Telephone the NASA Access Help Desk at 301–621–0390

- Write to:
  NASA Access Help Desk
  NASA Center for AeroSpace Information
  7121 Standard Drive
  Hanover, MD 21076

NASA/CR—2005-213328

Large Engine Technology Program: Task 22—Variable Geometry Concepts for Rich-Quench-Lean Combustors

J.M. Cohen and F.C. Padget
United Technologies Research Center, East Hartford, Connecticut

D. Kwoka, Q. Wang, and R.P. Lohmann
Pratt & Whitney, West Palm Beach, Florida

Prepared under Contract NAS3–26618

National Aeronautics and
Space Administration

Glenn Research Center

February 2005

Acknowledgments

The NASA Project Manager for this task was Mr. Robert Tacina of NASA Glenn Research Center, Cleveland, Ohio. Dr. Robert P. Lohmann was the Pratt & Whitney Program Manager. Mr. David Kwoka and Mr. Qiang Wang were responsible for the design and analysis efforts at Pratt & Whitney while Dr. Jeffrey Cohen and Mr. Frederick Padget were principal investigators for the activity at United Technologies Research Center and directed the design, analysis and experimental evaluations of the injectors. S. Crocker conducted computational analyses at CFDRC.

Document History

This research was originally published internally as HSR062 in November 1997.

Note that at the time of writing, the NASA Lewis Research Center
was undergoing a name change to the
NASA John H. Glenn Research Center at Lewis Field.
Both names may appear in this report.

Available from

NASA Center for Aerospace Information
7121 Standard Drive
Hanover, MD 21076

National Technical Information Service
5285 Port Royal Road
Springfield, VA 22100

Available electronically at http://gltrs.grc.nasa.gov

FOREWORD

This report documents the activities conducted under Task 22 of the NASA Large Engine Technology program under Contract NAS3-26618 to define and evaluate variable geometry concepts suitable for use with a Rich-Quench-Lean combustor. The specific intent was to identify approaches that would satisfy High Speed Civil Transport cycle operational requirements with regard to fuel-air ratio turndown capability, ignition and stability margin without compromising the stringent emissions, performance and reliability goals that this combustor would have to achieve.

The NASA Project Manager for this task was Mr. Robert Tacina of NASA Lewis Research Center, Cleveland, Ohio. Dr. Robert P. Lohmann was the Pratt & Whitney Program Manager. Mr. David Kwoka and Mr. Qiang Wang were responsible for the design and analysis efforts at Pratt & Whitney while Dr. Jeffrey Cohen and Mr. Frederick Padget were principal investigators for the activity at United Technologies Research Center and directed the design, analysis and experimental evaluations of the injectors. S. Crocker conducted computational analyses at CFDRC.

TABLE OF CONTENTS

FOREWORD ii

SECTION I - SUMMARY 1

SECTION II - INTRODUCTION 3

SECTION III - VARIABLE GEOMETRY DESIGN CONSTRAINTS AND OBJECTIVES 6

Design Constraints 6
Design Objectives and Evaluation Strategy 8

SECTION IV - EXPERIMENTAL APPARATUS 10

Airflow Capacity and Laser Velocimetry Test Facility 10
Spray Patternation and Atomization Test Facility 11
Modular RQL Combustor Rig 13
RQL Combustor Test Facility and Instrumentation 14

SECTION V - VARIABLE GEOMETRY CONCEPT DEFINITION 16

Tri-Swirler Aerating Injector 17
Radial-Inflow High-Shear Injector 21
Aerated Injector with Translating Ramp 26
Axial Flow High Shear Injector 27

SECTION VI - COMBUSTOR EVALUATION 29

Combustor Test Results with Baseline Injectors 29
Combustor Test Results with Variable Geometry Injectors 31

SECTION VII - CONCLUSIONS 35

REFERENCES 36

SECTION II FIGURES 37

SECTION III FIGURES 39

SECTION IV FIGURES 40

SECTION V FIGURES 43

SECTION VI FIGURES 65

APPENDIX A - COMPUTATIONAL FLUID DYNAMICS CALCULATIONS ..... A

SECTION I - SUMMARY

The objective of the task reported herein, which was conducted under Task 22 of the NASA sponsored Large Engine Technology program (Contract NAS3-26618), was to define and evaluate variable geometry concepts suitable for use with a Rich-Quench-Lean combustor. The specific intent was to identify approaches that would satisfy High Speed Civil Transport cycle operational requirements with regard to fuel-air ratio turndown capability, ignition and stability margin without compromising the stringent emissions, performance and reliability goals that this combustor would have to achieve.

The effort was initiated with an analytical study to define the optimum variable geometry scheduling to operate the Rich-Quench-Lean combustor over the entire flight envelope while avoiding domains of local stoichiometry that would produce unacceptable emissions and/or compromise durability. The study identified a mode of operation in which the rich zone was operated at below stoichiometric mixture strengths at low, overall fuel/air ratio conditions such as idle and the low-power descent-approach flight regime. When the control requires a fuel/air ratio above a predefined threshold in the range of 0.015 to 0.020 the variable geometry system abruptly shifts the size of the combustor air admission orifices so that a mixture strength well above stoichiometric is produced in the rich zone. A regime of prohibited operation, in which heat loads on the combustor liners might exceed steady state limits, is crossed only as a transient event with minimal thermal impact on the liner. Further power-up beyond this transition point is achieved by increasing fuel flow and modulating the rich zone airflow along the rich branch of the characteristic rich zone equivalence ratio versus overall fuel/air ratio behavior and produces optimum Rich-Quench-Lean emissions at the high power end of the operating range. This mode of operation involves the use of a variable geometry, air admission system only on the inlet to the rich zone where it can be integrated with the fuel injectors. The quantity of airflow being shifted is not excessive so this approach has the distinct advantage of not requiring another variable geometry component elsewhere on the combustor to compensate for the airflow shift. This approach does produce excursions in total pressure drop across the combustor, but the variation in overall combustor inlet area is moderate, making the resultant pressure drop shifts tolerable.

The major technical effort on this task involved the definition and optimization of candidate variable geometry concepts. Four potential configurations were identified and three of these were refined and tested in a high-pressure modular Rich-Quench-Lean combustor rig. The tools used in the evolution of these concepts included models built with rapid fabrication techniques that were tested for airflow characteristics to confirm sizing and airflow management capability, spray patternation and atomization characterization tests of these models and studies that were supported by Computational Fluid Dynamics analyses.

A two-passage aerating fuel injector was defined and tested in the Modular RQL combustor rig as a baseline for comparison with the variable geometry injectors. Its technology base is well established in commercial engine application. Effort was also directed at the evaluation of an alternate multi-passage premixing fuel injector for the cylindrical Rich-Quench-Lean combustor rig. The intent of the evaluation was to establish a database on the influence of fuel-air mixture preparation on the performance and emissions characteristics of the RQL combustor concept in preparation for designing rich zone components later in this task. The multi-passage premixing design was intended to produce a spatially uniform fuel/air mixture in the rich zone, should this be critical to NO_x emissions.

The first approach to the definition of a variable geometry axial flow aerating injector was to extend the baseline aerating injector by increasing the airflow capacity of the outer swirler. Combining an existing, but smaller airflow two-passage injector with a variable geometry airflow component located co-axially with the core two-passage injector was the preferred implementation of this tri-swirler approach because of the advantage of divorcing the fuel atomization process from the modulated airflow feature.

A radial inflow injector concept that was a variation of a standardized fixed geometry design that has been under investigation at Pratt & Whitney and United Technologies Research Center was also investigated. The configuration consists of radial inflow swirlers with air introduced through inner and outer passages. A centrally mounted fuel injector delivered fuel through radial jets. These fuel jets penetrated through the inner airflow and impinged on the inner side of the wall between the two air passages where a film of fuel was developed. An axially translating band sliding over the inlet to the swirler stages could provide the required airflow modulation. The preferred embodiment allowed for two variable-geometry flow passages.

The third injector concept refined and tested in the high-pressure modular Rich-Quench-Lean combustor rig was the translating ramp injector concept. This concept parallels the three-passage approach of the tri-swirler injector in that the innermost two passages provide an aerating fuel atomization function and substantially provide the minimum airflow requirement of the injector while a third outboard air system provides the variable airflow demands. Fuel is introduced through a series of 12 radially directed orifices on a centrally mounted wall between the inner and intermediate air passages. A larger, outer airflow, sufficient to meet the maximum airflow requirement, is introduced through a radial-inflow air swirler. The airflow through this swirler is modulated by using a translating ramp, which slides axially along the central core of the injector blocking a variable part of the axial height of the swirler discharge.

Combustion tests were performed with each of these concepts at supersonic cruise conditions and at other critical conditions in the flight envelope, including the transition points of the variable geometry system, to identify performance, emissions and operability impacts. Based upon the cold flow characterization, emissions results, acoustic behavior observed during the tests and consideration of mechanical, reliability and implementation issues, the tri-swirler configuration was selected as the best variable geometry concept for incorporation in subsequent Rich-Quench-Lean combustor evolution efforts for the High Speed Civil Transport.

SECTION II - INTRODUCTION

Environmental impacts will dictate substantial constraints on the High Speed Civil Transport (HSCT) aircraft that will in turn establish its economic viability. Emissions output, and in particular the oxides of nitrogen generated during supersonic flight in the stratosphere, is especially significant because of their potential for participating in the destruction of ozone at these high altitudes. These concerns lead to the need to severely constrain the output of NO_x from the engines for this aircraft. Comprehensive studies of the dynamics of the upper atmosphere as it influences ozone concentrations are being conducted under the NASA sponsored Atmospheric Effects of Stratospheric Aircraft program (Ref. 1). The initial results from these studies have led to a goal of an emissions index of 5 gm of NO_x/kg fuel at the supersonic cruise flight condition. Since this level is five to eight times lower than that achievable with current engine combustor technology only the most aggressive and advanced low emissions technology can be considered for the power plants for this aircraft. Pratt & Whitney and General Electric are studying two combustor concepts in the NASA-sponsored High Speed Research program to define a burner that achieves this NO_x emissions goal at the supersonic cruise operating condition. Such a burner must also preserve high efficiency, broad operability, and low emissions at all other operating conditions as well as being durable and economically competitive.

The effort at Pratt & Whitney has focused on the Rich-Quench-Lean (RQL) combustor. A conceptual embodiment of this combustor is shown in Figure II-1. This combustor concept incorporates separated zones of combustion to preserve combustor stability while achieving emission control. The combustion process is initiated in a fuel-rich combustion zone and completed in a fuel-lean combustion zone, with a rapid transition between them. All of the fuel is introduced in the rich zone but with only a fraction of the air required for complete combustion. The rich combustion process provides the combustor stability and, being deficient in oxygen, completes a significant portion of the overall energy release without forming oxides of nitrogen. The combustion products proceed to a quench section where the remainder of the combustion air is introduced in a rapid, intense mixing process. The downstream lean zone is used to complete CO and soot burn-off. Low NO_x emissions will be achieved only if the quench or transition process between the zones is sufficiently vigorous to avoid significant flow residence time near stoichiometric mixture proportions. Sub-scale testing of a single injector or modular version of the RQL combustor at the HSCT engine supersonic cruise operating conditions has demonstrated the low emissions potential of this concept and generated a significant design data base. This effort has been conducted at United Technologies Research Center (UTRC) and was performed as Task 3, HSR Low NO_x Combustor, of NASA Lewis Research Center contract NAS3-25952, Aero-Propulsion Technology Research Program, with Pratt & Whitney of the United Technologies Corporation (Ref. 2).

For the High Speed Civil Transport engine application the aerothermal design point of the Rich-Quench-Lean combustor is the supersonic cruise condition. The results of the evaluations performed in Ref. 2 indicate that the equivalence ratio in the rich zone should be about 1.8. This equivalence ratio is sufficiently high to preclude NO_x emissions at the exit of the rich zone while minimizing the proclivity for smoke formation. To minimize NO_x production in the quench and lean zones, liner cooling airflow to the lean zone is minimized and the remainder of the combustor air enters through the quench air system. This air serves a dual function in that it provides convective cooling of the rich zone liner while being directed to the quench section by an enclosing hood. Based on an overall fuel/air ratio of 0.030 at supersonic cruise, these considerations lead to a combustor airflow distribution of about 24% in the rich

zone, 70% through the quench system and 6% for lean zone liner cooling. Figure II-2 shows the rich zone operating characteristics, on a stoichiometry diagram, for a fixed geometry combustor that incorporates this airflow distribution. It is evident that the characteristic of any combustor with a fixed rich zone airflow fraction is a line that must pass through the origin of the graph. For the particular engine cycle under consideration, both the high-power, supersonic cruise operating point and the low-power, ground-idle point are shown on the characteristic line. This range of "rich zone" equivalence ratios, from 0.6 to 1.8, is similar to many gas turbine combustors typically used for subsonic aircraft, implying that a fixed geometry combustor with 24% combustor airflow in the "rich" zone might satisfy the operational requirements of this engine.

However, while this airflow distribution is optimized from the point of view of supersonic cruise operation, as the engine is operated at fuel/air ratios less than supersonic cruise, the mixture strength in the rich zone would approach and eventually pass through stoichiometric proportions. Since the highest gas temperatures occur in the products of stoichiometric or near-stoichiometric combustion, steady state operation at points in this regime could have adverse effects on durability of the rich zone liner and on the emissions output at some intermediate power levels. This effect is demonstrated graphically on Figure II-2, where a regime of prohibited steady state operation, labeled "Durability", is indicated around stoichiometric proportions.

While not immediately relevant to the fixed geometry 24% rich zone airflow configuration, Figure II-2 also indicates another area of prohibited steady state operation. This second prohibited region occurs at low, overall engine fuel/air ratios and high rich zone equivalence ratios. This regime indicates the operation of the rich zone at above stoichiometric conditions that will generate large quantities of CO and smoke but for which there is inadequate temperature levels in the quench and lean zones to oxidize these products. Consequently, the so-called "rich" zone (at high power) can only be operated at lean, or below stoichiometric proportions at low power to avoid large quantities of CO and smoke in the exhaust. With the constraints of avoiding steady state operation in the prohibited zones of the rich zone stoichiometry diagram while still achieving the operational capability of a flight engine, variable geometry approaches to manipulate combustor airflow distribution may be considered an enabling technology.

Figure II-3 shows the rich zone stoichiometry diagram for the Rich-Quench-Lean combustor in the High Speed Civil Transport engine for a combustor which incorporates variable geometry technology. The intent is to operate the "rich zone" at lean (below stoichiometric) mixture strengths at lower fuel/air ratio conditions such as startup, idle and the low power, descent-approach flight conditions. Modulation of the variable geometry system at these low power conditions, up to the point of transition, maintains a lean "rich zone" stoichiometry, avoiding the prohibited rich zone equivalence ratios. When the control requires a fuel/air ratio above a predefined threshold, in the range of 0.015 to 0.020 (shown as 0.017 on Figure II-3), the variable geometry system abruptly shifts the size of the combustor air admission orifices. The change in orifice size is designed so that a mixture strength well above stoichiometric is produced in the rich zone. The regime of prohibited operation is crossed only as a transient event with minimal thermal impact on the liner. Further power-up beyond this transition point is achieved by increasing fuel flow and modulating the rich zone airflow so that the combustor is operated along the rich branch of the characteristic stoichiometry curve (conceptually shown in Figure II-3). This rich branch characteristic curve is designed to maintain optimum Rich-Quench-Lean emissions at the high power end of the operating range.

The objective of the task reported herein, which was conducted as Task 22 of the NASA-sponsored Large Engine Technology program (Contract NAS3-26618), was to define and evaluate variable geometry, airflow modulation concepts for use with a Rich-Quench-Lean combustor. The specific intent was to identify approaches that would satisfy High Speed Civil Transport cycle operational requirements with regard to fuel/air ratio turndown capability, ignition and stability margin without compromising the stringent emissions, performance and reliability goals that this combustor would have to achieve. Emphasis was also placed on robust designs that could be introduced with minimal additional development and refinement because of the rapid-paced High Speed Research program requirements. Specific objectives of the task were to:

- Analytically define and evaluate three different variable geometry, air modulation concepts consistent with the requirements of the High Speed Civil Transport application of the Rich-Quench-Lean combustor.

- Conduct cold flow calibrations and velocity field definitions on models of each concept to confirm sizing and airflow management capability of each.

- Evaluate the spray patternation and atomization characteristics of each concept to anticipate its performance and emissions characteristics.

- Perform combustion tests with each concept at supersonic cruise conditions and at other critical conditions in the flight envelope, including the transition points of the variable geometry system, to identify performance, emissions and operability impacts.

- Select the best variable geometry concept for incorporation in subsequent Rich-Quench-Lean combustor evolution efforts for the High Speed Civil Transport.

The activities performed in this program were consistent with the above objectives. The non-reacting evaluations of the candidate variable geometry concepts were conducted in dedicated facilities at the United Technologies Research Center. An existing high inlet air temperature Rich-Quench-Lean combustor rig used in the concept demonstration and design base data acquisition activities of Ref. 2 was the test vehicle for the performance, emissions and operability validation portions of the task. This facility was located in Cell 1E of the Jet Burner Test Stand at United Technologies Research Center. The facility is capable of testing at combustor pressures up to 200 psia, combustor inlet air temperatures of 1400°F, and contained airflow control features to alter the airflow rates delivered to the rich-zone combustor and to the quench mixer. The combustor rig contained a modular, 5-inch diameter RQL combustor that allowed evaluation of variable geometry components in a size scale consistent with the next major test vehicles in the High Speed Research program.

This report details the activities and results of the evaluation of the variable geometry rich-zone air modulation concepts. Section I provides a Program Summary, while Section II includes introductory and background information. Section III provides concept definition strategy and design constraints and Section IV provides a description of the test facilities, including the modular RQL combustor rig. Section V presents the details of the variable geometry concept definitions and their evolution through the influence of the supporting non-reacting evaluations of models of those components while the results of the combustion test program are discussed in Section VI. Conclusions presented in Section VII.

SECTION III - VARIABLE GEOMETRY DESIGN CONSTRAINTS AND OBJECTIVES

The technical effort on this task was initiated with a review of candidate variable geometry concepts that might be incorporated in the Rich-Quench-Lean combustor for application to the High Speed Civil Transport engine. This initial review disclosed four potential configurations, three of which were ultimately evolved and tested in the modular RQL combustor rig. This section describes the design constraints on these candidate systems and the processes by which the systems were evolved towards viable approaches.

Design Constraints

Initial studies of the requirements and constraints on a variable airflow system for the Rich-Quench-Lean combustor indicated that the simplest design approach involves the use of a variable geometry, air admission system on the inlet to the rich zone. As previously shown on Figure II-1, this approach allows direct control of the airflow entering the rich zone and can be integrated with the fuel injectors. If the quantity of airflow being shifted is not excessive, this approach has the distinct advantage of not requiring another variable geometry component elsewhere on the combustor to compensate for the airflow shift. This approach does produce excursions in total pressure drop across the combustor. But if the variation in overall combustor inlet area is moderate, as one would expect from manipulation of a region that accounts for less than 25% of the total combustor effective area, the resultant pressure drop shifts are tolerable.

Figure III-1 and Figure III-2 show the variation in rich zone equivalence ratio and the fraction of total combustor airflow, respectively, as a function of overall combustor fuel/air ratio for key operating conditions of the HSCT cycle. The figures represent the above-described type of variable geometry system, applied to the Rich-Quench-Lean combustor in the Turbine Bypass-type study engine for the High Speed Civil Transport. (Subsequent studies in other engine cycles, including low bypass ratio turbofans have indicated the fundamental operating characteristics of the variable geometry concept of this figure are retained and systems for these cycles would differ only in minor details.)

The operating environment at the fuel injector/air admission modules is further identified in Table III-1 for each of the engine power level conditions of Figure III-1 and Figure III-2. Parameters specified include the total pressure and total temperature of the air approaching the combustor dome and the air and fuel mass flows passing through the individual fuel injector/air admission modules. It is assumed that an annular combustor would be fed by a multiplicity (18 to 30 or more depending on airflow size of the test vehicle) of these fuel injector/air admission modules spaced circumferentially. Also indicated is the effective flow area (ACd) of the module and the pressure drop across the bulkhead of the rich zone at each condition. As indicated, the effective flow area of the fuel injector/air admission module must vary from about one half to twice the nominal area at supersonic cruise during the rich to lean transition process. These transition points represent the extremes of the variable geometry system, operating envelope.

Power Condition	Inlet Total Pressure psia	Inlet Total Temp F	Overall Fuel/Air Ratio	Rich Zone Equivalence Ratio	Per Module Fuel Flow lb/sec	Per Module Air Flow lb/sec	Per Module Effective Flow Area ACd in^2	Bulkhead Press Drop %
Ground Idle	67	424	0.0091	0.60	0.026	0.62	0.98	7.5
Subsonic Cruise	92	634	0.0139	0.60	0.046	1.12	1.77	4.7
Lean Transition	227	766	0.0160	0.60	0.123	3.00	2.20	3.9
Rich Transition	227	766	0.0160	1.55	0.123	1.16	0.61	8.1
Supersonic Cruise	207	1250	0.0288	1.80	0.164	1.34	1.05	6.0
Takeoff	264	818	0.0373	1.80	0.272	2.22	1.50	3.6
Subsonic Climb	104	666	0.0402	1.80	0.116	0.94	1.67	3.0

Table III-1 Design Parameters for Rich-Quench-Lean Combustor Fuel/Air Modules

In the sizing of the fuel injector/air admission modules it must be noted that the effective flow area is the representation of all pressure losses in the air side of the module. The effective flow area is represented as a single orifice supplied by air at the total pressure of the flow approaching the combustor dome. If the module has significant internal losses, the controlling aperture size (physical geometric area) may have to be substantially larger than the effective area. Likewise, there may be cross-flows close to the combustor hood and fuel injector/air admission modules due to the significant quench and turbine cooling air flows bypassing this region. Injector/air admission modules that do not recover the full ram effect of the approaching velocity operate at lower effective pressure drops and would, therefore, require larger airflow components (physical geometric size).

The bulkhead pressure drops cited in Table III-1 are those available for flowing the rich zone inlet system and reflect the absence of any compensation for the change in overall combustor orifice area. While these drops strongly influence combustor section total pressure loss, and hence cycle efficiency, the loss levels, particularly at the cruise conditions where fuel burn can be substantial, are moderate. High bulkhead pressure drops are conducive to stable combustion and tend to enhance the atomization characteristics, so the higher pressure drops at the low inlet temperature idle and the high fuel loaded rich transition point can be considered advantageous.

The fuel/air ratio at which the lean to rich transition point occurs was chosen based on Nitric Oxide (NO_x) formation and Carbon Monoxide (CO) oxidation criteria. The flame temperature at the transition point should be high enough so that CO can be burned off, but low enough so that thermal NO_x is not created in great quantities. Lean and rich transitions represent the same overall engine power level and fuel/air ratio, but operate the combustor in different modes. The lean transition point of Table III-1 requires an effective injector airflow area of 2.2 in^2 to achieve $\phi_{rich} = 0.6$, while rich transition requires an area of 0.6 in^2 to achieve $\phi_{rich} = 1.6$. Power levels between idle and lean transition require increasing

airflow, and therefore larger effective nozzle areas, to keep the "rich" zone operating in a lean mode. Power levels between rich transition and subsonic climb require increasing airflow (and therefore area) to keep the rich zone from becoming too rich as the fuel flow rate is increased.

Design Objectives and Evaluation Strategy

The objective of this study was to generate designs for and evaluate the performance of fuel injection devices intended to achieve the necessary variations in effective airflow area. Guidelines for the design process were established to enhance the probability of a successful result:

- The range of effective airflow areas that must be covered was 0.60 in^2 to 2.20 in^2.
- Any moving parts or actuators that were required to achieve the necessary geometry variations should not be directly exposed to the flame itself or to high radiative heat loads from the flame.
- The performance characteristics of the injector should not change substantially as a function of varying operating condition.
- The physical size of the injector and the associated actuation mechanisms should be minimized.
- While the mechanical design of the actuation mechanism proper was not a specific requirement of this task, consideration must be made of this aspect. This implied that the requisite mechanism be as simple as possible, requiring only a small but repeatable linear or rotary motion.

Three candidate variable geometry injectors were ultimately evaluated in the modular RQL cylindrical combustor test rig. The process through which these three designs were selected utilized non-reacting tests to characterize the air and fuel flow distributions, as well as the area variations achieved by different candidate concepts. The initial phase of the program was to generate designs for several concepts that met the above criteria. Prototypes for these concepts were then fabricated using rapid-turn-around fabrication techniques, such as stereolithography. This allowed for several design/fabricate/test iterations for each concept. Several techniques were employed to evaluate of the performance of injector models:

- Using a calibrated air flow system, determine the range of effective airflow areas achievable by the model.
- Using laser velocimetry, determine the effects of varying the airflow passage geometry of the model on the air velocity distribution near the exit of the injector.
- Using spray patternation, determine the effects of varying airflow passage geometry along with fuel and airflow rates on the fuel flux distribution produced by the injector model.
- Using optical droplet sizing techniques, determine the effect of changing effective airflow area, fuel flow rate and air flow rate on fuel atomization.

- Using computational fluid dynamics to predict the reacting-flow performance of candidate designs under both lean and rich conditions. Two-dimensional, axisymmetric calculations for both reacting and non-reacting cases were performed by CFD Research Corporation. Included in these analyses were the calculation of an unmixedness parameter and the calculation (under lean conditions) of total rich zone NO_x EI. The results of these calculations are detailed in Appendix A.

These results, along with the other design criteria, acted as a guide by which three final designs were selected and optimized. Three hot-test models and an actuation mechanism common to two of them were then fabricated.

SECTION IV - EXPERIMENTAL APPARATUS

This section describes the test facilities used to support the evolution of the variable geometry, air-fuel admission concepts and verify their performance/emissions characteristics in a combusting environment. These included the dedicated facilities for non-reacting characterization tests and the modular RQL combustor rig.

Airflow Capacity and Laser Velocimetry Test Facility

Airflow capacity and laser velocimetry measurements were performed in a facility especially designed for the cold-flow evaluation of fuel injector airflows. A schematic layout of the facility is shown in Figure IV-1. The injector was mounted on the end of a 10-in. diameter cylindrical plenum, from which air was supplied to the injector. The flow rate of air into the plenum was measured using a choked (either 0.453-in. or 0.150-in. diameter) venturi, equipped with static and total pressure measurements. The pressure in the plenum was also monitored, so that the pressure drop across the injector airflow passages could be measured (injector airflow is exhausted to atmospheric conditions). Using the measured air flow rate, and knowing the pressure drop, it was then possible to calculate the effective area (ACd) of the injector air flow passages:

$$AC_d = \frac{\dot{m}_{air}}{\sqrt{2\rho_{air}\Delta P_{inj}}}$$

where $\dot{m}_{air}$ is the mass flow of air, ρ_{air} is the density of air, and ΔP_{inj} is the pressure drop across the injector. The same flow facility was used for laser velocimetry. The injector was mounted on the downstream end of the plenum, so that the flow issuing from the injector was unconfined. Seed material was introduced into the upstream plenum using a spray nozzle. The seed material was polystyrene latex beads (1 μm) suspended in methanol. The methanol evaporated quickly, leaving only the small seed particles in the flow.

A schematic of the laser velocimetry system and its installation in the facility is shown in Figure IV-2. The two-component laser velocimeter used two TSI 1998 counter signal processors, feeding their signals into an Apple IIe computer. This computer controlled the data acquisition and reduction processes, including positioning. The system used the 488-nm and 514-nm lines of a Spectra Physics 5W Argon - Ion laser. Frequency shifting (50 MHz) was employed in order to detect reverse velocities. This was accomplished using TSI 9168 Bragg Cells. The frequency shift was set against the mean flow direction in all cases and was reversed for the tangential component upon crossing the geometric center of the flow. Scattered light was collected using on-axis forward-scattering collection optics. The velocimetry probe volume was positioned in the flow field using a Centurion IV numerically controlled milling machine base, to which the velocimetry system was mounted. The milling machine was driven automatically, using the Apple IIe computer.

All velocimetry tests were conducted at a fixed air pressure drop of 7-in. H_2O across the injector. The flow was unconfined in all cases. Geometric (ACd) changes were made to the injectors in order to provide the proper effective flow area for different operating conditions. The tangential and axial air velocity components were measured along diametrical traverses of the flow field at a given axial plane. The acquisition routine was set to acquire a fixed number (512) of valid samples from each channel in non-coincident mode. The reduction software then calculated the mean and fluctuating velocity components and stored these along with the probability distributions for each set of samples. The computer then signaled the milling machine to move to the next radial position and begin collecting data. On a diametrical traverse through a swirling flow, the frequency shift for the tangential velocity must be reversed upon crossing the aerodynamic center of the flow, because the mean direction of the swirl velocity changes. It was assumed, for the sake of simplicity, that the aerodynamic center of the flow and the geometric center of the fuel nozzle exit were coincident.

Spray Patternation and Atomization Test Facility

All spray tests were performed in a facility that offered the capability to characterize the sprays formed by fuel injectors under ambient conditions. A schematic of this facility is shown in Figure IV-3. It consisted of a computer-positioned plenum mount for the injector, a receiver tank containing a high-resolution patternator, and the necessary controlling and metering devices for air and fuel flow rates. The test injector was mounted on the bottom end of the plenum and sprayed downward into the receiver. Injector airflow was fed into the plenum. Fuel lines were plumbed through the plenum to the injector.

A unique feature of the facility was the high-resolution patternator. This system consisted of a "wagon-wheel" array of probes that fed liquid collection devices. This patternator rake contained 60 tubes, 10 each on six equally spaced radii within a 4-in. diameter. The plenum was positioned above the patternator to place the injector axis at the center of the rake. The separation distance between nozzle and rake was either predetermined or adjusted so that the rake intercepted an entire cross section of the spray cone. Liquid collected by a probe accumulated in a cylinder. The quantity of fuel collected there was determined by measuring changes in liquid column pressure in the cylinder, as sensed by a Scanivalve ZOC electronic transducer.

The patternation process was automated and controlled by an Apple IIe computer. Initially, the fuel flows and airflows were established with covers over the collection tubes. The computer recorded initial readings on each collection cylinder. Upon initiation of patternation, the covers were withdrawn. The computer monitored each collector and terminated the process by returning the covers when a set point collection volume was reached. After a one-minute pause to assure complete drainage into the cylinders, ZOC readings were acquired and, via calibration factors and the initial reading, were used to compute the local fuel mass flux. An ejector system was actuated to empty each cylinder and a new zero ZOC reading was acquired. At this point, the computer repositioned the plenum and the entire process was repeated. Typically, the plenum was rotated to cover the spray in 10-degree increments, providing 360 points of spray mass flux. Data were saved on floppy disks and later transferred to an IBM RSC6000 computer. Subsequent processing yielded information on averaged circumferential and radial spray distributions, cone angles and spray fuel flux contours.

The 360 measurements of local fuel flux were processed to produce contour plots (two dimensional representations with lines of constant mass flux), three dimensional projections of these contours, a radial mass flux profile obtained by averaging the 36 data points at a common radius, and a 45-degree sector analysis. The 45-degree sector analysis integrated the mass flux data to evaluate the circumferential uniformity of the spray. In particular, the quantity of the spray contained in a 45-degree flow sector was evaluated, with the normalized peak-to-peak deviation from the average [denoted: (Max-Min)/Ave] used as an indicator of non-uniformity. "Error bars" on the radial profile indicate azimuthal variations at each radius.

A spray cone angle was computed from the mass flux data by integrating them outward from the centerline until 90% of the total mass flow was accounted for. The radius at this location and the downstream sampling location defined one half of the 90% spray angle. A "peak" spray angle was also calculated, corresponding to the location of the peak of the radial fuel flux profile. For sprays originating from a finite diameter (i.e. not a point on the injector centerline), the radius of the source was included to provide a cone angle representing the expansion of the spray beyond the source diameter. All cone angles were measured from the inner diameter of the filming surface or the final point of fuel injection. This reference accounted for the effects of different filming diameters in the cone angle calculations.

The test conditions for ambient spray tests were scaled from nominal engine operating conditions. The velocity of the air through the nozzle/swirler was matched, and the fuel flow was set at the value required to match the fuel/air momentum ratio of the engine condition. This procedure, preserving momentum ratio and shear-scaled mechanisms, is believed to be important for atomization and patternation, especially for airblast type injectors. The geometric configuration of the injector was also changed, in order to provide the proper effective airflow area (and pressure drop) for the given flow condition.

This facility was also equipped with a Malvern 2600D, diffraction-based particle sizing instrument. Figure IV-4 shows a schematic of the instrument and its operation. The Malvern is a diffraction-based instrument that uses the on-axis scattering of laser light from all the particles in the measurement region. The measurement region consists of the entire Helium-Neon laser beam used as a light source. Hence, this diagnostic is not spatially precise. It collects sample from the entire path length of the beam. In a simple representation, small particles scatter light at high angles, due to their higher radius of curvature, whereas larger particles scatter light at lower angles. A series of photo-detector rings, concentric to the source beam path, measure the intensity of the scattered light at different radial positions. The light distribution is then transformed into a droplet size distribution, with each detector ring representing a range of droplet sizes. This instrument was fitted with a 300-mm lens system, enabling measurements between 5.8 μm and 564 μm.

The Malvern was controlled using a PC running dedicated acquisition software. Data were acquired, printed out and stored on the computer's internal hard disk. The light intensity distribution compensates for any variation in the background light intensity through a background reading, which was performed before each test. Data were fitted to the Rosin-Rammler droplet size distribution function:

$$R = e^{-\left(\frac{D}{X}\right)^N}$$

where R is the fraction of droplets in the spray with diameter greater than D. X represents a mean drop size for the distribution and N is a distribution width parameter. The values of X and N can be used to calculate the Sauter Mean Diameter (SMD), which characterizes the volume to surface area ratio of the spray.

As with many other optical diagnostic techniques, the Malvern loses effectiveness when used in dense sprays. An optically thick medium causes attenuation of the incident light and leads to multiple scattering effects. The instrument monitors the attenuation of the laser beam using the center photo-detector, and records this value as a relative "obscuration" level. An obscuration level of 1.0 indicates that no light penetrates through the spray to the center photo-detector. At high levels of obscuration (> 0.6) computed droplet sizes are often inaccurate due to multiple scattering effects. An analytical procedure is used to correct the two parameters in the Rosin - Rammler distribution to account for multiple scattering effects at high obscuration levels:

$$\frac{X_0}{X} = 1.0 + \left[N^{(1.9-3.437(OB))}\right] \times \left[0.036 + 0.4947(OB)^{8.997}\right]$$

$$\frac{N_0}{N} = 1.0 + \left[N^{(0.35-1.45(OB))}\right] \times \left[0.035 + 0.1099(OB)^{8.650}\right]$$

where X_0 and N_0 are the corrected levels of X and N, and OB is the obscuration level. The technique is applicable for obscuration levels between 0.6 and 0.98, over N = 1.2 to 3.8. A corrected SMD, SMD_0, may then be calculated using these two parameters and the mathematical Gamma function:

$$SMD_0 = \frac{X_0}{\Gamma\left(1 - \frac{1}{N_0}\right)}$$

The corrected SMD, SMD_0, are the values reported herein.

Modular RQL Combustor Rig

The modular RQL combustor rig, as it was defined and constructed for the effort of Ref. 2, is shown in Figure IV-5. As shown on the figure, the rig incorporated independent control of the airflow to the rich and quench zones of the combustor. The quench air-stream was directed into the gas path from a manifold around the quench section of the rig. The rich combustion zone consisted of a cylindrical length section followed by a conical convergent section to the quench entrance; these two sections were individual modules of the RQL combustor. Cylindrical spools of varying lengths were available to achieve different residence times in the rich zone. The convergent section was 1.6-inch long, transitioning from the 5-inch diameter combustor to the 3-inch diameter quench section at an included angle of 64 degrees. The lean zone consisted of a divergent section at the quench exit followed by a separate cylindrical section. The 3.2-inch long divergent section transitioned from the 3-inch diameter quench to the 5-inch diameter cylindrical section at an included angle of 34 degrees. Cylindrical spools of various lengths were also available to achieve alternative lean-zone lengths. All of these sections incorporated a double wall construction with an internal water jacket. The 8-inch nominal pipe size

spools contained a 1.25-inch thick ceramic liner to provide thermal insulation and achieve the gas path diameters mentioned above. The insulating liners were cast in place in the spools from Plibrico Plicast 40, a commercially available ceramic consisting of mostly alumina. This material was selected because of its favorable thermal shock properties and its ability to withstand combustor temperatures up to 3400°F.

Four candidate quench zone configurations, having different numbers and sizes of quench air orifices, were evaluated in the Ref. 2 program and an eight circular-hole quench configuration was used for these tests. The quench airflow was injected into the gaspath through eight, 0.719-in. diameter, equally spaced circular orifices. The quench section length and inner diameter was 3.375-in and 3-in, respectively, and the axial plane of the hole centerlines was equidistant from the quench entrance and exit. The eight hole quench section design had one air inlet and was fabricated from 316 SS. Heat loss to the cooled surface was minimized with use of a 0.03-in. thick, flame-sprayed coating of zirconia oxide. The design included two, 0.10-in. high annular water cooling passages located in a 0.75-in. thick wall that forms the quench-jet metal cylinder. Each cooling annulus was 1.10-in. wide and located to provide a 0.75-in. wide uncooled band at the center of the section for the quench-jet orifices. Water was supplied at a flow rate of 3 GPM to each cooling passage through flexible lines that passed across the quench manifold and out of the housing.

A Delavan Model 32740-3 Swirl-Air fuel injector had been used as a baseline for the combustion tests in the Ref 2. Program. The Delavan Swirl-Air nozzle is an internal mix, air-assist nozzle. The air-assist feature permitted control of the fuel atomization process independent of the test condition. The assist airflow was regulated and metered by a venturi to maintain a nozzle fuel-to-air flow rate ratio of about unity. This produced an included fuel spray angle of about 100 degrees. This nozzle was mounted in the center of an annular, axial-flow swirler. The effective airflow area of this nozzle-swirler assembly was 1.0 in^2.

The Delavan injector-swirler combination was mounted on the centerline of the front bulkhead of the rich zone with the metered airflow to the swirler being delivered to the upstream plenum. The experimental, variable geometry, fuel injector air admission devices evaluated during this task were mounted on similar bulkheads at this plane. On configurations incorporating remotely actuated variable geometry components, the actuation mechanism was installed in the upstream air plenum and the mechanical drive passed through a sealed fixture on the plenum wall.

RQL Combustor Test Facility and Instrumentation

The single nozzle modular RQL combustor test rig was installed in Cell 1E of the Jet Burner Test Stand at United Technologies Research Center. This combustor facility included a high-temperature airflow distribution and control system, the modular RQL combustor, and an exhaust system. The total combustor airflow was supplied to the test facility by continuous-flow compressors. Combustor inlet air temperatures up to 1300°F were achieved with multiple, non-vitiated heating systems. Two direct-contact, electrical resistance heaters were plumbed in series to obtain a 1300°F-inlet temperature at 200 psia. The airflow exiting the second heater was divided into the rich-zone combustor airflow and quench airflow.

A water-cooled instrumentation section containing six emissions sampling probes was located at the exit of the lean zone of the RQL combustor. Downstream of the instrumentation section, the combustor exhaust passed through diffuser and transition sections upstream of the combustor back-pressure control valve. The transition section diverted the flow through two 90-deg. turns prior to encountering high-pressure water sprays to cool the flow before entering the back-pressure valve. A window was located in the transition section along the combustor centerline to permit observation of the flame.

The instrumentation on the combustor rig consisted of two venturis to measure the total airflow to the rig and to the rich zone, with the quench zone/liner cooling airflow being determined by the difference between the two. Fuel flow meters measured the fuel flow to the fuel injector. Thermocouples were installed to measure air and fuel temperatures at each flow measurement site and in the rig air inlet plenums. Total pressure probes were also installed in the air plenums and static pressure taps in selected locations in the gas path provided measurements of the pressure differentials across components of the combustor. As indicated above, six water-cooled, gas-sampling probes were installed in the lean zone of the combustor. Further details on the baseline instrumentation on the rig and its operation are available in Ref. 2.

SECTION V - VARIABLE GEOMETRY CONCEPT DEFINITION

The major technical effort on this task consisted of a review of candidate variable geometry concepts that might be incorporated in the Rich-Quench-Lean combustor for application to the High Speed Civil Transport engine. This initial review disclosed four potential configurations, three of which were ultimately evolved and tested in the modular RQL combustor rig. The remainder of this section describes the evolution of these candidate systems including the non-reacting aero-thermal assessments conducted on models of the concepts as they developed.

Before proceeding with the assessment of the variable geometry injector/air admission concepts a viable baseline had to be established for combustor rig performance. During the tests of Ref. 2, the RQL modular combustor rig had been operated with an air-assisted fuel nozzle in which the atomization of the fuel is enhanced by introducing a high velocity air stream from an external source. The external assist feature provided greater test flexibility for these early development assessment tests by essentially eliminating atomization as a test variable while assuring a high degree of atomization. The quantity of assist air was small, on the order of the fuel flow, and the injector was centrally mounted in a swirler having an effective flow area, ACd, of one square inch. While it was an effective system for the initial validation and data base definition for a Rich-Quench-Lean combustor, the external air assist feature was not representative of a realistic engine injector, making this injector inappropriate as a baseline for this task of variable geometry injector definition for the HSCT application.

To establish a new baseline, a two-passage aerating fuel injector was defined and fabricated for this purpose under a prior contract (NAS3-25952) and tested in the Modular RQL combustor rig at the initiation of this task. The design of this injector is shown in Figure V-1 and photographs are shown in Figure V-2 and Figure V-3. Its technology base is well established in commercial engine application including the PW2000 and PW4000 models. The injector consists of two concentric swirling air streams, which in this application provide the entire airflow requirement of the rich zone. Fuel is introduced through an annular manifold in the wall between these air passages and passes through a metering plate to assure uniform circumferential distribution before being discharged from a filming lip into the air-streams. Contouring of the walls of the air passages in this fuel film impingement region is essential to good atomization and spray dispersion. The injector of Figure V-1was designed to have a nominal, effective flow area ACd of 0.96 in^2, with the area being split evenly between the outer and inner passages. The total ACd is the same as the swirler used in the Ref. 2 tests. Referring to Table III-1, this area would also be consistent with the requirements of a variable geometry injector at the idle and supersonic cruise conditions for the Turbine Bypass Engine selected as the reference for this task. The outside diameter of the air-cap on the outer air-stream of this injector was 2.60 inches while the diameter of the discharge orifice on the face of the injector was 1.70 inches. The inner air swirler contained 5 straight vanes inclined to a turning angle of 50-degrees. The injector was fabricated with interchangeable outer air caps having 40-degree and 60-degree swirl angle vanes in the outer air passage. Changing the swirl angle had a very small effect on the effective flow area of the injector but, as will be shown in Section VI, more significant differences in combustor rig performance. The cold flow spray characterizations of this injector are shown in Table V-1 and are typical of two-passage aerating fuel injectors

	40-Degree Outer Swirler	60-Degree Outer Swirler
Nozzle ACd (in^2)	0.96	0.88
Supersonic Cruise ($\Phi_{rich} = 1.8$)		
SMD (μm)	31	28
Spray Cone Angle (deg)	45	70
Idle ($\Phi_{rich} = 0.6$)		
SMD (μm)	51	60
Spray Cone Angle (deg)	53	71

Table V-1 Baseline Two-Passage Aerating Fuel Injector Cold Flow Characterization

While establishing a new baseline for the variable geometry evaluations, effort was also directed at the evaluation of alternate fuel injectors for the cylindrical Rich-Quench-Lean combustor rig. The intent of the evaluation was to establish a database on the influence of fuel-air mixture preparation on the performance and emissions characteristics of the RQL combustor concept in preparation for designing rich zone components later in this task. A multi-passage premixing fuel injection systems had been designed and fabricated for this purpose under a prior contract (NAS3-25952) and was the subject of this evaluation.

For the multi-passage premixing design, technical effort was directed at the experimental evaluation of this rich zone fuel injection system. Figure V-4 shows the details of the initial configuration of this system, which was designed with the intent of producing a spatially uniform fuel/air mixture in the rich zone, should this be critical to NO_x emissions. The injector system replaced the front bulkhead of the rich zone and admitted air into the rich zone through 19 distributed circular holes. The bulkhead was water cooled internally and was one inch thick. Jet A fuel was distributed to each of the 19 air passages through pressure balanced hypodermic tubes that protruded to the centerline of the passage. The tubes were constructed with a concentric heatshield and the annular passage between these tubes could have been used to admit a gaseous fuel, should this have been desirable for diagnostic purposes. The intent was to generate a premixed fuel/air mixture in each of the 19 passages. The thickness of the bulkhead and axial positioning of the injector 0.76 inches upstream into the passage were based on conservative criteria for avoiding auto-ignition in the passage.

Flow visualization tests were conducted on a single passage of this multi-source injector. The results indicated that liquid fuel discharged from the tube tended to accumulate in the wake of the tube. Retracting the heat shield tube and bending the liquid fuel injection tube to cant it in the downstream direction substantially inhibited the flow into the wake and enhanced dispersion. This enhanced design is shown in Figure V-5.

Tri-Swirler Aerating Injector

The first approach to the definition of a variable geometry axial flow aerating injector was to extend the baseline aerating injector of Figure V-1 by increasing the airflow capacity of the outer swirler. In

pursuing this approach, the injector has been designed and sized to accommodate the maximum rich zone airflow with an effective flow area (ACd) of 2.2 in^2 and variable airflow features are then incorporated to accomplish the required flow modulation. This would require increasing the outer air-cap diameter from 2.60 inches in the baseline configuration to about 3.75 inches.

The use of an axially translating aircap on the injector for flow modulation purposes appeared attractive initially from the aerothermal point of view. The essence of this concept is to have an injector similar in design to that shown in Figure V-1 but scaled up to meet the larger ACd requirements and to have the outer swirler air cap axially translate to provide the air modulating function. The air cap motion would modulate airflow in the outer passage sufficient for the desired stoichiometry change by controlling the axial gap between the fuel filming lip and the outer air cap. Mechanical execution of this approach could be difficult however because the downstream face of the air cap functions as part of the combustor bulkhead and is exposed to high radiant heat loads. Moving this hot part reliably and precisely while maintaining a seal with the combustor bulkhead could be difficult. This approach to airflow modulation was not pursued further.

The alternative could be to fix the outer air cap at the position necessary to pass the maximum airflow required and modulate the airflow through the outer swirler and passage with an upstream valve. This approach is akin to the design shown in Figure V-1 (with a larger outer swirler) with a valve positioned at the inlet to the outer air swirler feed. An advantage of this approach is that the variable mechanism is in a relatively cool and controlled temperature region. However with the upstream-modulated flow and the fixed-position outer air cap the variability of air velocity in the outer air passage must also be recognized. In a two passage aerating injector, this outer air stream strongly influences atomization of the fuel and the angle of the spray cone. Variability of these features would have to be accommodated with this design approach. This implementation was not pursued further because of this potential for variable flow field characteristics and injector performance.

An alternative approach to axial flow aerated operation involves combining an existing, but smaller airflow two-passage injector with a variable geometry airflow component located co-axially with the core two passage injector. The two passage aerating injector could be sized consistent with minimum rich zone air loading and surrounded by a variable geometry annular swirler that can open to meet the entire range of airflow demand. While building on an established injector system of known performance, experience indicates this approach must be executed judiciously to avoid unfavorable mixing or lack thereof between the "injector" stream and the tertiary variable stream. Nonetheless, this design approach offers the decided advantage of divorcing the fuel atomization process from the modulated airflow feature and was the preferred mechanical approach for the aerating injector.

Figure V-6 shows a cross-section of the tri-swirler aerating injector design. Two different valve mechanisms for controlling airflow are shown in the figure and are discussed below. The design is built on the baseline axial flow swirler, aerating or airblast injector geometry. Air was introduced through three airflow passages, each of which was equipped with independent vane swirlers (co-swirled). Fuel was introduced in a thin annular film in between the inner air stream and the intermediate air stream. High-speed airflows impinging onto and shearing the low-speed fuel sheet enabled a high level of atomization. In this concept, only the outer air passage flow area was modulated. The center-body, the inner air passage and the fuel distribution manifold are similar to the baseline injector of Figure V-1, but the swirl angle in the inner passage has been increased from 50-degrees to 60-degrees. The inner swirler

passage has about 0.35 in^2 of effective flow area, reflecting the swirl angle change. The intermediate swirler air-path provides two functions: 1.) to be the "outer", radially-positioned air-stream relative to the fuel filmer to shear and atomize the fuel (similar in function to the outer swirler of a two passage injector) and; 2.) to introduce the remainder (or nearly so) of the minimum airflow for the rich zone. The outer passage is never completely closed and is designed to have at least 10% of the minimum rich zone flow to purge the outer swirler region and prevent combustion products from recirculating into this region. The intermediate passage was consequently sized for about 0.20 in^2 of effective area at a 60-degree swirl angle so that in combination with the inner passage they provided about 90% of the minimum airflow of the injector. The outer air swirler and aircap were designed with 45-degree swirl vanes and sized to provide, in combination with the other two passages the total ACd of 2.20 in^2 required at the maximum flow position. This resulted in an air cap outside diameter of 3.90 inches. When installed in a combustor with a nominal bulkhead height of five inches it was evident the face of the aircap represented a substantial fraction of the cooled bulkhead surface. This was viewed as an advantage for this configuration because the aircap face could readily by cooled by the injector air flowing over the upstream face of the aircap.

The similarity between the tri-swirler and the baseline injector accelerated the fabrication of models of this configuration for non-reacting tests. The center-body and fuel manifold-filmer were common features, which allowed use of the metal parts from the baseline injector. The minor difference in the inner swirler angle, 50-degrees for the existing metal parts of the baseline injector versus 60-degrees for the tri-swirler, was deemed acceptable given the benefit of performing the non-reacting tests expediently. The outer two air passages were fabricated from parametric models using stereolithography procedures. The stereolithography parts were then mounted to the metal core using epoxy cement. The initial design of the outer air swirler revealed a deficiency in airflow capacity ACd relative to the 2.20 in^2 total area goal during the flow calibration tests of this model. Through the parametric computer design procedure the swirler was resized and an improved configuration with adequate flow area was produced rapidly through the stereolithography process.

Two different valving arrangements were considered to control the outer air passage flow. Both arrangements are shown on Figure V-6, one in the upper view and one in the lower view. One used a sliding dam to change the area feeding the air swirler. The other used a series of axially aligned sliding ribs, one for each swirl vane, which, when inserted to different degrees between swirl vanes, blocked off parts of each swirl passage. As shown in Figure V-7 this design required that a specific twist be applied to the outer swirl vanes, so that their leading edges would lie on an exact radial orientation. This allowed the sliding ribs to seal evenly along the entire span of the vanes. Stereolithography models of each valve concept were built and flow calibrated. Figure V-8, Figure V-9 and Figure V-10 show the assembled models used for non-reactive tests. The model of Figure V-9 and Figure V-10 include the sliding rib type of valve. While some advantage in swirler airflow uniformity at intermediate geometry positions had been anticipated for the sliding rib valve approach no significant difference in non-reacting performance was observed between the two blockage concepts. Consideration of design simplicity and avoiding extensive sealing and alignment issues made it obvious that the more elaborate rib valve approach should be discarded and the sliding dam valve development should be continued.

Figure V-11 shows axial velocity profiles measured with the laser velocimeter at a plane 0.25 inches downstream of the injector discharge with both the sliding rib valve and the sliding dam valve. The valve in both configurations was partially open to an intermediate position where the net effective flow

area of the system was determined to be 1.40 in^2. The profiles are very similar, with the only difference being a tendency for the sliding dam valve system to produce a slight velocity deficiency near the outer radii of the peak of the annular airflow cone.

In Figure V-12 the variation of the axial velocity profile at the injector exit, with changes in the extent of the outer swirler blockage, are illustrated over the entire range of variation. At the fully closed condition there was a central recirculation zone that extended to r = ± 0.4-inch with velocities of approximately 35 ft/s (reverse flow direction). Outside of this central recirculation zone, the peak axial velocity was approximately 80 ft/s and occurred at a fairly narrow peak. As the open area of the outer air swirler was increased, the central recirculation zone became narrower and weaker, with velocities of approximately 15 ft/s and an extent to r = ± 0.1-inch. To preserve continuity, the peaks in the axial velocity profile became broader and reached a slightly higher maximum level (approximately 90 ft/s).

Spray droplet size and patternation measurements were also made on the tri-swirler aerated injector model. Tests were conducted at seven flow conditions ranging from idle (lean) through transition to subsonic climb (rich). The effective area of the nozzle swirler was set to the appropriate value (see Table III-1) at each condition using results of earlier ACd testing. The concept demonstrated good atomization characteristics at all conditions, creating fuel sprays with SMD values between 5 and 35 microns. Typical spray droplet size results for the tri-swirler injector are shown below in Table V-2. As is expected, the atomization quality is most sensitive to the air velocity. The exceptional atomization performance of this injector was most probably due to the large filming diameter of the fuel preparation surface. A larger filmer diameter leads to the formation of a thinner film, and therefore smaller fuel droplets after the breakup of that film.

Test Condition Simulated	Fuel Flow Rate (pph)	Air ΔP (in. H_2O)	SMD (microns)
Supersonic Cruise	282	78.2	3.8-6.1
Rich Transition	171	77.9	4.4-5.7
Lean Transition	171	38.1	34.7-34.9

Table V-2 Typical Spray Droplet Sizes for the Tri-Swirler Injector

The injector also displayed consistent patternation characteristics. The fuel spray distribution was evaluated through monitoring of the fuel spray cone angles (peak and 90%) and the circumferential non-uniformity index. Both values were calculated from the results of tests performed at scaled conditions (as described in Section IV) representative of the entire range of operation. As shown on Figure V-13, a total variation of peak spray cone angle of only 15 degrees was observed over the entire operating range. The minimum cone angle was observed at the lean transition condition, where the injector airflow rate was the highest and the injector is in the fully open position. This one deviation represented the majority of the total variation in spray cone angle, and the spray cone angle variation across the other conditions was less than 10 degrees.

Figure V-14 shows the circumferential 45-degree sector fuel flux non-uniformity index as a function of the seven test conditions. Lower values indicate a more uniform distribution. There was only significant non-uniformity at the idle condition, at which the fuel flow rate was the lowest. This is behavior typical of low pressure, pre-filming fuel systems, in which the hydraulics of the fuel passage at low flow rates

can have large effects on the spray distribution and can actually enhance the injector's stability characteristics at these conditions.

Following completion of the non-reacting tests with extremely satisfying results, the design activity on the tri-swirler concept focused on the design of the high temperature metal configuration for evaluation in the cylindrical RQL combustor rig. After review of the anticipated test program, it was concluded that the design would include an actuating mechanism for the variable airflow valve of this configuration so that the test operator could externally control this system. This approach, as opposed to the simpler exchange of shims or spacers during shutdowns of the rig, was based on consideration of savings in test time, experience gained with an actuation mechanism in a hostile environment and versatility, in that the same mechanism may be adaptable to other concepts. Figure V-15 shows a photograph of the assembled tri-swirler injector including the non-flight type actuation system. Note that in this configuration of the injector, the sliding rib valve is shown.

Cold flow testing of this injector showed that the maximum effective area achieved by this design was 2.21 in^2 versus the required ACd of 2.20 in^2. The minimum effective flow area, measured with the sliding rib valve in the fully closed position, was 0.96 in^2 versus the design intent of 0.60 in^2. Testing indicated that this was a result of leakage around the sliding rib valve. The minimum ACd achieved by the injector when the variable passage was completely blocked off with tape was 0.52 in^2. Limited spray patternation and laser velocimetry tests were performed on this model to verify its similarity to the prototype and to quantify its performance. Both tests revealed behavior that virtually met or exceeded the prototype. Fuel and air flux profiles acquired at a plane 1.5 inches downstream of the injector exit are shown on Figure V-16 and Figure V-17 for subsonic cruise and supersonic cruise respectively. They indicate juxtaposition of the air and fuel mass flux peaks implying significant homogeneity of the fuel/air distribution at these simulated conditions.

Radial-Inflow High-Shear Injector

A schematic view of a radial inflow injector (without variable geometry enhancements) is shown in Figure V-18. This concept is a variation of a standardized fixed geometry design that has been under investigation at Pratt & Whitney and United Technologies Research Center for some time. An extensive database on its definition was evolved in the effort of Ref 3. The configuration consists of radial inflow swirlers with air introduced through inner and outer passages. Each of these passages contained tangential slots through which the air was admitted, imparting a swirl component to the flow. A centrally mounted fuel injector delivered fuel through radial jets, spaced at even azimuthal intervals. These fuel jets penetrated through the inner airflow and impinged on the inner side of the wall between the two air passages. There, a film of fuel was developed, flowing axially downstream until it left the surface of that wall and was sandwiched between the two high-speed shearing air flows. For the variable geometry application, designs were considered in which either one or both of the airflow paths were modulated. An axially translating band sliding over the inlet to the swirler stages (shown in Figure V-19) could provide the required airflow modulation. The collar shown in this figure is the design that modulates the inner swirler air only. Figure V-20 shows an actuation system that could control precise positioning of this collar using a coarse thread collar guide.

The experience-base for design of these swirlers was derived from studies performed for devices with effective areas of 0.5 in^2 or smaller, approximately one-fourth the maximum RQL requirement. Nonetheless, the analytical model formulated from these studies was exercised to specify geometries that are predicted to achieve a maximum effective flow area of more than 2.20 in^2. The process involves iterating the swirler geometry to achieve desired inner and outer airflow rates and exit swirl strengths, for a desired pressure loss. The geometry is specified by swirler inlet slot height, width, and angle for both the inner and outer swirler; the layout circle of their inner edge; and the exit diameter of both flows. Particular attention is given to the slot layout to achieve a high percentage of open area at the inner radius of the slot array. High open areas reduce the maximum diameter of the swirler and minimize flow expansion losses at the slot exit. Definition of the variable geometry system recognized that the majority of the total swirler airflow passes through the inner swirler and the initial configurations were designed to modulate only this inner swirler airflow.

Three compound radial-inflow swirlers (identified as HSCT1, HSCT2, and HSCT7) were specified and their dimensions are given in Table V-3. These three designs each have effective flow areas of 2.1 in^2, within 95% of the design requirement, and required a large outside diameter, 4.00 or 4.35-inches, to achieve this flow area. The three designs differ in the slot height-to-width (H/W) aspect ratio or the calculated airflow split between the inner and outer swirler. The HSCT1 design has H/W=2, while the others are near 1.5. The HSCT1 and HSCT2 designs predict a 90/10, inner/outer airflow split, while HSCT7 projects an 80/20 split. Both of these features affect the strategy to throttle the total airflow.

	HSCT1	HSCT2	HSCT7
Inner Swirler (angle ≈ 63°)			
Inlet OD (in)	4.00	4.35	4.00
Exit ID (in)	2.36	2.36	2.26
Number of Slots	32	24	28
Height (in)	0.469	0.469	0.431
H/W	2.0	1.5	1.6
% of Total Flow	90	90	80
Outer Swirler (angle ≈ 75°)			
Inlet OD (in)	4.00	4.35	4.00
Exit ID (in)	2.71	2.71	2.79
Number of Slots	32	24	20
Height (in)	0.179	0.179	0.259
H/W	2.0	1.5	1.6
% of Total Flow	10	10	20

Table V-3 Geometry of the Initial Series of Radial Inflow Swirlers

The focus of the airflow throttling strategy initially was to reduce the inner swirler flow rate only. Hence the design inner-to-outer flow split will vary during throttling, with the inner flow (percentage of total) decreasing as the variable geometry mechanism is closed. For example configurations HSCT1 and

HSCT2 have flow splits of 90/10 at the maximum flow capacity. At the minimum required capacity of 0.6 in^2, the inner flow has been reduced, resulting in a 60/40 split. These two extreme flow split values span the previous design experience. Similar predictions for HSCT7 result in a flow split range from 80/20 to 40/60. Depending on spray quality, the reduced inner flow of the HSCT7 configuration would result in a smaller swirler diameter (4.00 versus 4.35 inch) for $H/W \approx 1.5$, as seen by comparing the HSCT2 and HSCT7 designs.

Aluminum versions of each of these three swirlers were fabricated and one is shown in Figure V-21 with the sliding collar removed for clarity. Cold flow calibration tests confirmed that the swirlers did achieve the target, effective flow area capacity at the desired inner/outer airflow split. These studies also mapped the airflow throttling achieved by progressive coverage of the inner swirler slots as shown in Figure V-22.

Figure V-23 shows the axial velocity profiles measured 0.25 inches downstream of the discharge plane of the HSCT2 swirler model as the inlet of the inner swirler passage was progressively blocked. At all but the minimum inner-swirler inlet area, a substantial and strong recirculation zone exists at the center. In contrast, at low inner swirler flows, this region is very wide and composed of essentially dormant air, a feature that will be the subject of further discussion.

The design of the centrally mounted radial-jet fuel injector for this type of swirler required significant experimental assessment. For good performance, it was necessary that the fuel jets leaving the injector should have sufficient momentum to reach the filming surface on the inside of the swirler. The liquid penetration is least favorable at the idle condition because the momentum of the pressure driven fuel jet is minimal while the air momentum is high during this lean mode of burner operation. As a consequence, the body of the fuel injector must be large to reduce the fuel jet penetration distance. The combination of a large injector body diameter and sufficient jet penetration must not compromise injector pressure drop or circumferential fuel distribution considerations. To address this issue, patternation tests with several different injectors were conducted with one representative air swirler (HSCT1). The defining geometric parameters of the injectors investigated experimentally are listed in Table V-4.

Injector Diameter inches	Number of Evenly Spaced Radial Jets	Diameter of Jets inches
2	6	0.040
2	12	0.020
2	8	0.020
1.75	8	0.020

Table V-4 Geometric Parameters of Injectors for High-Shear Swirlers

Figure V-24 shows the variations in azimuthal frequency mode of the spray from each of the injectors as a function of fuel flow when installed in the HSCT1 swirler and evaluated on the patternator. An azimuthal frequency of unity indicates the fuel was dispersed as a relatively uniform annular spray while a frequency mode of "N" implies the spray was dominated by "N" concentrated areas. The data indicate that both eight-orifice injectors produced one-per-orifice fuel concentrations at fuel flows representative of the subsonic cruise condition, 165.6 pph, but that these tended to coalesce when fuel flow was

increased. These results imply adequate fuel jet penetration to the swirler wall but inadequate transverse dispersion until the fuel jet-to-air momentum ratio became higher at the higher fuel flow. Conversely, the six-orifice configuration, with larger orifice diameters and subsequently low fuel pressure drop and velocity, did not generate sufficient momentum for fuel filming. Even when fuel flow was high and the jets reached the swirler surface, they were dispersed as six relatively discrete sprays. The twelve jet orifice appears to provide the best performance in that, while there may have been some film merging between films generated by jets from adjacent orifices at low flow rates, at the moderate and high fuel flows the desired transverse uniformity of fuel spray was observed.

Figure V-25shows the 90% spray cone angle measured with the patternator with the injectors of Table V-4 in the HSCT1 swirler. The cone angle variation had been measured over the entire range of effective flow area with the six-orifice injector. The spray angle remained in a 27-degree wide band (55° - 82°) through all simulated power conditions except for Lean Transition with the 6-orifice injector, where the spray tended to collapse. This Lean Transition point is the condition of highest inner swirler air velocity, and with less than ideal jet penetration and dispersion anticipated based on the data for this injector as shown in Figure V-24, this collapse of the spray cone is not surprising. The other three injectors, which had better penetration characteristics as described above, produced higher spray cone angles consistent with all the fuel being atomized from the filming surface. The injector with 12 evenly spaced holes provided adequate fuel jet penetration in the spray visualization apparatus and the best overall spray dispersion and circumferential uniformity. With this injector, droplet size was small at most conditions, with Sauter Mean Diameters of 10 to15 microns.

The totality of non-reacting flow evaluations on the first three swirler configurations (HSCT1, HSCT2 and HSCT7) indicated this design approach needed further refinement. Airflow profiles at the injector exit had indicated significant variations in flow structure as the injector airflow was modulated as previously shown in Figure V-23. Previously discussed velocimetry measurements made near the exit plane of the swirler demonstrated that as the inner swirler inlet was closed off, a large central wake region developed, as shown in Figure V-23. This wake region became wider with increasing blockage, until at minimum effective flow area, a large "dead zone" of airflow occupied the center portion of the flow. It was determined that this large variation in the airflow field downstream of the injector was undesirable because of the unknown effects it would have on reacting-flow performance. Of specific concern was injector durability. A large wake region in the center of the flow would allow hot combustion products to be re-circulated back into the swirler, where hardware damage could result. In addition, the patternation tests discussed above also raised the issue of fuel jet penetration from the center-body injector through the inner air stream to the filming surface on the inside of the inner swirler. At high airflow conditions such as the Lean Transition condition, the airflow rate passing through the inner swirler was also very high, making it difficult for the fuel jets to reach the filming surface. Studies of the design approach suggested that the modulation of the airflow through the inner passage of the swirler was excessive and consideration should be given to modulation of both the inner and outer airflow passages. These findings led to the definition of three additional configurations of this concept with different inner to outer swirler airflow splits and alternate variable geometry schedules.

Three new configurations of the radial-inflow concept were defined as shown in Table V-5. They differed from the first set in that they allowed for two variable-geometry flow passages, as opposed to only the inner passage, as used in earlier designs. The inner/outer flow split between the two-swirler passages at maximum flow capacity was also decreased, so that more air would be introduced on the

outboard side of the spray cone to accommodate the flow modulation of that passage while maintaining spray quality. Within the set, the three configurations differed in the inner/outer swirler flow split and in the nominal intensity of air swirl. Figure V-26 shows a cross-section through this type of swirler including the collar that would control the inlet flow area of both swirlers.

	HSCT11	HSCT12	HSCT13
Flow Split (Inner/Outer)	70/30	70/30	50/50
Swirler Angles (Inner/Outer)	60/50	70/40	60/50

Table V-5 Geometry of the Revised, Constant Flow Split Series of Radial Inflow Swirlers

Laser velocimetry tests were conducted on aluminum models of the three new radial-inflow high-shear injector concepts and exhibited performance improvement relative to original designs of this type. Because the flow split between the inner and outer air passages did not change as the variable geometry mechanism was actuated, the flow field changes as a result of actuation are less pronounced. As shown in Figure V-27, one of the new configuration swirlers (HSCT13), representative of all three new configurations, designated "Constant Flow Split" on this figure, produces a narrower central wake region surrounded by higher energy airflow cone at the minimum flow area setting. Centerbody fuel injection was accomplished using 8 x 0.020-in. diameter fuel injection orifices on a 1.5-in. diameter centerbody, which provided reliable fuel filming at all test conditions. Spray patternation tests indicated that these devices produced sprays that changed only slightly with varying flow condition and geometry as shown on Figure V-28. This is in sharp contrast to the initial series of configurations with variable airflow split (HSCT1, HSCT2 and HSCT7) which had exhibited large variations in spray cone angle and circumferential fuel distribution. This improvement was achieved by holding the inner/outer flow split constant as the air flow capacity was varied. Spray atomization results showed very good levels of atomization, with drop sizes of less than 25 microns at all conditions.

The high temperature metallic version of the variable geometry radial inflow high shear system was defined on the constant airflow split basis and incorporated the eight orifice central injector used in the patternation tests. The externally controlled actuating mechanism defined for the tri-swirler injector was adapted to the translating collar that modulated the swirler inlet airflow areas on this injector for combustion tests. Prior to being installed in the combustor rig, fuel/air homogeneity measurements were obtained at ambient conditions to determine the fuel air ratio distributions at a plane one-half inch downstream of the injector discharge. These fuel/air homogeneity measurements were acquired at injector mixture proportions and variable airflow settings simulating both subsonic and supersonic cruise of the HSCT engine. Based on the individual air velocity measurements and fuel spray patternation data, the radial profiles of Figure V-29 and Figure V-30 were constructed. Coincidence of the air and fuel profiles is indicative of a highly homogeneous fuel/air mixture. Comparison of these profiles to those observed in Figure V-16 and Figure V-17 for the tri-swirler injector indicates that there is slightly more displacement between the peaks of the fuel and air profiles for the radial inflow swirler than there was in the tri-swirler case. This result would imply that, while retaining good mixture preparation characteristics, the high shear concept does not produce quite as homogeneous a mixture.

Aerated Injector with Translating Ramp

CFD Research Corporation defined this translating ramp injector concept during the computational support effort that they provided to this task. The concept parallels, in the large sense, the three-passage approach of the tri-swirler injector in that the innermost two passages provide an aerating fuel atomization function and substantially provide the minimum airflow requirement of the injector while a third outboard air system provides the variable airflow demands. However, as shown in Figure V-31 the method of providing these functions and hence the configuration of the injector differ substantially from the tri-swirler concept. Fuel is introduced through a series of 12 radially directed orifices on a centrally mounted wall between the inner and intermediate air passages. The jets are atomized by impact with the air approaching from orthogonal directions. The intermediate air passage discharges in the axial direction while a comparable fraction of the injector air entering along the centerline of the injector is swirled and discharged in a substantially radial direction. This intermediate airflow stream is oriented axially such that it impacts the fuel jets causing them to be atomized and the resulting droplets to be evenly dispersed. The combined airflow through these two passages represents slightly less than that required at the minimum injector flow condition. A larger, outer airflow, sufficient to meet the maximum airflow requirement, is introduced through a radial-inflow air swirler. The airflow through this swirler is modulated by using a translating ramp, which slides axially along the central core of the injector blocking a variable part of the axial height of the swirler discharge. The radially inward direction of outer passage flow was expected to provide strong interaction and mixing with the fuel-air mixture emanating from the inner section of the injector. The positioning of the ramp at minimum injector flow condition leaves a small portion of the outer swirler exit free to generate a film of cooling airflow on the downstream face of the ramp. The overall outside diameter of the injector, measured to the leading edge of the outer swirler vanes, is 3.87 inches. This diameter represents a substantial fraction of the frontal area of a combustor bulkhead and the fact that this surface would be cooled by the flow through the outer swirler passage was seen as an advantage of this concept. However, there was concern over the successful actuation and the long-term durability of the variable geometry mechanism in that the translating ramp was directly exposed to hot combustion gases and radiant heat loading. Back-spray of fuel or recirculation of hot gas onto the cylindrical surface on which the ramp slid was also a concern since either fuel deposition or thermal distortion of the metal parts could potentially interfere with component motion.

A cold flow model of the translating ramp injector concept was fabricated using a combination of stereolithography and aluminum parts and is shown on Figure V-32 and Figure V-33. Fuel filmer parts were made using aluminum to ensure strength and dimensional accuracy. The hypodermic tubing emerging from the model convey fuel to the internal manifold while the three metal pins protruding from the upstream face are the positioning pins for the translating ramp. The effective airflow area of the model ranged from 0.3 to 2.3 in^2, meeting the requirements specified in Table III-1. Laser velocimetry measurements were made in the airflow at 0.30 inches downstream of the injector exit plane of this model under ambient conditions to show the variation of the velocity profile as a function of the effective area of the injector. As the results of Figure V-34 indicate, there were no large changes in the airflow field as the effective airflow area was changed. A slight broadening of the axial velocity peaks with increasing ACd was observed. However, the character of the central recirculation zone may be shifting as the ACd approaches the minimum value. The axial velocity profile shifts from a flow field characterized by upstream, reversed or recirculating flow on the centerline to a flow field with

downstream, non-recirculating flow on the centerline surrounded by an annulus of upstream, recirculating flow, implying a different flow structure.

Spray patternation tests showed a 30-degree variation in spray cone angle across the entire range of test conditions, i.e. as a function of fuel flow, air flow and ramp position, as presented in Figure V-35. The sudden drop in spray cone angle at the Supersonic Cruise condition is unexplained, but was repeated in subsequent testing. At all airflow conditions, the spray exhibited circumferential streaks in the fuel distribution pattern. As seen in the patternator data distribution of Figure V-36, twelve peaks are evident and apparently correspond with the 12 discrete fuel injection sites. At all airflow rates, the mixing of these fuel jets with the airflow was incomplete, and hence streaking was observed. These peaks were small and, because of the large number of them, nearly approached a continuous azimuthal distribution. Spray droplet sizing tests showed good atomization characteristics, with SMD values of between 10 and 25 μm at all tested conditions.

Based on the favorable results in the non-reacting assessment of the translating ramp injector, a metal version of the injector was designed and fabricated for combustor testing. However, no effort was made to incorporate the externally actuated variable geometry mechanism used with the tri-swirler and the radial inflow concepts. Rather, shims were designed to fit axially behind the translating ramp and position it so that variable geometry could be simulated in a series of fixed geometry configurations, each tested at the pertinent rig inlet conditions. Figure V-36 shows a comparison of the fuel spray produced by the metal injector with that of the model at the simulated supersonic cruise condition and indicates excellent similarity in both the spray cone angle and the qualitative features of the spray.

Axial Flow High Shear Injector

A fourth concept considered for adaptation to a variable geometry injector is shown on Figure V-37. The intent of the concept was to produce the effect of radial inflow swirlers in the high-shear injector concept with axial-flow air swirlers. This approach offers the possibility of delivering the same airflow capacity in a smaller diameter package and one that could more effectively capture the ram effect of the upstream diffuser discharge flow. This concept also replaces the center-body fuel injector of the radial inflow swirler system with an annular fuel filming system on the filming lip proper. This avoids the need to spray jets of fuel across the inner swirler air stream to generate the fuel film, but raises the issue of needing a large surface area, annular fuel manifold at the filmer radius with attendant thermal isolation requirements. The requirements of airflow modulation were not addressed in detail, but some form of modulation of the inner swirler flow with an upstream register, while maintaining the outer swirler flow area constant (as in the earlier versions of the radial inflow concept) was envisioned. The sliding rib valve concept, shown originally in Figure V-7 and first proposed on the tri-swirler injector, could be implemented on the inner swirler of this axial flow high shear injector. This approach would offer the potential of minimizing radial flow variations in the inner swirler at all ACd settings.

A stereolithography model of the axial flow high shear injector was fabricated and limited non-reacting assessments were conducted on it. This model, at 4.0 inches diameter to the outer cowl of the outer swirler inlet, met the full range of required effective areas as shown in Table III-1. Laser velocimetry tests showed that at high airflow conditions, the central recirculation zone did not penetrate inside the injector. In fact, measurements indicated that no recirculation was apparent as far downstream as 0.25 favorably to those obtained with prior injectors. It is evident that the compositional uniformity of the

inches. At low airflow conditions, however, the same wake profile observed in the radial-inflow devices was observed and is illustrated in Figure V-38. Spray patternation data indicated the circumferential uniformity of the spray was poor at most conditions, showing large streaks in the spray. A typical spray patternation distribution acquired at simulated subsonic cruise conditions for this injector is shown in Figure V-39. This poor patternation behavior is most probably due to high axial momentum of the fuel jets, which inhibited the fuel filming into the transverse direction. There was little variation in spray cone angle from condition to condition. On the basis of these results and more favorable observations in the evaluation of the other three injector concepts, it was concluded that no further work would be done on the axial flow high shear concept.

SECTION VI - COMBUSTOR EVALUATION

The technical effort on this task was initially directed at the evaluation of alternate fuel injectors for the cylindrical Rich-Quench-Lean combustor rig. The intent of the evaluation was to establish a database on the influence of fuel-air mixture preparation on the performance and emissions characteristics of the RQL combustor concept. Two fuel injection systems had been designed and fabricated for this purpose and were the subject of this combustor evaluation. These systems were based on the aerating fuel injector and the multi-passage premixing design approaches adapted to the air and fuel flow requirements of the rich zone of the cylindrical combustor.

Following the initial evaluation of these alternate fuel injectors, the tri-swirler variable geometry injector was installed in the cylindrical RQL combustor rig for evaluation under fired conditions. The injector was installed on the front bulkhead of the rich zone with the airflow supplied from the upstream plenum. The variable geometry actuating mechanism on the injector included a rotary shaft penetrating the wall of the plenum and was, in turn, driven by a remotely operated stepper motor. The motor was calibrated against the effective flow area schedule of the injector and provided independent control of the geometry. The combusting tests of the injector were conducted at six different conditions typical of the entire range of operation of a representative HSCT engine. These included idle, subsonic cruise, supersonic cruise, takeoff, and the end points of the transition between rich and lean operation. The latter represent the extremes of injector airflow variation.

The reacting flow investigation continued with the evaluation of the radial inflow injector in the cylindrical RQL combustor. The test injector was installed on the front bulkhead of the rich zone with the airflow supplied from the upstream plenum similar to the tri-swirler injector. The radial inflow configuration was also driven by the variable geometry actuating mechanism used on the tri-swirler injector. The motor was re-calibrated against the effective flow area schedule of this injector. The combustion tests on this injector concept were also conducted at the six different conditions typical of the entire range of operation of a representative HSCT engine as described for the tri-swirler concept.

The reacting flow investigation of the variable geometry concepts was completed with the evaluation of the translating ramp injector in the cylindrical RQL combustor. The translating ramp injector was not compatible with the externally controllable actuator, so ramp motion was simulated during the evaluation by interrupting the tests, opening the rig and installing or removing inserts behind the ramp to alter its position. Again, the combustion testing focused on the six different conditions typical of the entire range of operation of a representative HSCT engine.

Combustor Test Results with Baseline Injectors

The aerating fuel injector was initially installed in the combustor rig with the 40-degree outer air swirler. Table VI-1 shows a comparison of emissions and performance acquired during these tests with corresponding measurements obtained when the combustor rig was operating with the external, air-assisted fuel injector. This comparison is also shown graphically in Figure VI-1 and Figure VI-2. The external, air-assisted fuel injector was the injector used for the combustion testing of Ref. 2. At lean mode idle condition, NO_x emissions are considerably lower and carbon monoxide an order of magnitude

higher with the aerating fuel injector. However, much of this difference can probably be associated with the combustor configuration since the rich zone of the combustor is shorter and the quench section performance more effective in the current configuration with the aerating fuel injector. In either case, the performance is acceptable and adequate for idle operation. At the other operating conditions listed, the combustor is operating at above stoichiometric rich zone equivalence ratios. While there is a general trend toward slightly higher NO_x output and lower carbon monoxide emissions with the aerating injector, the performance is quite comparable to that achieved with the more idealized external, air-assisted injector.

					Delavan Air-Assist Injector		40 Degree Aerating Injector		60 Degree Aerating Injector		Premixed Multi-source	
Condition	P3 (psia)	T3 (°F)	f/a	Φ_{rich}	NO_x EI	CO EI	NO_x EI	CO EI	NO_x EI	CO EI	NO_x EI	CO EI
Nominal Supersonic Cruise	150	1200	0.030	1.8	8.1	1.4			8.8	1.1		
Reduced T3 SS Cruise	119	865	0.030	1.8	4.1	9.9	4.8	5.8	5.1	7.2	4.6	5.0
De-rated (Reduced P3) SLTO	104	830	0.037	1.8	4.2	15.0	6.6	6.1	9.8	19.9		
Idle	67	440	0.009	0.6	4.5	1.8	2.7	18.0	2.4	24.6		

Table VI-1 Emissions Results for Baseline Injectors

The 40-degree swirl angle outer air passage vanes were replaced with the vanes having 60-degrees angle and combustion tests conducted. A comparison with the 40-degree outer air swirler vanes and the previously employed external air assist fuel injector is also shown in Table VI-1 and graphically in Figure VI-1 and Figure VI-2. These results continue to indicate that the overall performance of the aerating fuel injector is very good relative to the fine atomizing external, air-assisted fuel injector. NO_x emissions at the higher fuel air ratios are slightly higher with the increment being about three-fourths of a gm/kg in the emissions index at supersonic cruise. The only pronounced effect of outer air swirler angle appears to be a significant increase in both NO_x and carbon monoxide at takeoff with the 60-degree outer air swirler vanes. The takeoff condition is at nearly the maximum fuel air ratio of a turbine bypass engine cycle and this difference may be attributable to injector fuel loading effects. However, previously discussed fuel patternation tests on the injector had indicated the injector produced a wider and more dispersed spray which might be considered conducive to more uniform mixtures with the 60-degree out air swirler.

Data was also acquired with the multi-source combustor rig configuration. Table VI-1 shows a comparison of the emissions characteristics of the combustor with the multi-source fuel injector with those observed with the other baseline fuel injection configurations employed in this rig. Again, this comparison is shown graphically in Figure VI-1 and Figure VI-2. As shown, the emissions compare favorably to those obtained with prior injectors. It is evident that the compositional uniformity of the

combustor exit flow must be dictated by quench zone mixing effects and is not influenced by the use of a potentially more homogeneous source in the rich zone.

Combustor Test Results with Variable Geometry Injectors

After completion of the tests with the baseline configurations, the rig was reconfigured to incorporate the variable geometry injectors and the externally controllable actuation mechanisms installed.

Table VI-2 provides the RQL combustor emissions characteristics at the six operating conditions investigated for all of the variable geometry injectors evaluated. This comparison is also shown graphically in Figure VI-3 and Figure VI-4. As indicated by the table and comparison with the previously describe baseline injectors, the performance of the tri-swirler injector paralleled or bettered that of the fixed geometry configurations at the points of comparison. The combustion efficiency with all three injectors was above 99.5% at all steady state operating conditions including idle and dropped only to about 98.5% at the rich end of the transition point. Note that the lean and rich transition test points were conducted at a lower inlet pressure than previously described by the design parameters listed in Table III-1. This modification to the test plan was intended to keep the test program focused on the most up-to-date engine cycle parameters available from the on-going HSCT engine cycle studies. The reduction in pressure from 227 psia in the design table to 78 psia as-tested, also represented a more conservative test condition for the transition point. The critical characteristic evaluated at the transition point would be combustion efficiency and hence, the ability to maintain engine thrust through the transition. Carbon monoxide emissions typically increase, decreasing combustion efficiency, as pressure is reduced, making this revised test condition a more aggressive, conservative comparison point. In the high-power burning mode, i.e. the rich transition, takeoff and supersonic cruise conditions, the NO_x emissions from all three injectors are comparable. At idle and subsonic cruise, where the combustor is burning in the lean mode in the rich zone, some variations in NO_x emissions are evident with the tri-swirler injector configuration producing slightly higher levels. The variable geometry actuation system functioned properly at all inlet temperature levels.

					Tri-Swirler Injector		Radial Inflow Injector		Translating Ramp Injector	
Condition	P3 (psia)	T3 (°F)	f/a	Φ_{rich}	NO_x EI	CO EI	NO_x EI	CO EI	NO_x EI	CO EI
Idle	67	425	0.009	0.60	5.5	8.7	3.3	5.1	2.3	6.7
Subsonic Cruise	92	635	0.014	0.60	10.0	7.5	8.4	1.9	9.4	0.6
Lean Transition	78	766	0.016	0.60	9.6	2.0	10.1	2.2	12.6	1.6
Rich Transition	78	766	0.016	1.55	6.1	67.2	4.9	71.8	5.0	57.6
Scaled Supersonic Cruise (Reduced P3,T3,f/a)	120	818	0.028	1.80	6.1	6.5	5.5	8.6	5.3	11.7
Nominal Supersonic Cruise	150	1210	0.030	1.80	9.9	1.0	9.3	1.8	8.4	1.3

Table VI-2 Emissions Characteristics of Variable Geometry Injectors

Beyond the variable geometry injector evaluations, additional combustor evaluations focused on the ascertaining the influence of fuel-air mixture preparation on the performance and emissions characteristics of the RQL combustor concept.

The multi-source fuel system was modified, as shown in Figure VI-5, to supply fuel to 18 of the 19 air passages in the bulkhead. The intent of the unfueled air jet, which accounted for nominally 1.3% of the combustor airflow at supersonic cruise, was to simulate a "leak" of air into the rich zone. Data was acquired at rig inlet conditions identical to the configuration with all passages fueled. The results indicated that the carbon monoxide emissions index measured at the end of the lean zone was low and qualitatively comparable to that measured with no simulated air leak in the rich zone. However, the NO_x emissions index at the same plane was measured at 6.8 gm/kg as opposed to only 4.6 when there was no "leak" in the rich zone. In both cases the profile of NO_x emissions, as defined by readings at the five individual gas samplings in the lean zone, was flat. Carbon monoxide distributions at this plane exhibited some non-uniformity, but the dominant features were comparable between the "leaks" and "no leak" configurations, which implied that they were caused by quench zone effects as opposed to phenomena in the rich zone.

On the basis of these observations, it was concluded that the leakage of air into the rich zone of an RQL combustor could have substantial adverse impact on NO_x formation in that zone. Evidently, significant quantities of NO_x can be formed in the diffusion burning zones that exist around the periphery of the entering jet. It does appear, however, that the configuration investigated may be a severe case because, other than the recirculation zones formed by the entering jets at the bulkhead, the flow in the rich zone is relatively quiescent. This would have permitted the diffusion burning zones to persist and promote NO_x formation. By contrast, the swirling rich zone flow structures created by the aerating injectors of prior

cylindrical rig configurations would be expected to stir reactants throughout the zone and dilute the diffusion burning zones around a leak more rapidly.

Parametric tests were also conducted with the tri-swirler injector at low pressure/temperature, scaled supersonic cruise simulation and idle conditions to assess the effect of reduced residence time in the combustor, using the variable geometry feature, to support studies of revised RQL configurations. NO_x and carbon monoxide emissions results are shown in Figure VI-6 and Figure VI-7 for the scaled supersonic cruise and idle conditions, respectively. In general, the results of these tests indicate that up to 40% reductions in residence time in the rich and lean zones of the combustor could be accommodated without compromising NO_x emissions. However, carbon monoxide emissions at both idle and low pressure/temperature scaled supersonic cruise and lean stability margin at low power levels could be adversely affected by the associated velocity scale increases.

Tests were also conducted on the cylindrical RQL combustor to assess a significant aspect of an alternative configuration of this combustor concept. The intended final configuration of the RQL combustor was considered to be annular with a multitude of variable geometry, air admission/fuel injector modules mounted on the front bulkhead of the rich zone. An alternate configuration involves a similar ensemble of cylindrical rich-quench modules, each with its own variable geometry injector. The combustion products from these modules would be discharged into a common annular lean zone where specie oxidation would be completed and the products delivered to the turbine. However, because of geometric constraints on the combustor, this transition from module to annular gas path involves an abrupt expansion of the flow and the potential of significant additional NO_x formation in the recirculation regions associated with the expansion was a concern.

Back-to-back tests were conducted on the cylindrical combustor rig using different lean zone configurations. Most of the combustion testing with the variable geometry injectors had been conducted with a 3.12-in. long divergent conical section between the quench and the cylindrical part of the lean zone of the rig. This conical section was removed and a cylindrical lean zone three inches longer than the baseline configuration was installed to account for the space previously occupied by the divergent conical section. This left the effective length of the lean zone (as measured from the end of the confined region of the quench zone to of the emissions probes) nearly unchanged at approximately 6 inches. However, this configuration introduced a 3-in. to 5-in. diameter sudden expansion rather than a conical transition at the juncture with the quench section. Testing of this configuration at simulated supersonic cruise conditions indicated no substantial NO_x generation associated with the sudden expansion.

Operability considerations were also addressed during the reacting flow evaluations. At the idle condition, the rich zone equivalence ratio at lean blowout was 0.28 and 0.31 for the tri-swirler and translating ramp configurations respectively. Blowout was a distinct event for both of these configurations with no evidence of instability as the fuel flow was reduced towards this condition. The lean blowout equivalence ratio for the rich zone of the radial inflow injector was 0.17 but as fuel flow was reduced below the nominal idle equivalence ratio of 0.6, flame pulsing and instabilities occurred when the equivalence ratio dropped below 0.4. The radial inflow injector also produced a distinct low frequency tone noise at all power levels. This noise was not observed in the evaluation of the other variable geometry injectors nor in any prior configuration of this rig.

In summary, the tri-swirler showed stable flow fields insensitive to variable geometry positioning, good fuel/air uniformity, and a strong central recirculation zone. Emissions performance of the tri-swirler configuration was acceptable and further development would be expected to improve its performance. Cold flow characterization of the radial inflow swirlers showed an inclination towards a lazy central recirculation when the injector approached low effective airflow settings. In addition, combustion testing showed a potential for operability problems in that combustion was unstable and erratic below rich zone equivalence ratios of 0.4. In addition, this radial inflow injector had pronounced low frequency tones at most power levels. The translating ramp injector performed admirably in its combustion emissions performance. However, cold flow characterization of the translating ramp configuration showed a potential flow field shift was occurring as the variable outer swirler air passage neared the fully closed position. In addition, the surface that the variable geometry mechanism slides on is exposed to radiant heat load from the rich zone combustion products, which may cause reliability problems for long term exposure applications. Finally, no significant experience base exists for the translating ramp configuration where as a substantial experience base exists for the aerating and radial inflow configurations. Based upon the cold flow characterization, emissions results, acoustic behavior observed during the tests and consideration of mechanical, reliability and implementation issues, the tri-swirler configuration was selected as the best variable geometry concept for incorporation in subsequent Rich-Quench-Lean combustor evolution efforts for the High Speed Civil Transport.

SECTION VII - CONCLUSIONS

Based on the results presented in this report the following conclusions are reached:

- A mode of operating the Rich-Quench-Lean combustor was identified in which the rich zone is maintained well below stoichiometric conditions at low power and abruptly changes to well above stoichiometric conditions at high power.

- A variable geometry, air admission system on the inlet to the rich zone is the only variable geometry device necessary to achieve the desired rich zone stoichiometry schedules.

- While excursions in total pressure drop are produced, the quantity of airflow modulated is not excessive and the overall variation in combustor effective area is moderate, making the excursions in pressure drop tolerable.

- A variety of variable geometry injector designs are feasible that are capable of meeting the requirements for a wide range in effective flow area while maintaining good injector performance characteristics.

- The Rich-Quench-Lean combustor concept is robust in its emissions performance by demonstrating tolerance to fuel/air mixture non-homogeneity. Low emissions are observed over a wide range of conditions representing the range of operation of an HSCT engine while operability margins are maintained.

- Operating the rich zone of a Rich-Quench-Lean combustor at above stoichiometric conditions at low power levels can yield marginally acceptable carbon monoxide emissions and combustor efficiency performance.

- Unmanaged leakage of air into the rich zone of a Rich-Quench-Lean combustor can adversely impact NO_x emissions performance.

- Moderate reductions in rich zone and lean zone residence times can be accommodated without impacting NO_x emissions performance.

- A sudden expansion between the quench zone and lean zone can be incorporated into Rich-Quench-Lean combustor configurations without substantial increase in NO_x emissions performance.

- A variable geometry actuating mechanism can be successfully implemented to operate at High Speed Civil Transport combustor inlet conditions. Further development may be necessary to advance the mechanism design to an engine-worthy configuration.

REFERENCES

1) The Atmospheric Effects of Stratospheric Aircraft: A Fourth Program Report, NASA Reference Publication 1359, January 1995

2) Rosfjord, T. J. and Padget, F. C., Experimental Assessment of the Rich/Quench/Lean Combustor for High Speed Civil Transport Aircraft Engines, Final Report on Task 3 of NASA Contract NAS3-25952, December 1995

3) Cohen, J. M. and Rosfjord, T.J., Influences on the Sprays Formed by High Shear Fuel Nozzle/Swirler Assemblies, Journal of Propulsion and Power, AIAA, Vol. 9, No. 1, 1993

SECTION II FIGURES

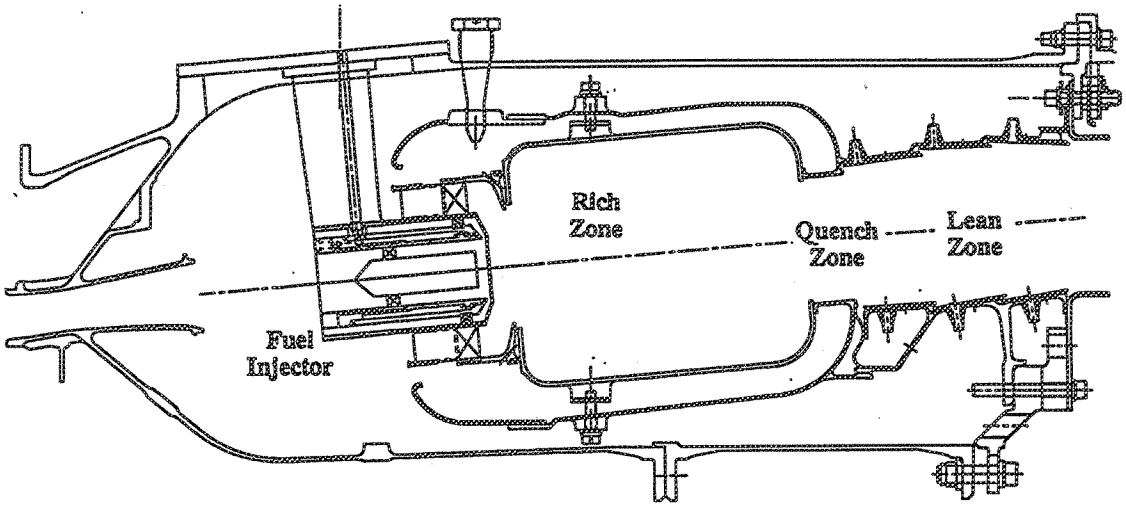

Figure II-1 Rich-Quench-Lean Combustor Concept

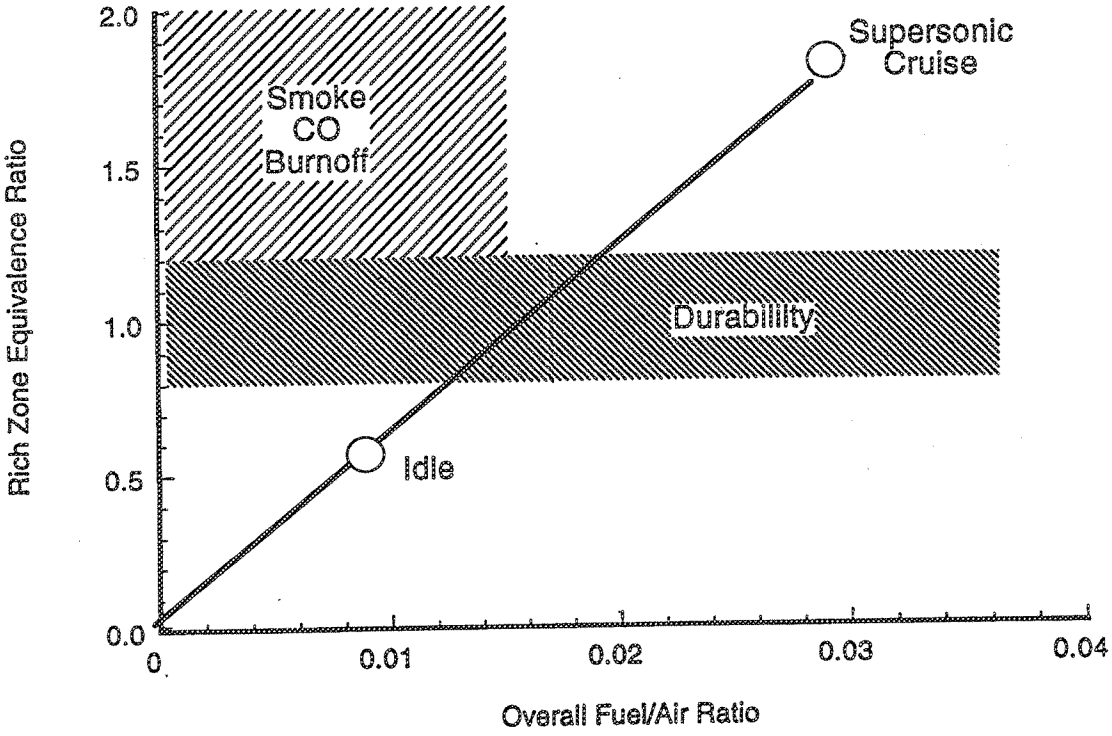

Figure II-2 Rich Zone Stoichiometry of a Fixed Geometry Combustor
(24% rich zone, 70% quench zone, 6% lean zone cooling).

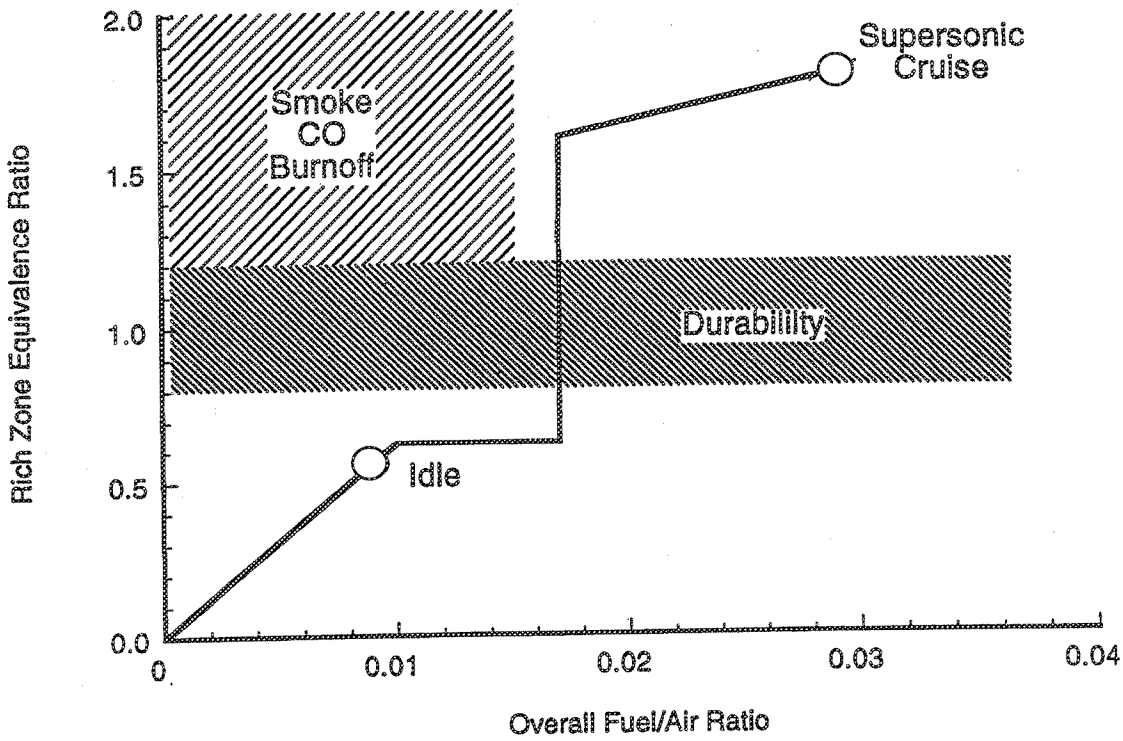

Figure II-3 Rich Zone Stoichiometry Schedule for a Variable Geometry RQL Combustor

SECTION III FIGURES

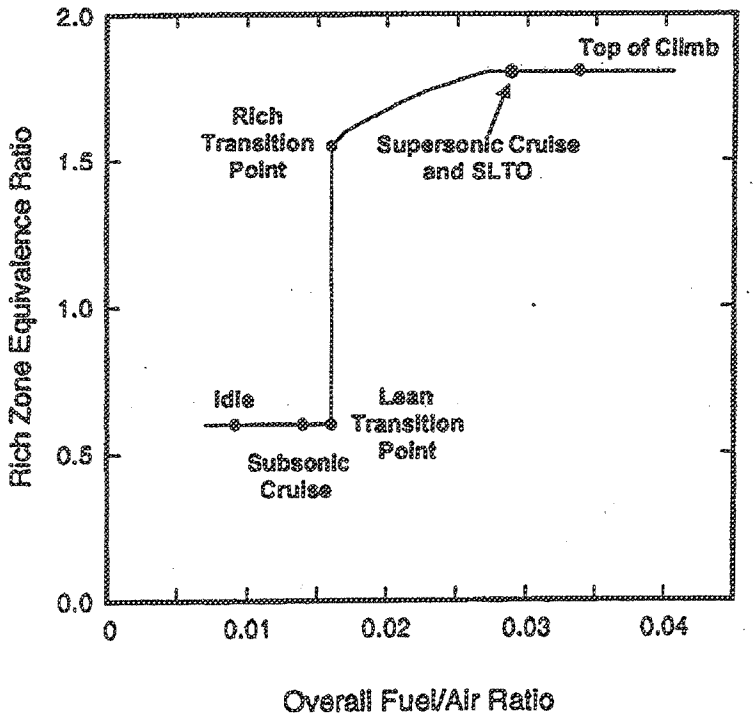

Figure III-1 Rich Zone Stoichiometry Schedule of a Variable Geometry RQL Combustor.

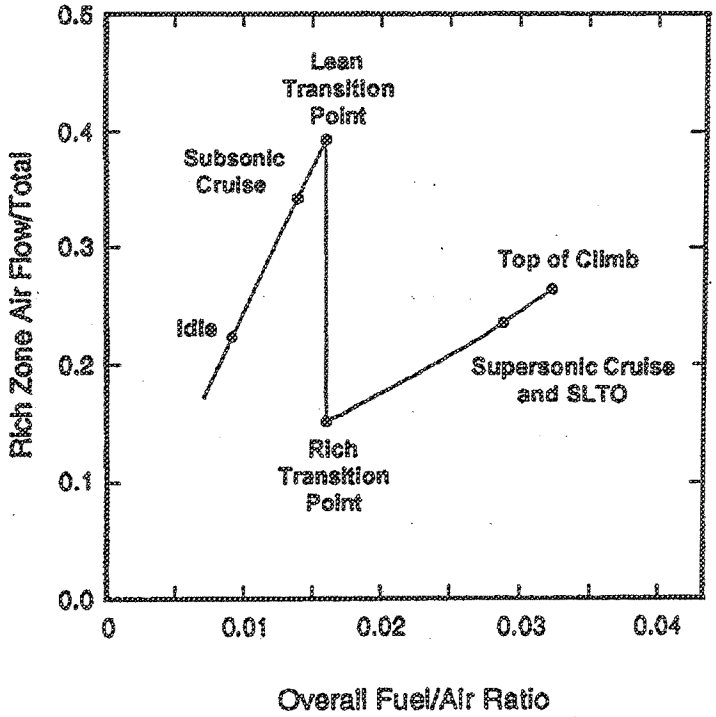

Figure III-2 Rich Zone Air Loading Schedule of a Variable Geometry RQL Combustor.

SECTION IV FIGURES

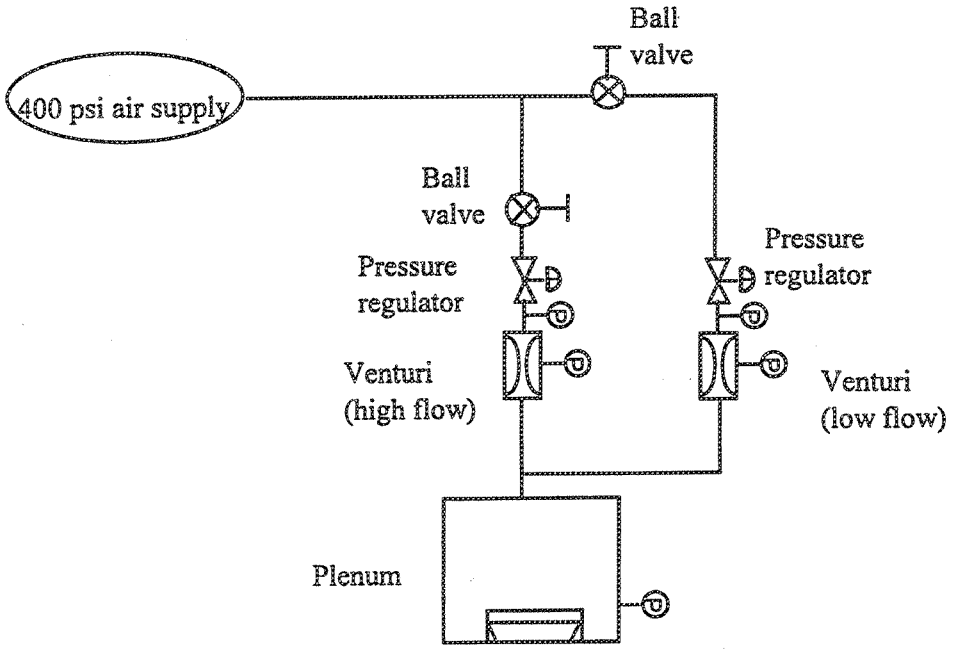

Figure IV-1 Airflow Supply System for ACd and Laser Velocimetry Testing.

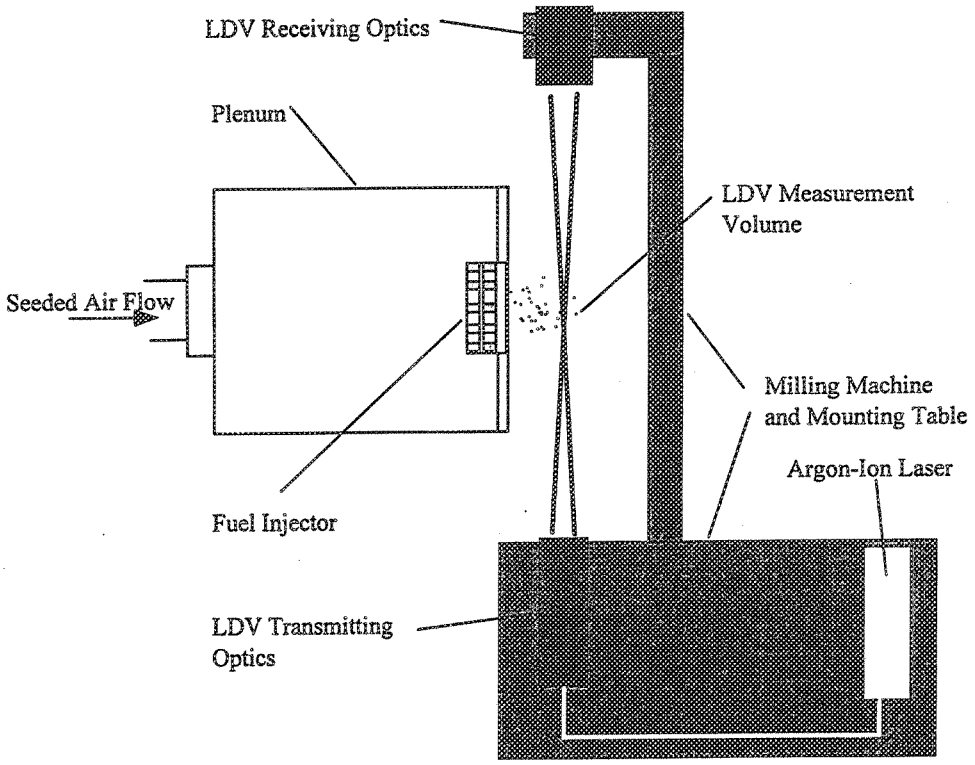

Figure IV-2 Schematic of Laser Velocimetry System.

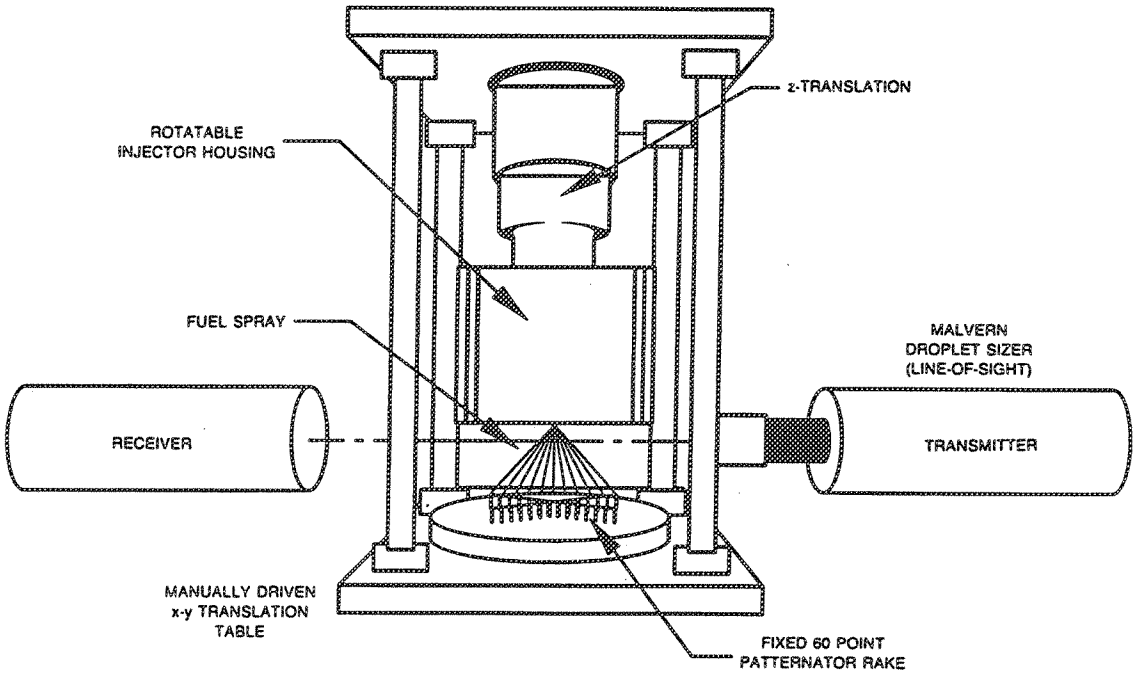

Figure IV-3 High Resolution Ambient Spray Patternator.

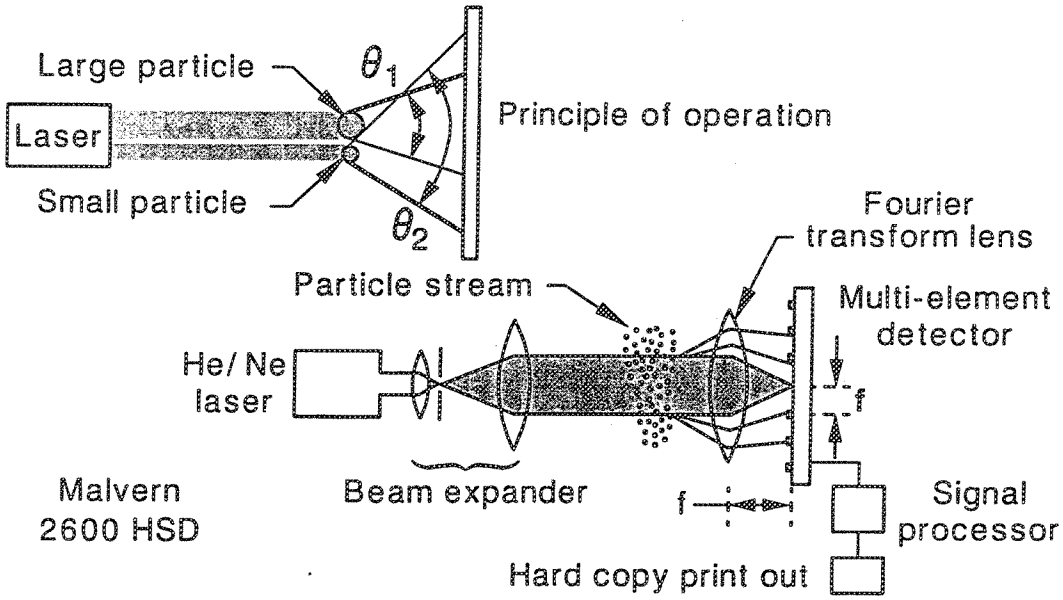

Figure IV-4 Schematic Diagram of the Malvern Particle Size Analyzer.

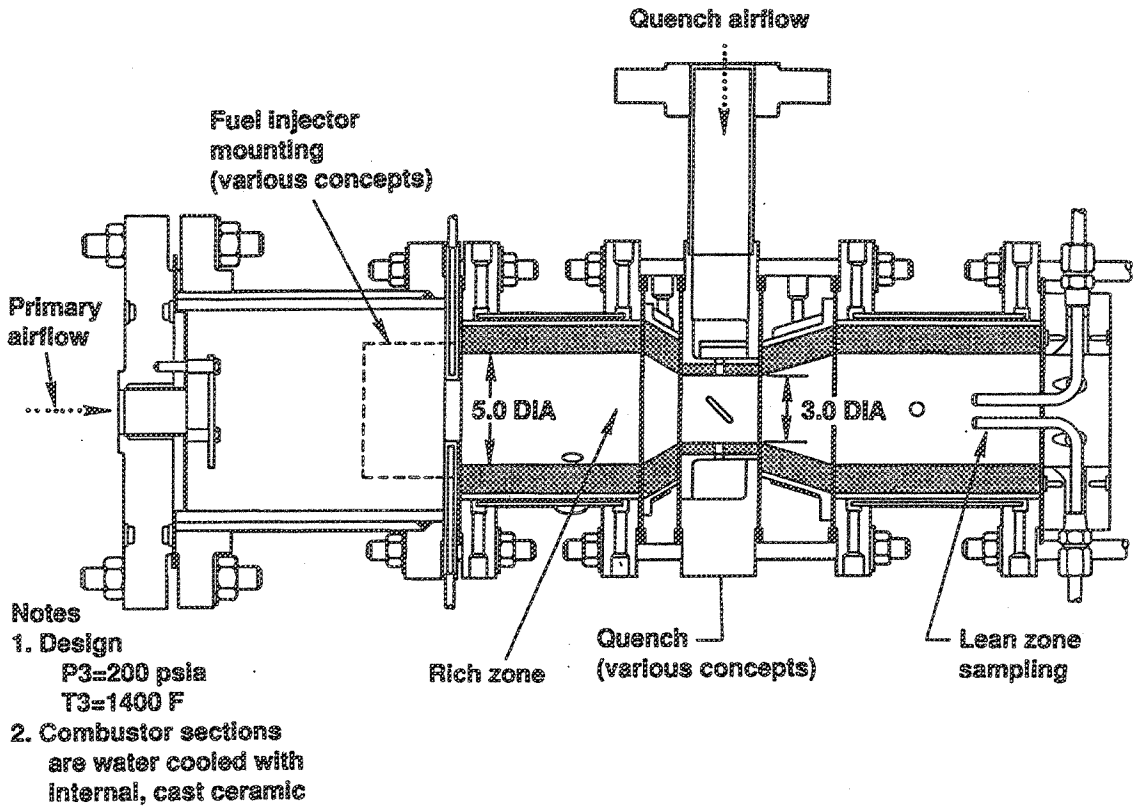

Figure IV-5 Cylindrical RQL Combustor Rig.

SECTION V FIGURES

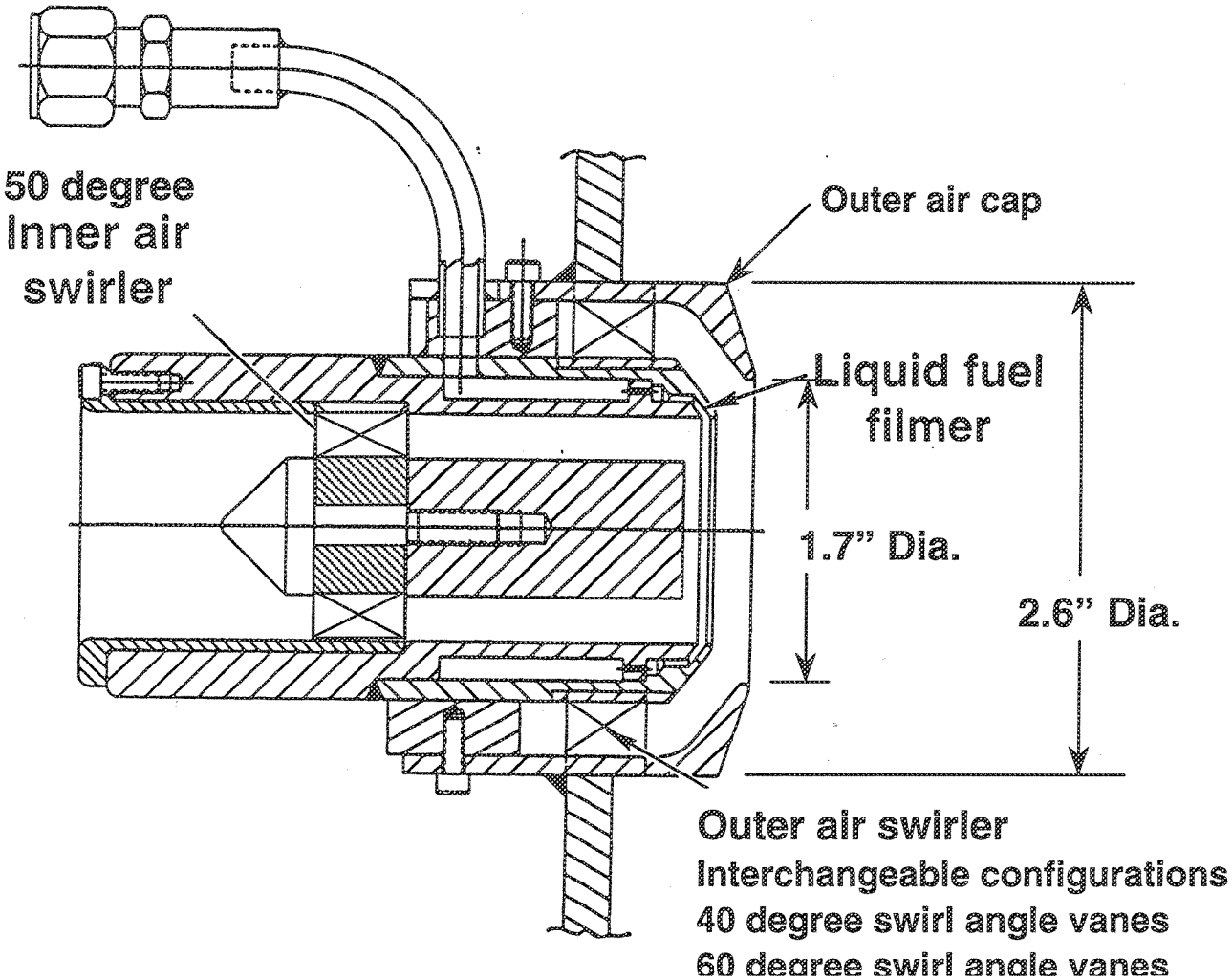

Figure V-1 Baseline Two Passage Aerating Fuel Injector Design.

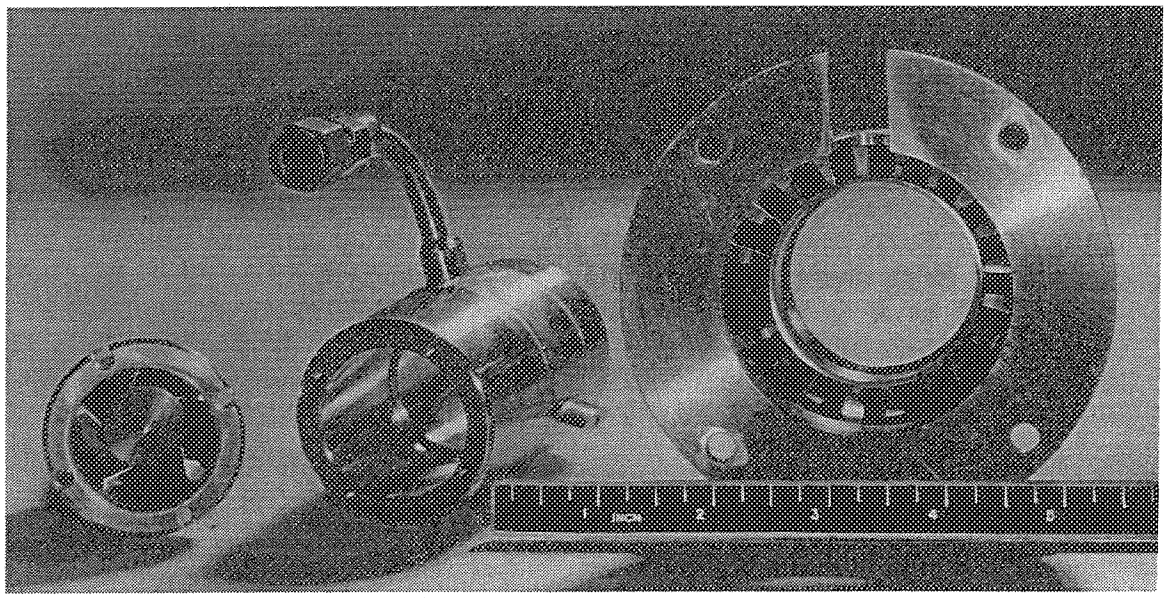

Figure V-2 Baseline Two Passage Aerating Fuel Injector Components.

Figure V-3 Baseline Two Passage Aerating Fuel Injector Assembly Used in Combustion Tests.

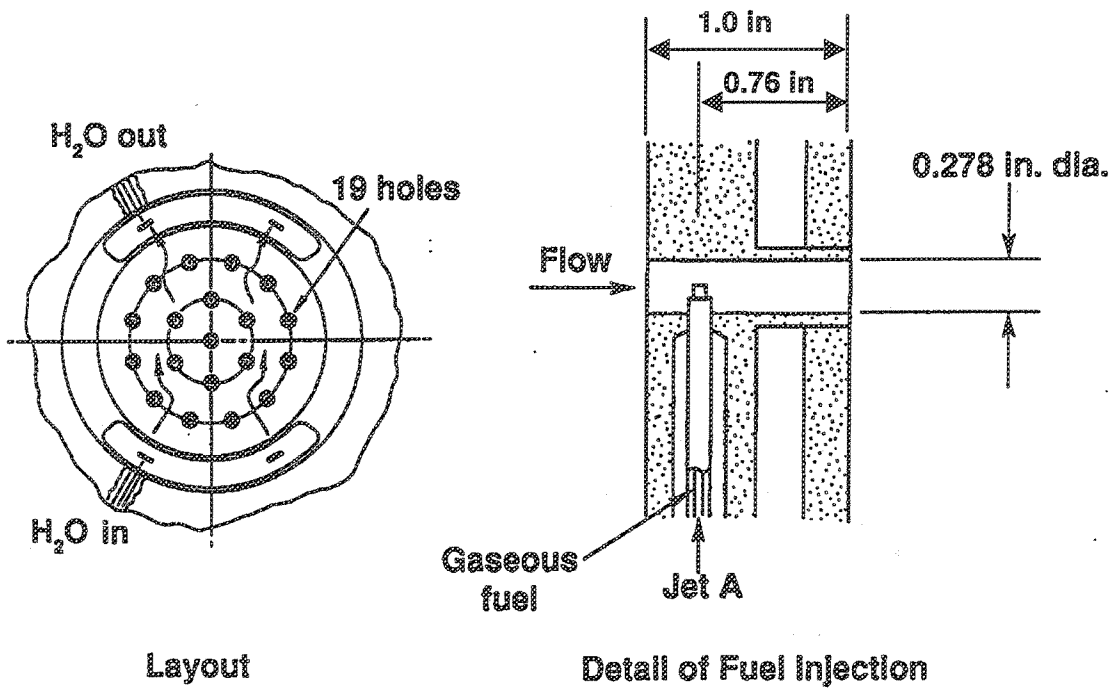

Figure V-4 Pre-Mixed Multi-Source Fuel Injector Design.

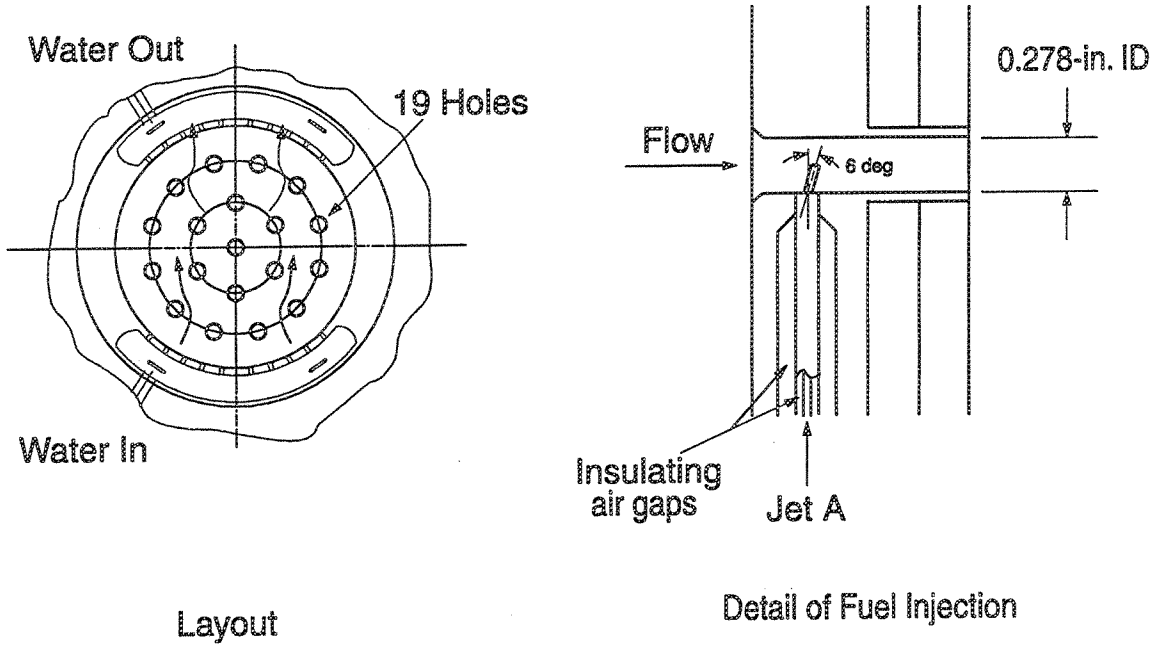

Figure V-5 Modified Pre-Mixed Multi-Source Fuel Injector Design for Enhanced Fuel Dispersion.

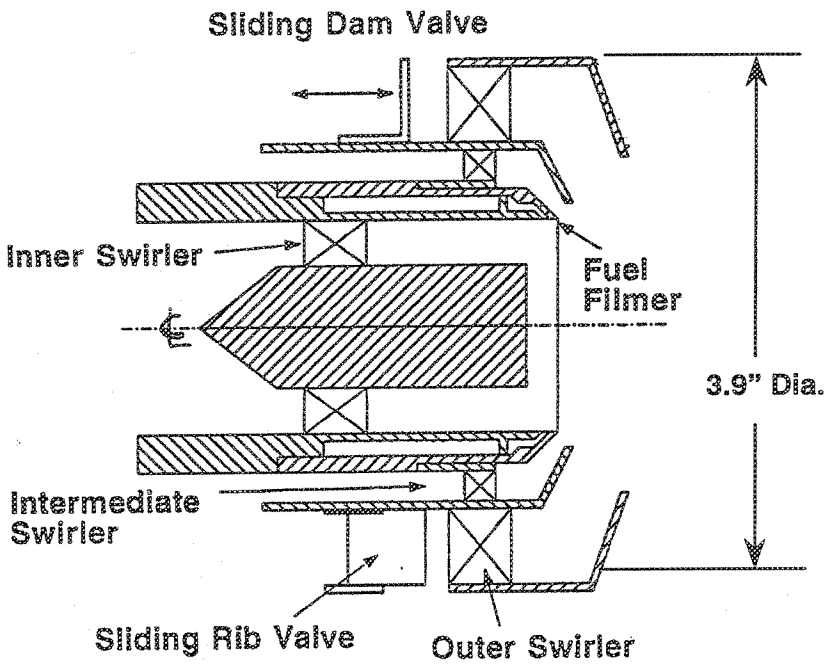

Figure V-6 Tri-Swirler Variable Geometry Fuel Injector Design.
Top Half: Sliding Dam Valve Approach
Bottom Half: Sliding Rib Valve Approach

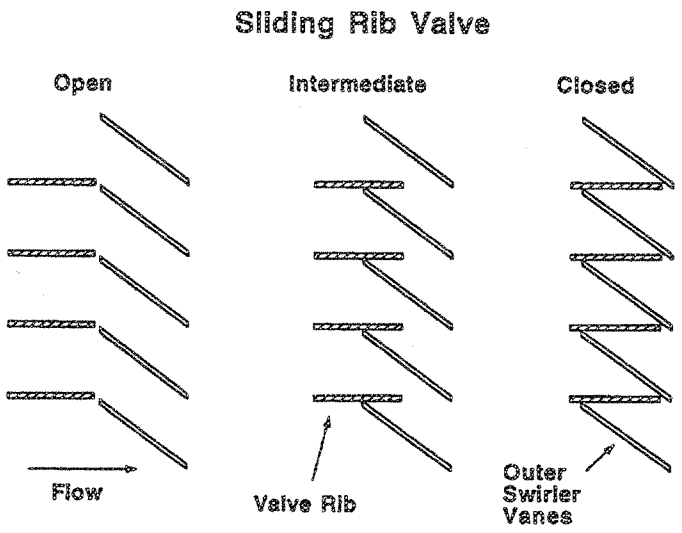

Figure V-7 Tri-Swirler Variable Geometry Fuel Injector Sliding Rib Valve Positioning for Airflow Modulation.

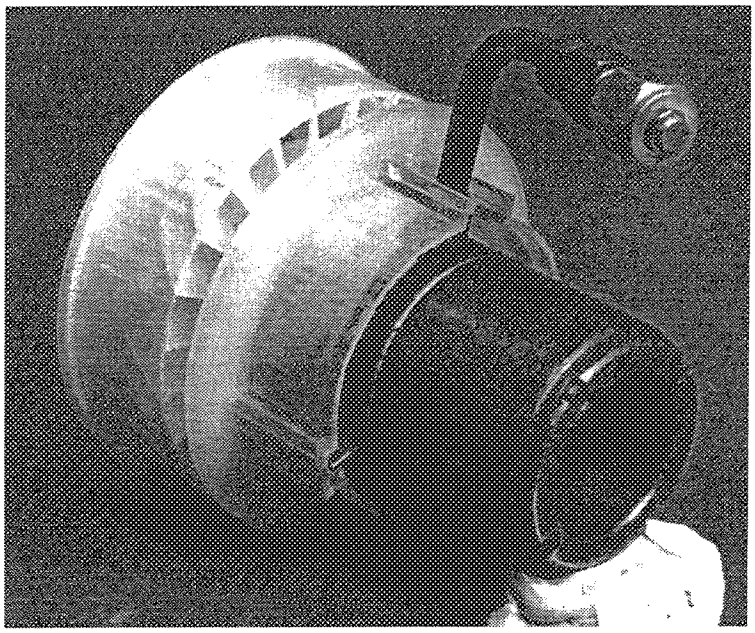

Figure V-8 Tri-Swirler Injector Used for Non-Reacting Tests; Combining Metal centerbody Inner Swirler & Fuel Filmer with SLA Intermediate & Outer Swirler with Sliding Dam Valve. Forward Looking Aft Trimetric View.

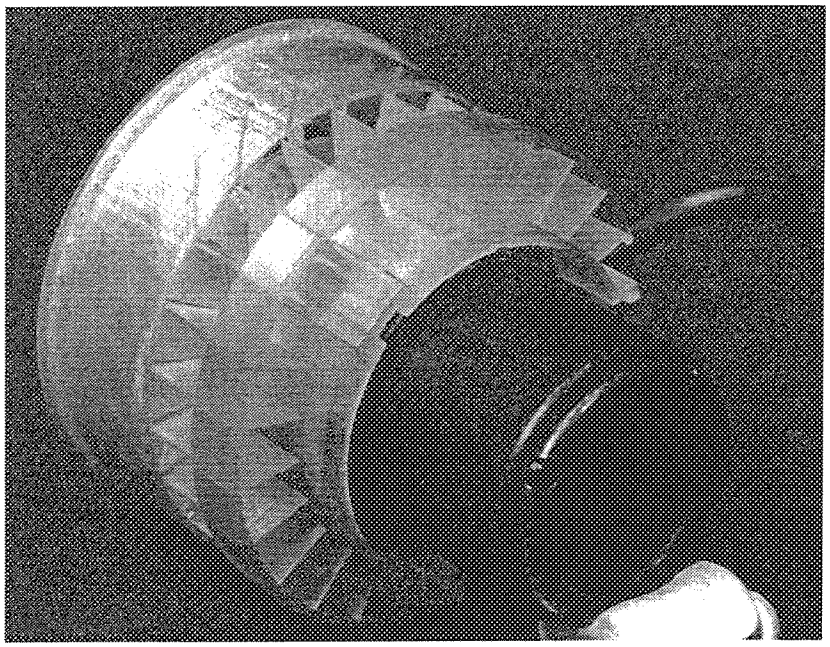

Figure V-9 Tri-Swirler Injector Used for Non-Reacting Tests; Combining Metal centerbody Inner Swirler & Fuel Filmer with SLA Intermediate & Outer Swirler with Sliding Rib Valve. Forward Looking Aft Trimetric View.

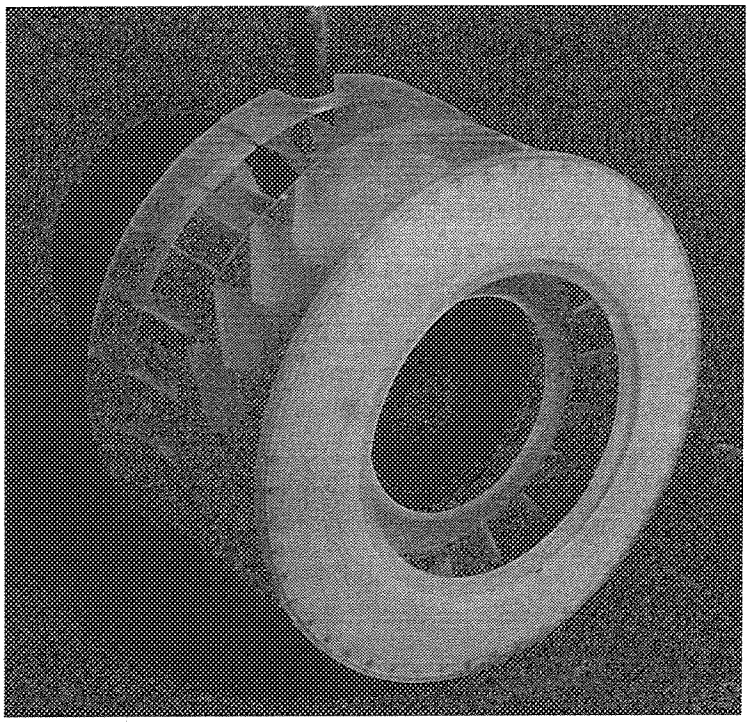

Figure V-10 Tri-Swirler Injector Used for Non-Reacting Tests; Combining Metal centerbody Inner Swirler & Fuel Filmer with SLA Intermediate & Outer Swirler with Sliding Rib Valve. Aft Looking Forward Trimetric View.

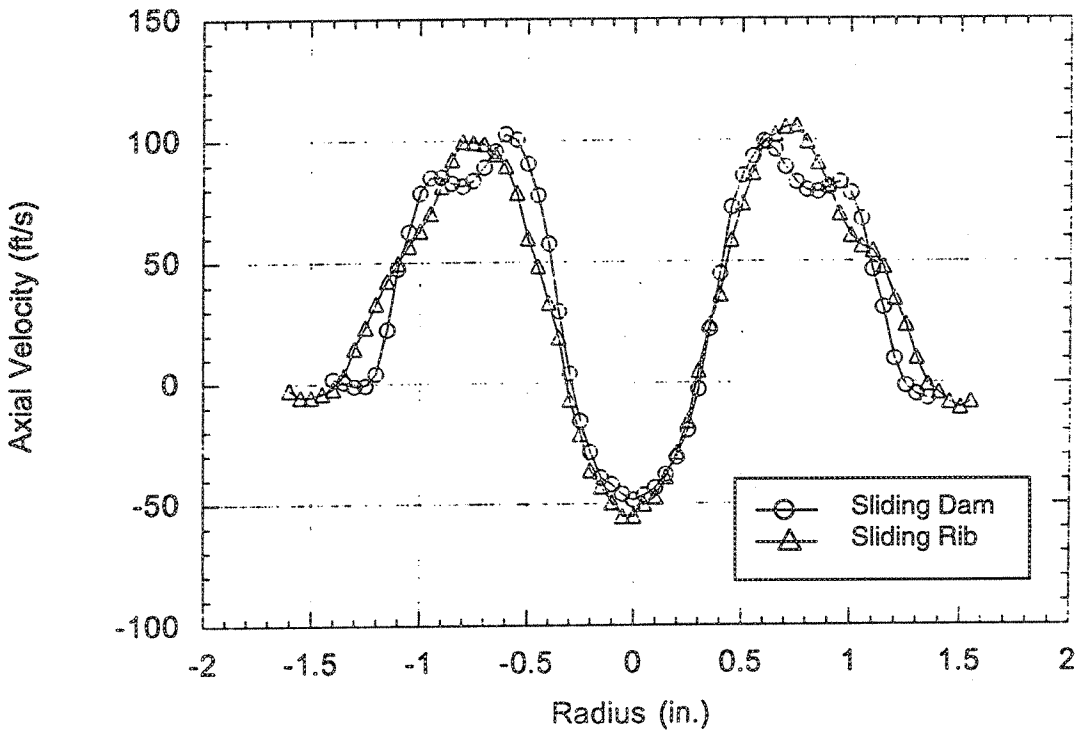

Figure V-11 Effect of Valve Type on Axial Velocity Profile from Tri-Swirler Injector. (ACd = 1.4 in^2; Measurements Taken 0.25 in Axially Downstream From Injector Face)

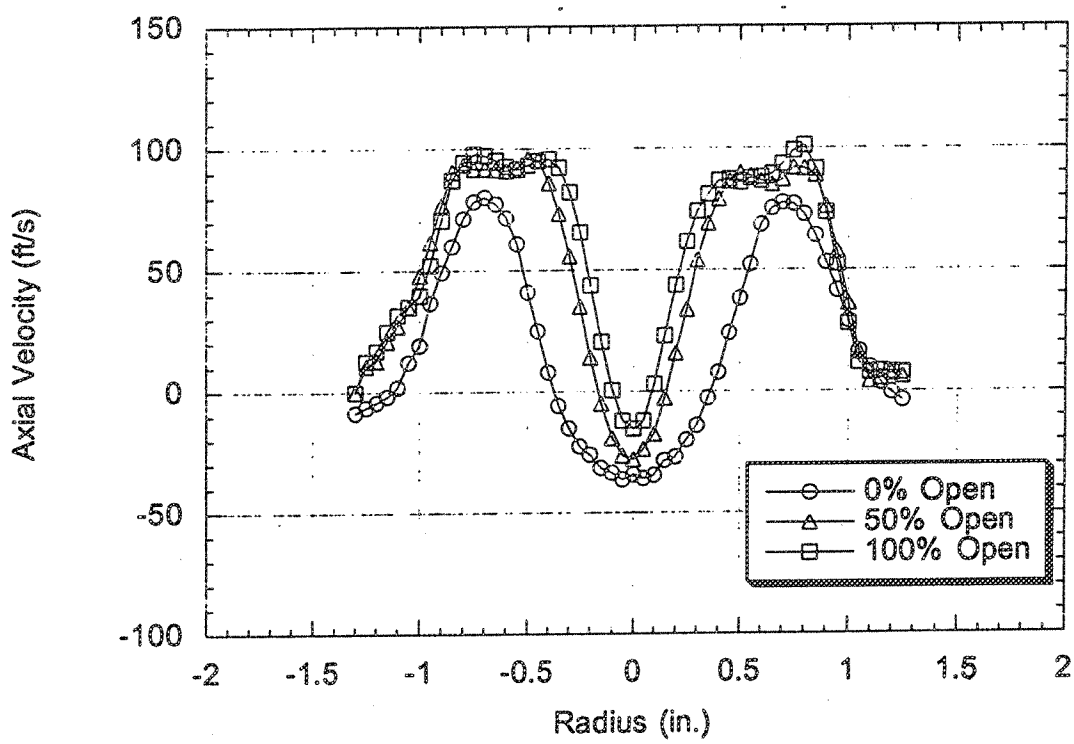

Figure V-12 Effect of Flow Area Variation on Axial Velocity Profile for the Tri-Swirler Injector with Sliding Dam Valve. Measurements Taken 0.25 in. Axially Downstream from Injector Face

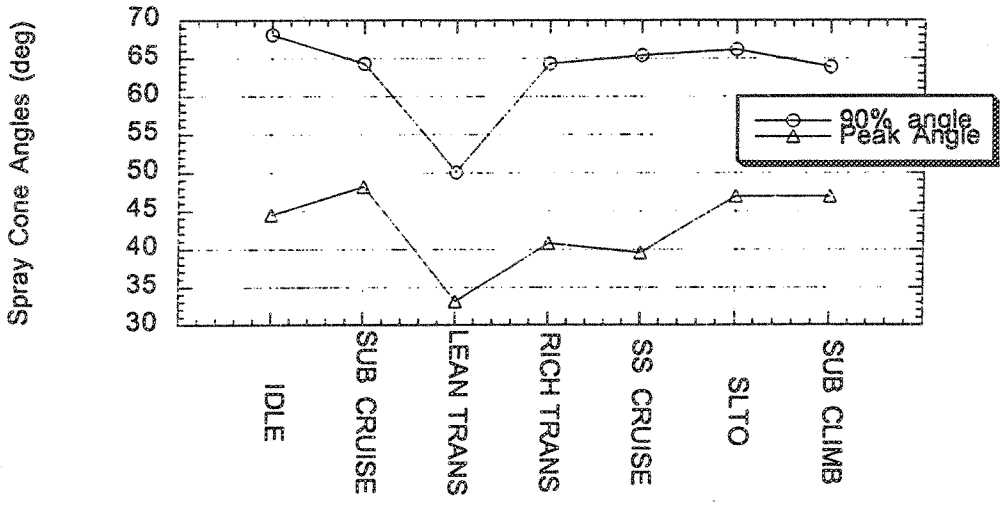

Figure V-13 Tri-Swirler Injector with Sliding Dam Valve Spray Cone Angle Dependency on Flight Condition.

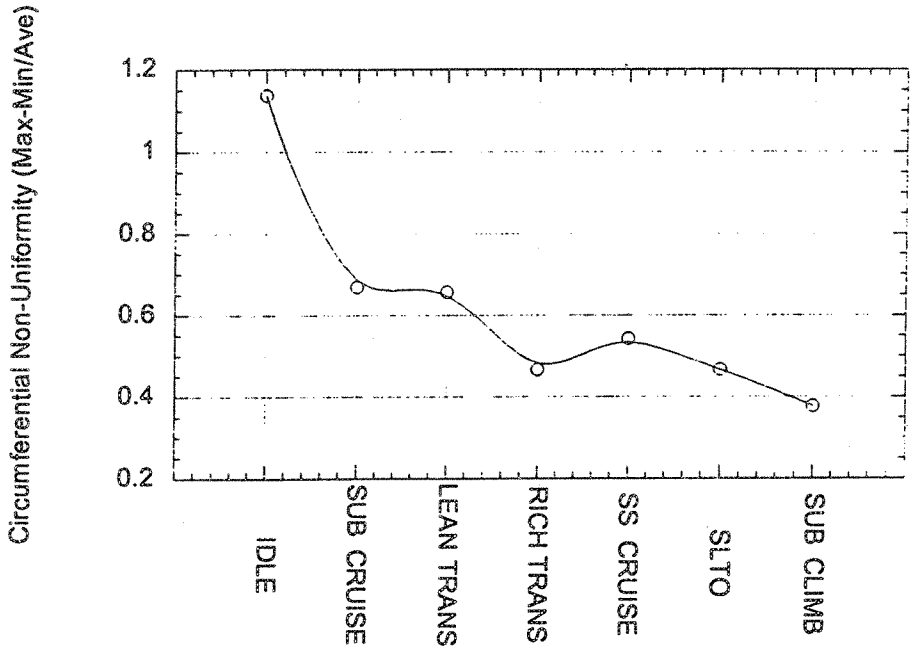

Figure V-14 Circumferential Spray Uniformity of Tri-Swirler Injector with Sliding Dam Valve as a Function of Flight Condition. 45-Degree Sector Analysis of Fuel Mass Flux.

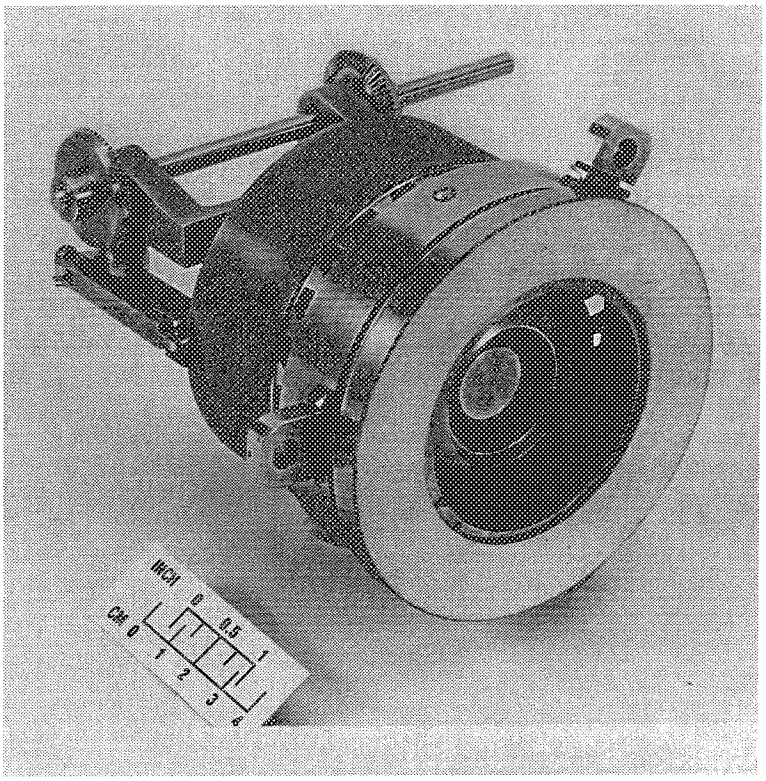

Figure V-15 Externally Controllable Tri-Swirler Injector with Sliding Rib Valve Used in Cylindrical RQL Combustor Rig Tests.

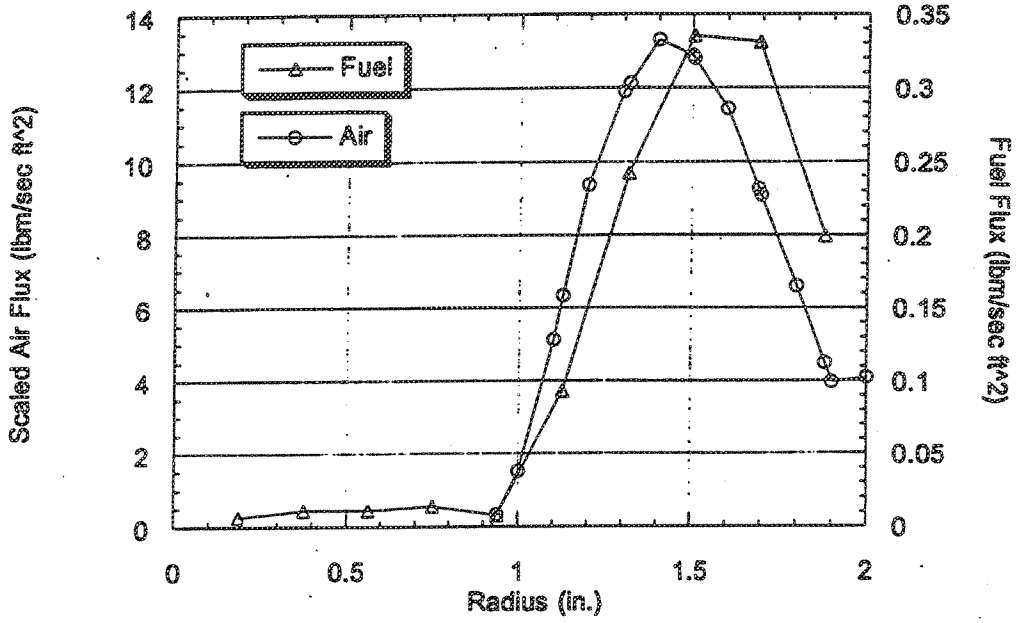

Figure V-16 Fuel and Air Flux Profiles from Tri-Swirler Injector for the Combustor Rig. Subsonic Cruise Condition Simulation. Measurements Taken 1.5 in. Axially Downstream from Injector Face.

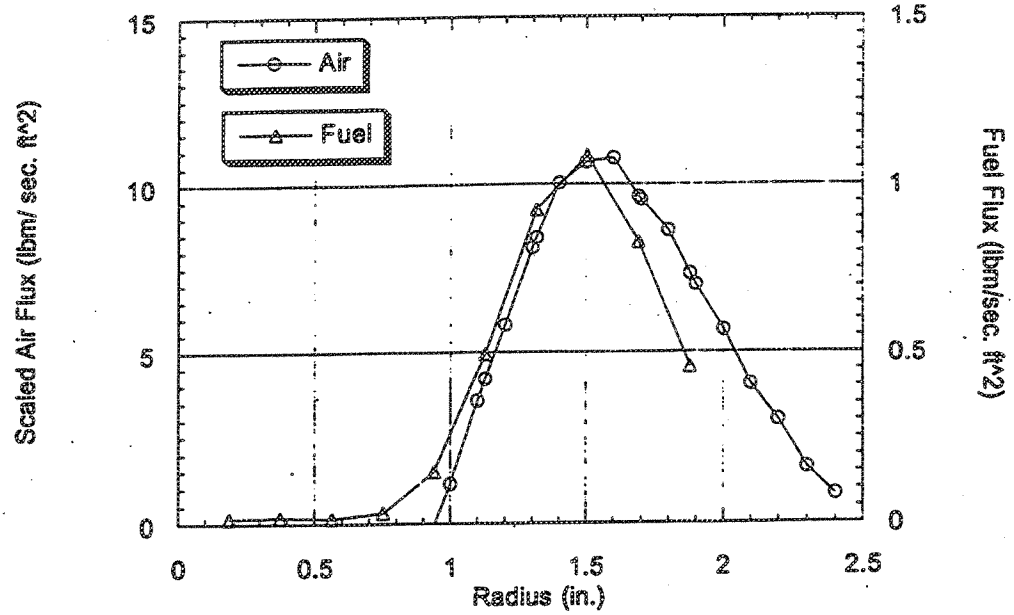

Figure V-17 Fuel and Air Flux Profiles from Tri-Swirler Injector for the Combustor Rig. Supersonic Cruise Condition Simulation. Measurements Taken 1.5 in. Axially Downstream from Injector Face.

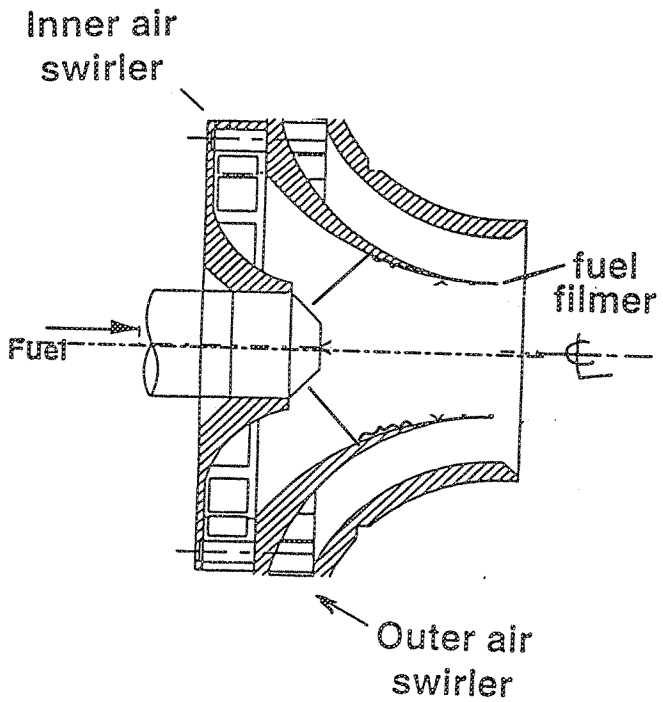

Figure V-18 Radial Inflow Swirler/Fuel Injector Concept.

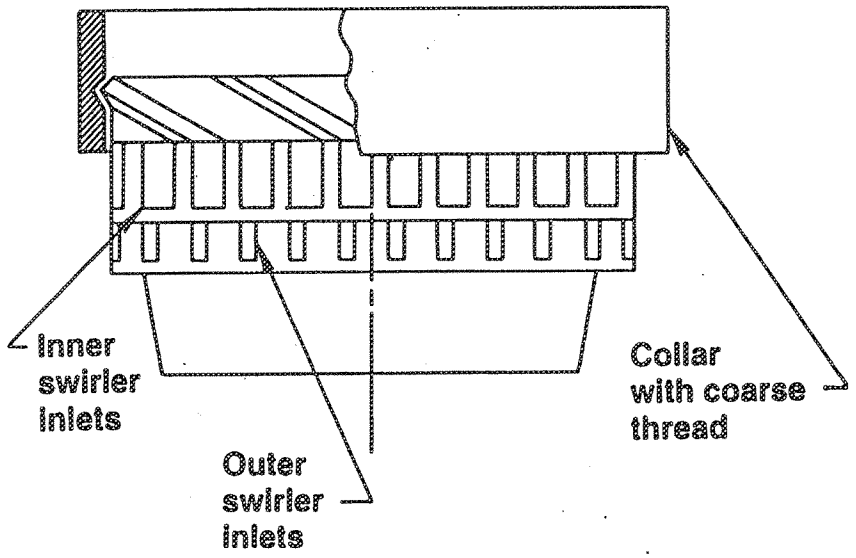

Figure V-19 Variable Airflow Configuration of Radial Inflow Swirler Design. Inner Air Passage Modulation Only.

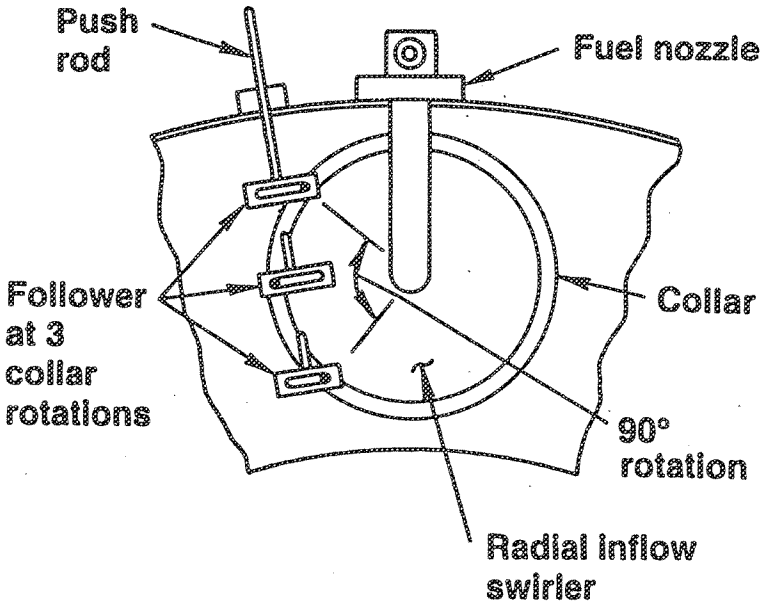

Figure V-20 Actuation Mechanism for Variable Geometry Radial Inflow Swirler.

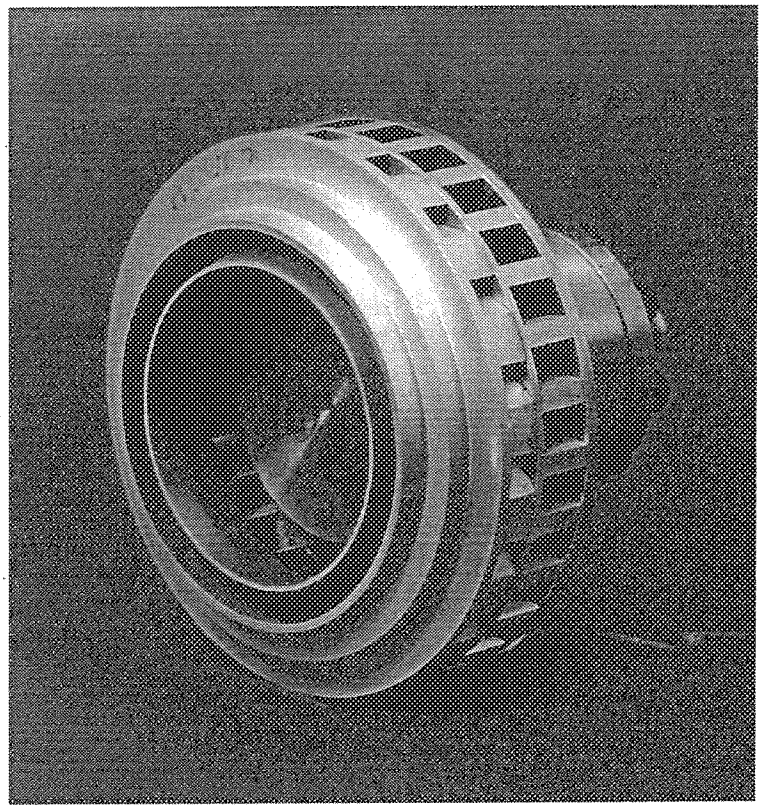

Figure V-21 Aluminum Radial Inflow Swirler Used in Cold Flow Calibration Tests. Sliding Collar Removed for Clarity

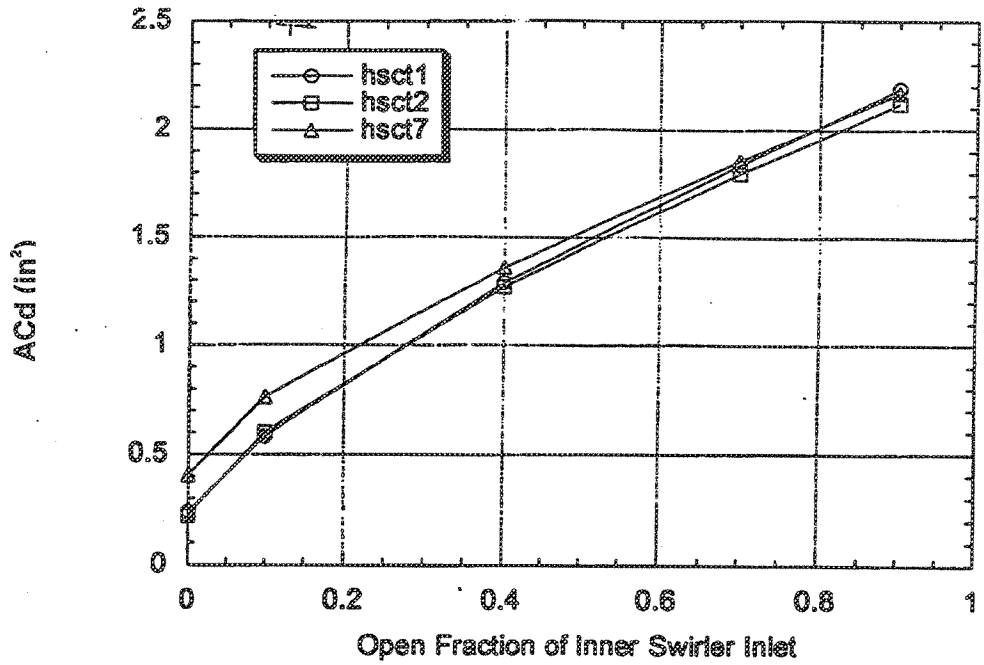

Figure V-22 Effective Flow Area Throttling of Radial Inflow Swirlers.

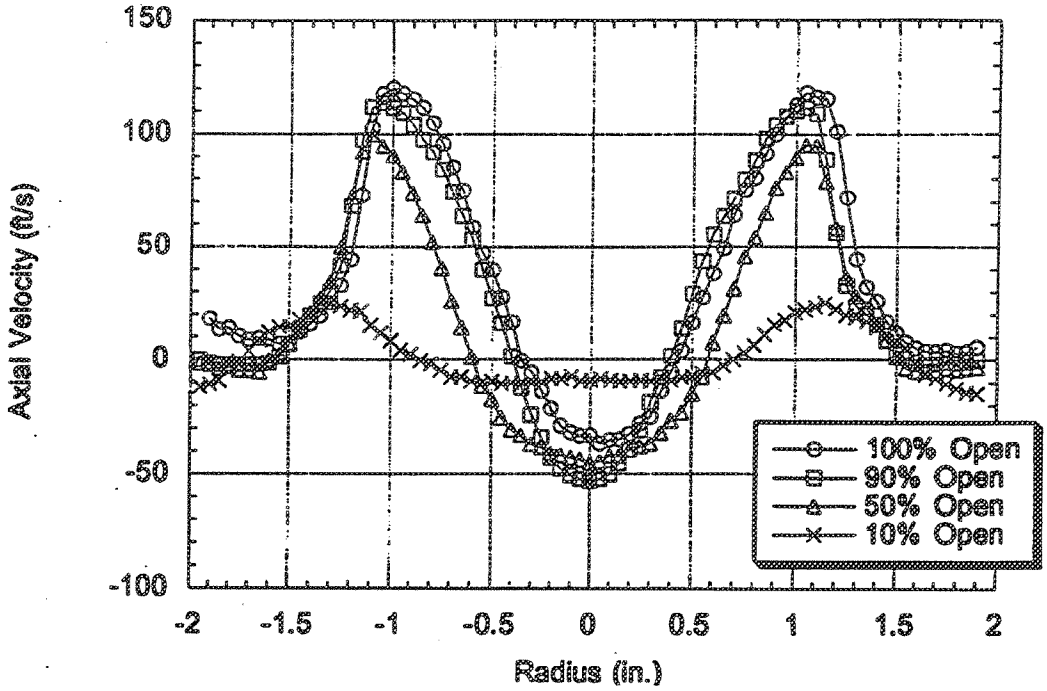

Figure V-23 Effect of Flow Area Variation on Axial Velocity Profile for the Radial Inflow Swirler (HSCT2). Measurements Taken 0.25 in. Axially Downstream from Injector Face.

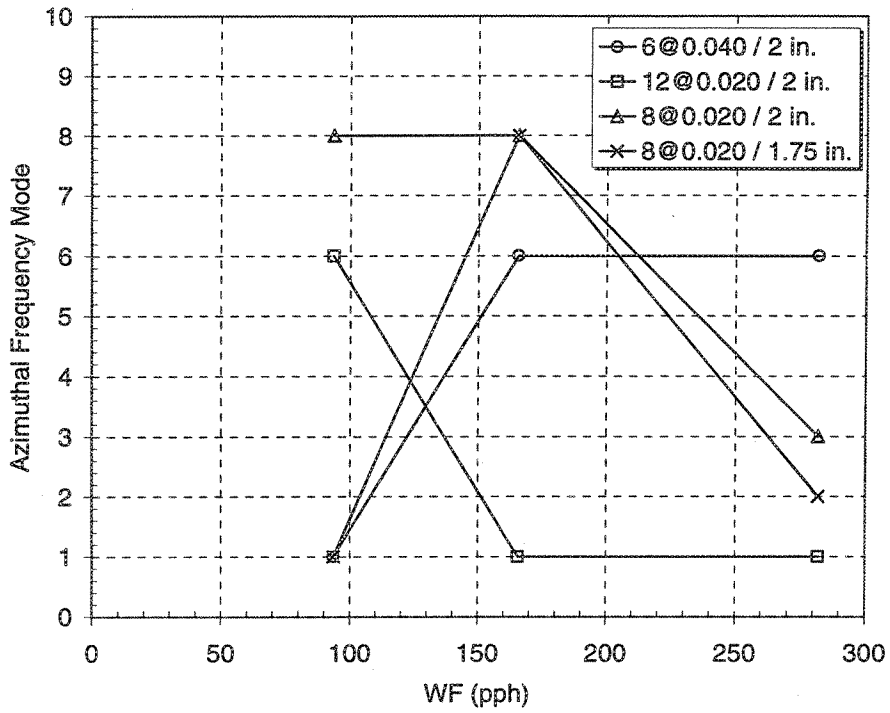

Figure V-24 Comparison of Azimuthal Spray Distribution for Various Fuel Injectors Installed in the Radial Inflow Swirler (HSCT1).

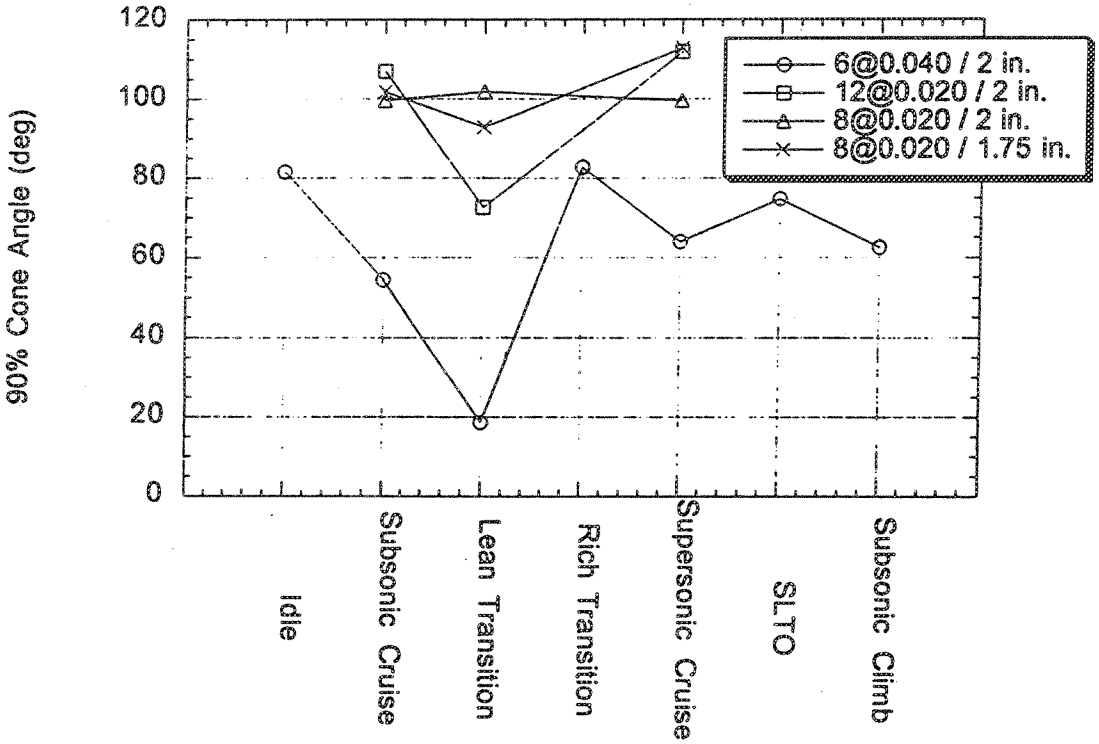

Figure V-25 90% Spray Cone Angle Variations as a Function of Flight Condition for Various Fuel Injectors Installed in the Radial Inflow Swirler (HSCT1).

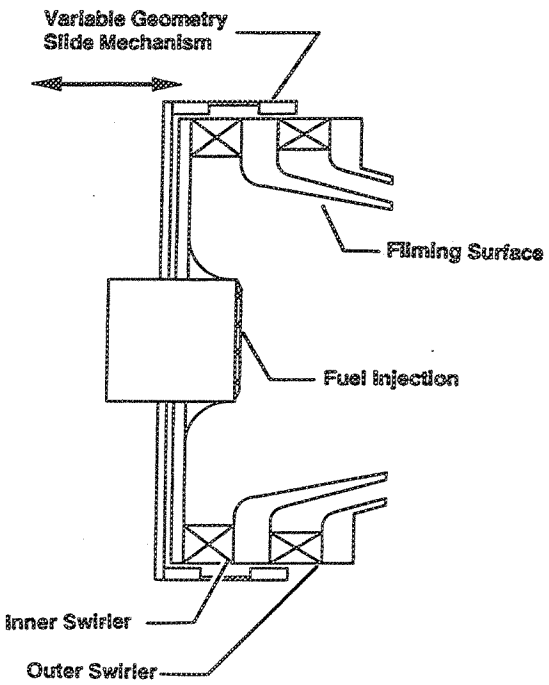

Figure V-26 Radial Inflow Swirler/Fuel Injector with Variable Airflow in Both Swirler Passages.

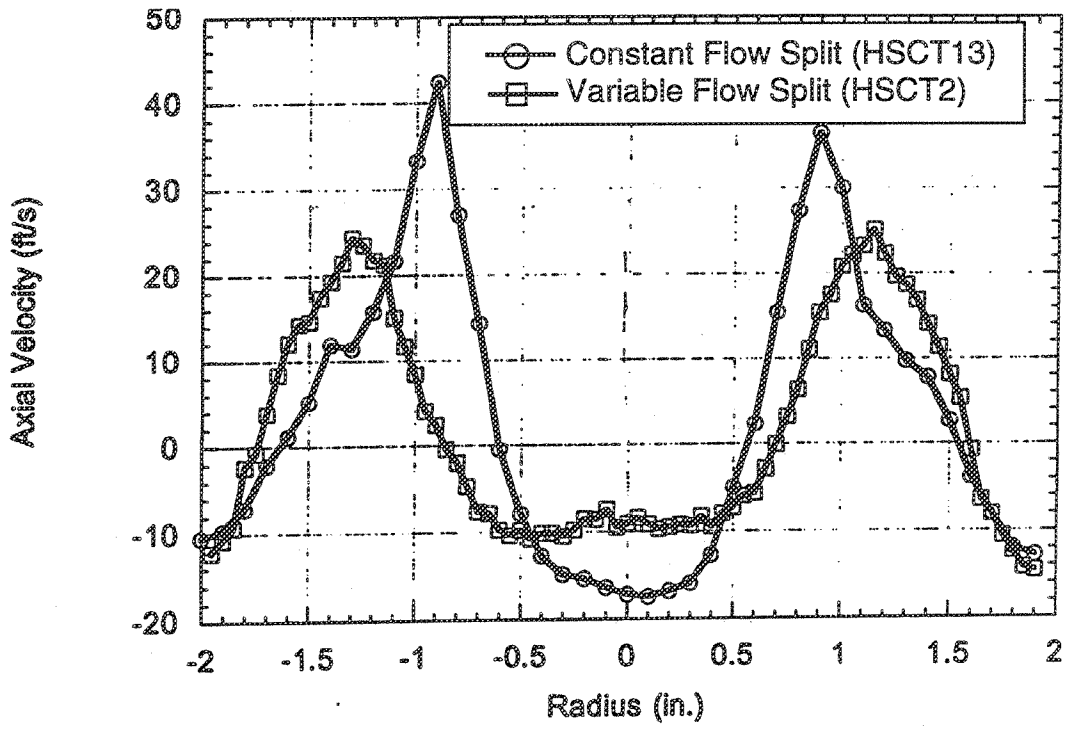

Figure V-27 Comparison of Axial Velocity Profiles for Radial Inflow Swirlers with Different Variable Airflow Management Approaches at Low ACd Setting, 10% Open.

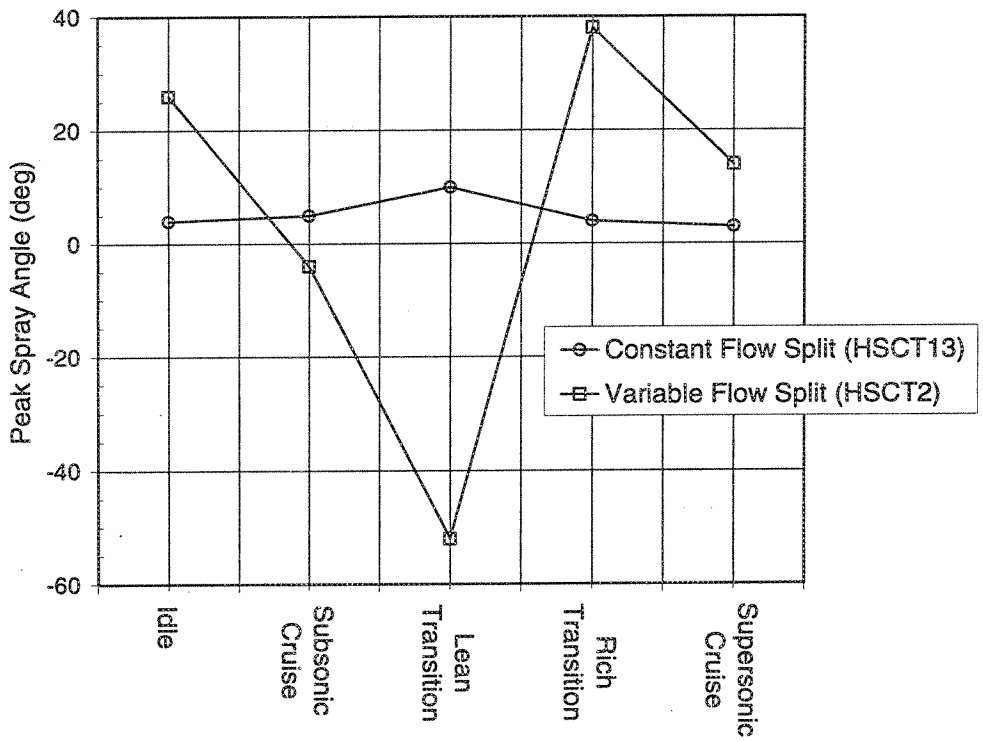

Figure V-28 Comparison of Peak Spray Angle as a Function of Flight Condition for Radial Inflow Swirlers with Different Variable Airflow Management Approaches.

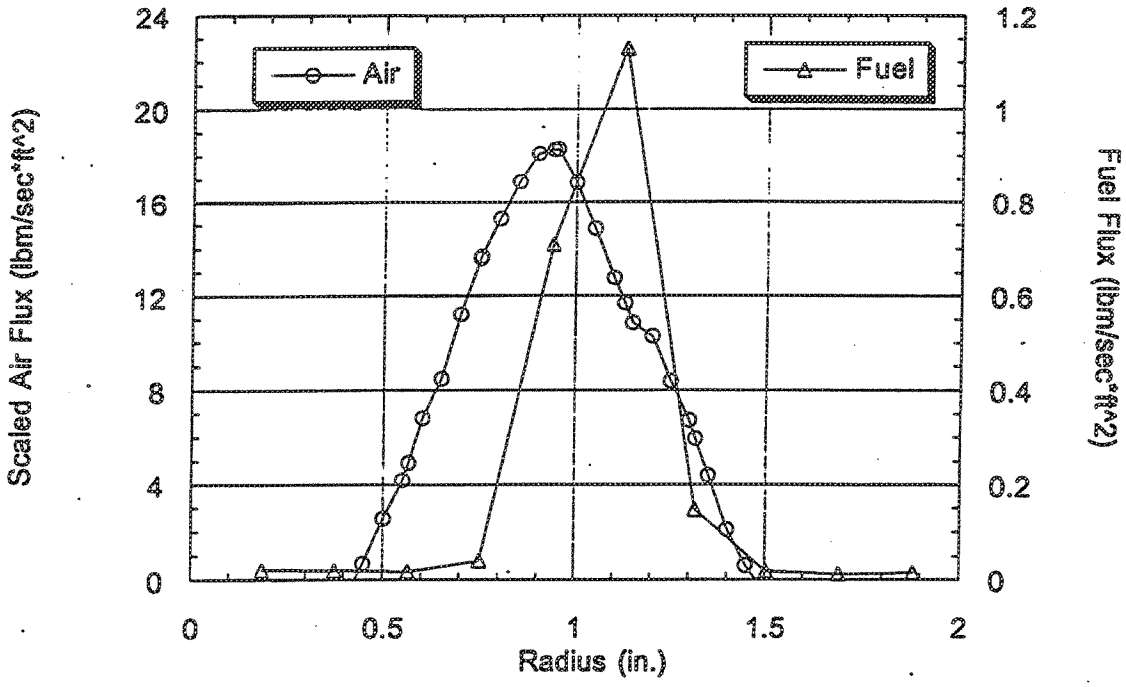

Figure V-29 Fuel and Air Flux Profiles from Radial Inflow Swirler (HSCT16) Injector for the Combustor Rig. Subsonic Cruise Condition Simulation. Measurements Taken 0.5 in. Axially Downstream from Injector Face.

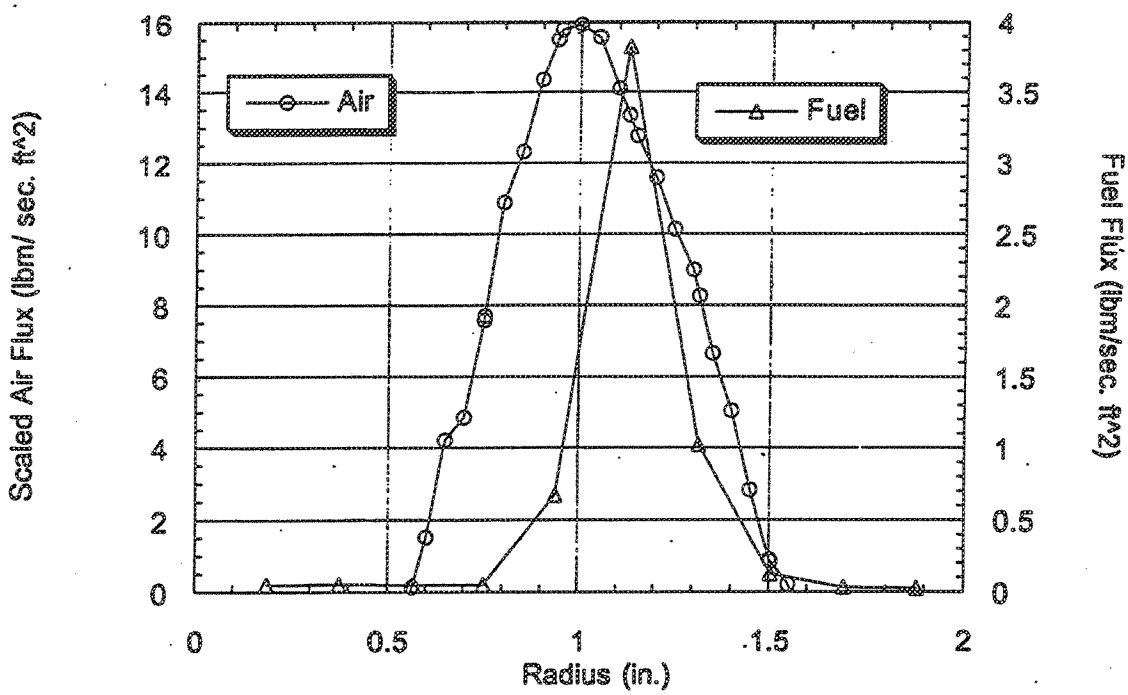

Figure V-30 Fuel and Air Flux Profiles from Radial Inflow Swirler (HSCT16) Injector for the Combustor Rig. Supersonic Cruise Condition Simulation. Measurements Taken 0.5 in. Axially Downstream from Injector Face.

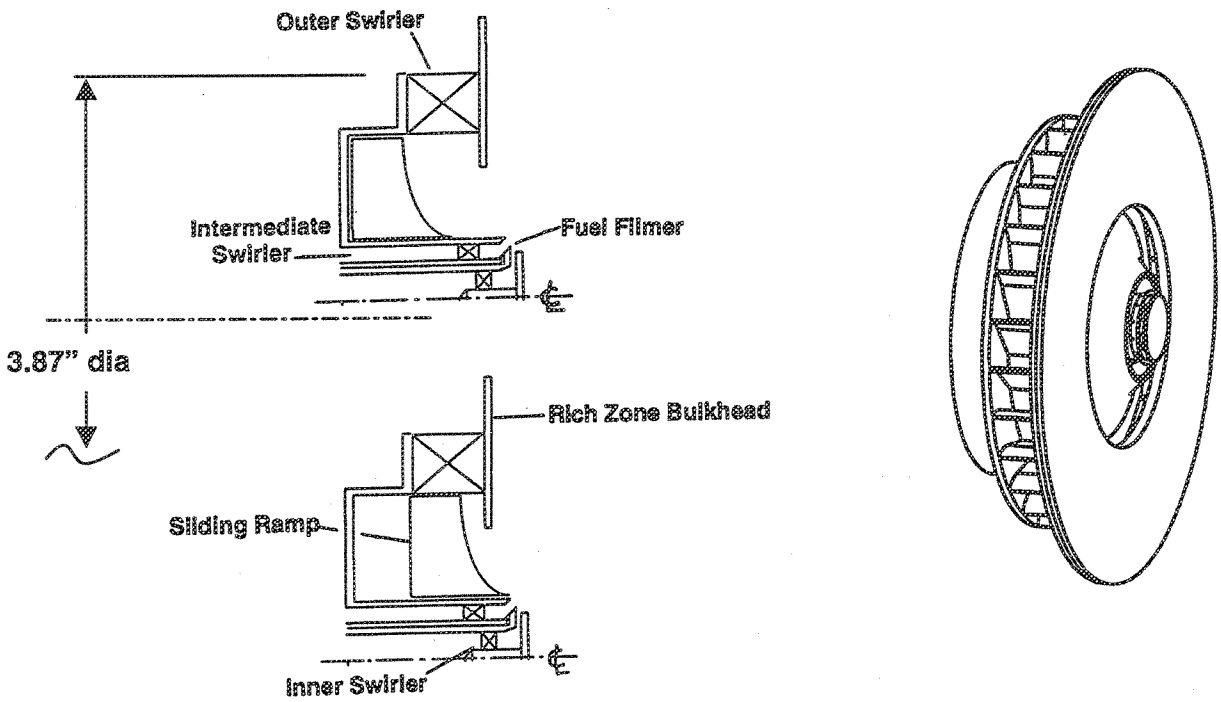

Figure V-31 Translating Ramp Variable Geometry Fuel Injector Design.
Top: Ramp in High Flow Position; Bottom: Ramp in Low Flow Position

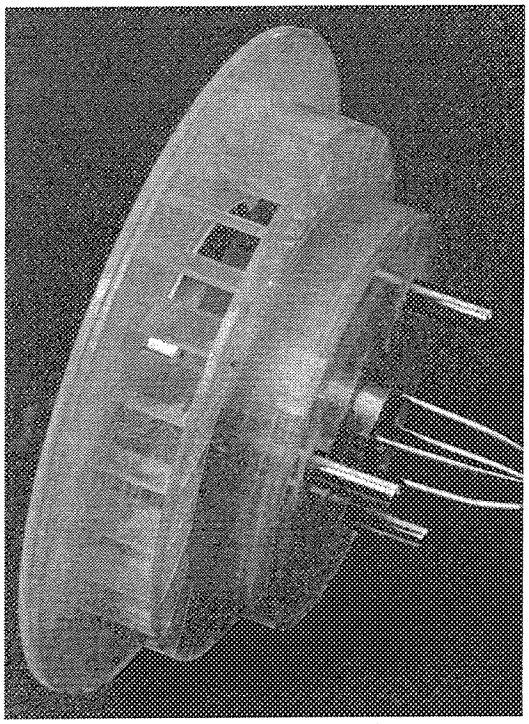

Figure V-32 Translating Ramp Injector Used for Non-Reacting Tests; Combining Metal Fuel Filmer with SLA Outer Swirler. Forward Looking Aft Trimetric View.

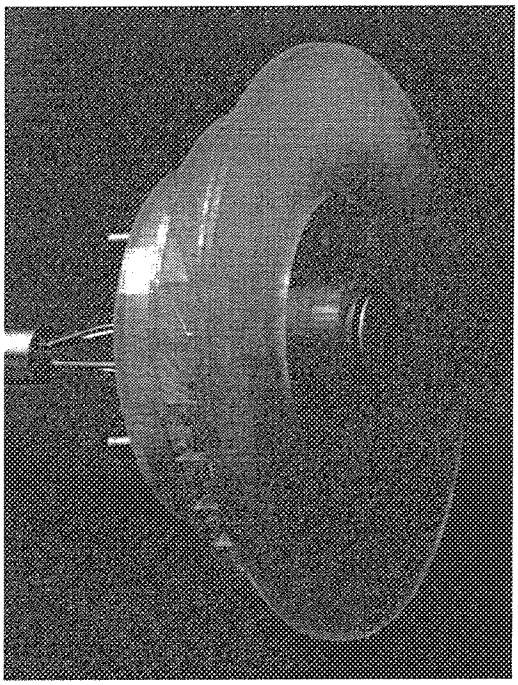

Figure V-33 Translating Ramp Injector Used for Non-Reacting Tests; Combining Metal Fuel Filmer with SLA Outer Swirler. Aft Looking Forward Trimetric View.

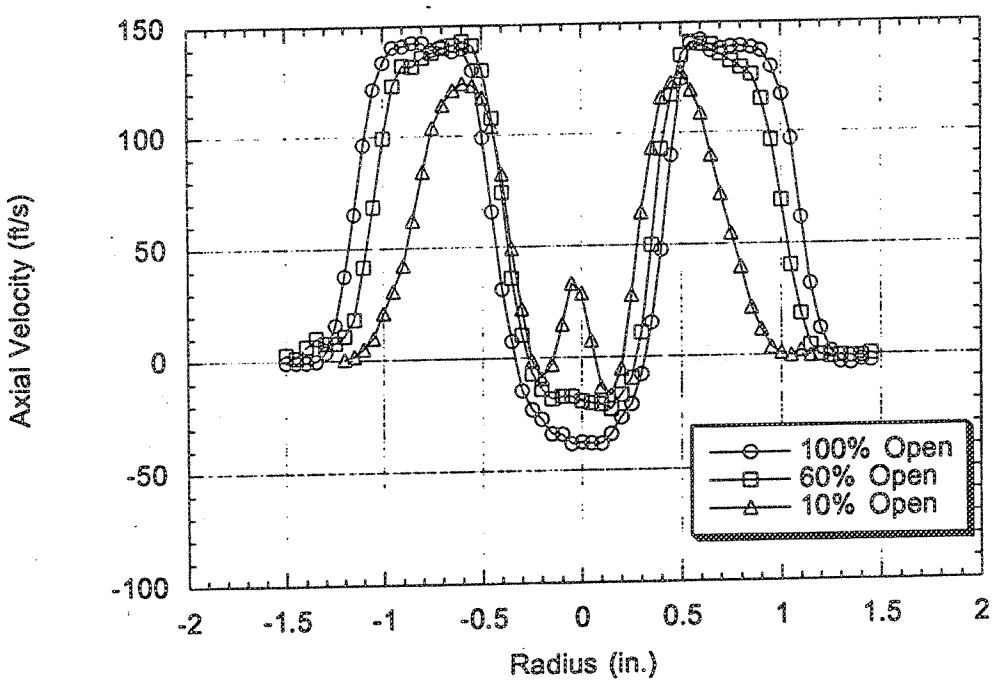

Figure V-34 Effect of Flow Area Variation on Axial Velocity Profile for the Translating Ramp Injector. Measurements Taken 0.3 in. Axially Downstream from Injector Face.

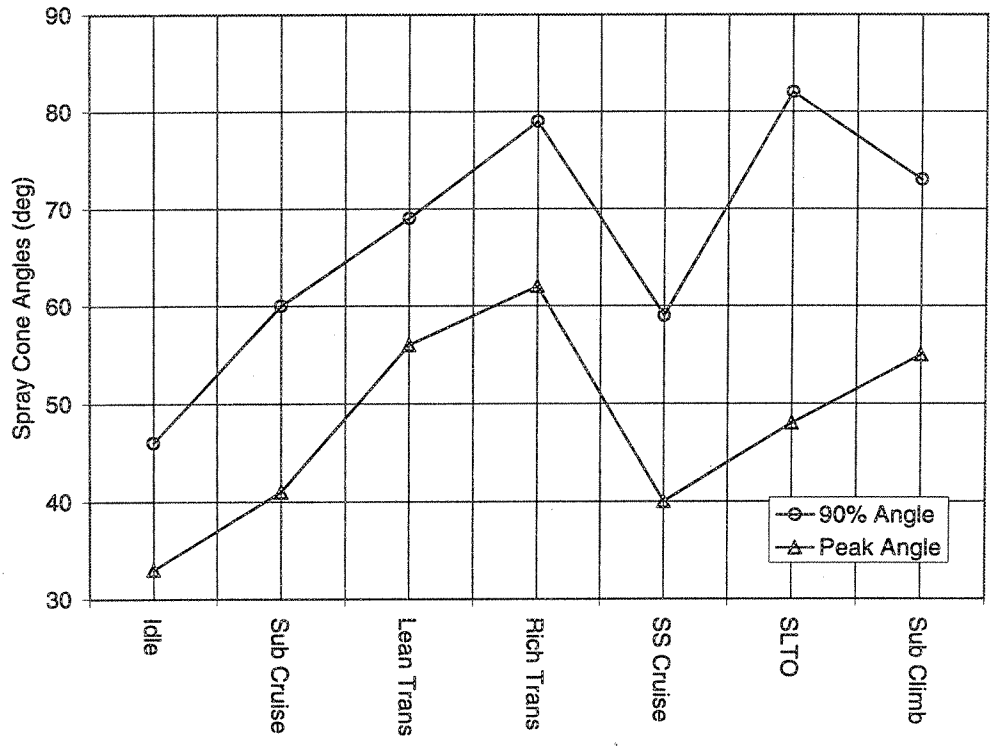

Figure V-35 Translating Ramp Injector Spray Cone Angle Dependency on Flight Condition.

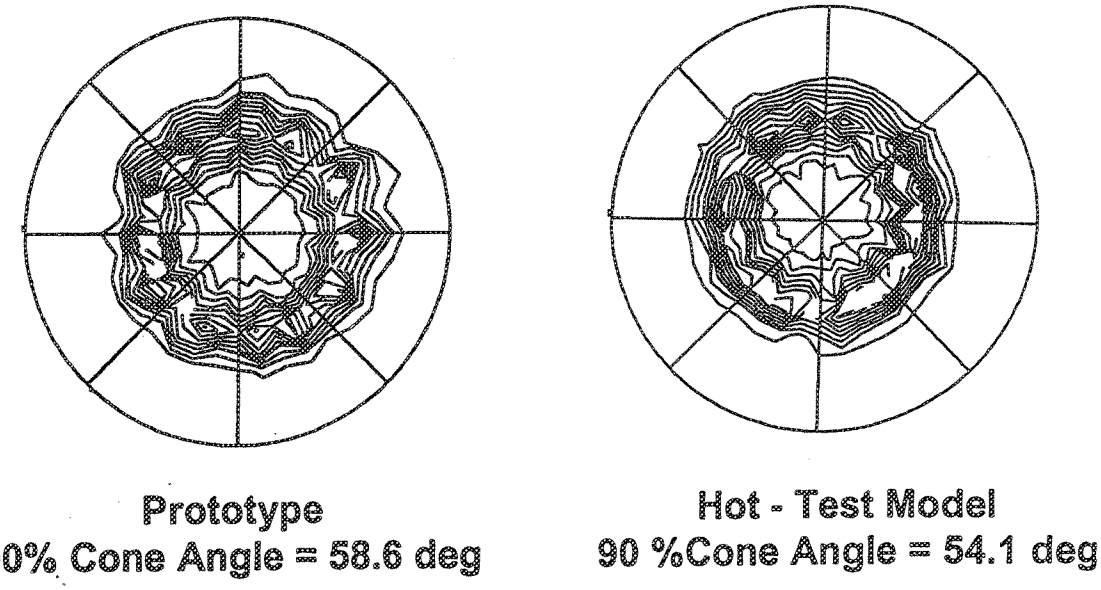

Figure V-36 Comparison of Prototype and Hot-Test Model Spray Distribution for the Translating Ramp Injector. Supersonic Cruise Simulation.

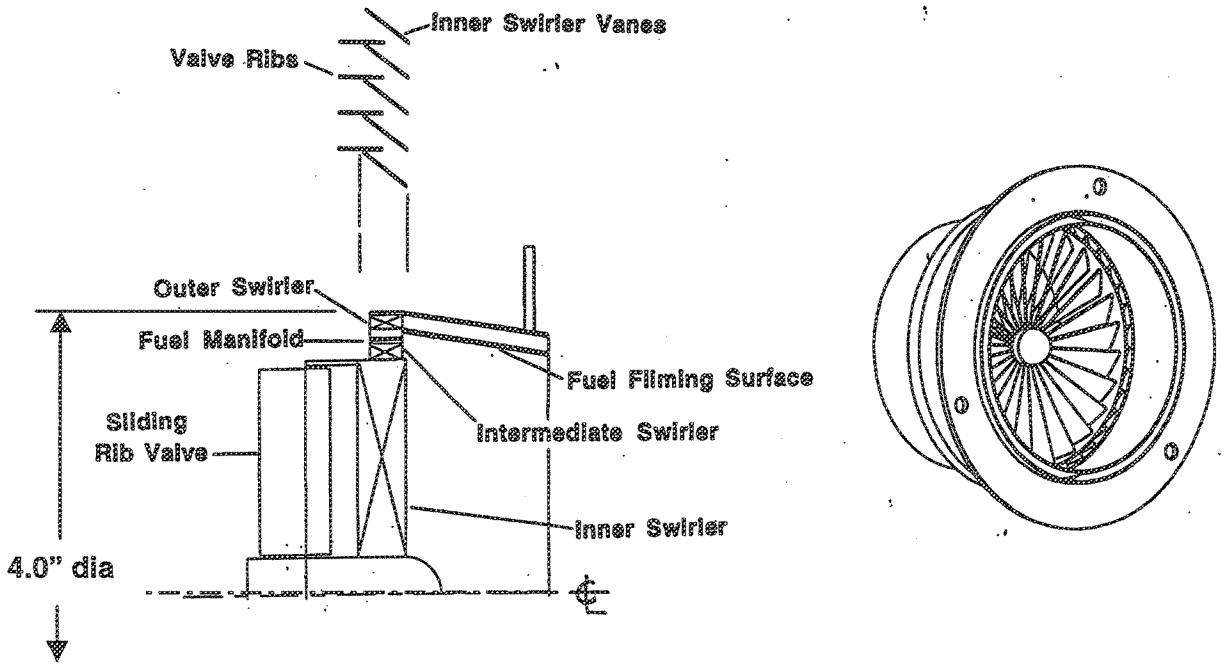

Figure V-37 Axial Flow High Shear Variable Geometry Injector Concept.

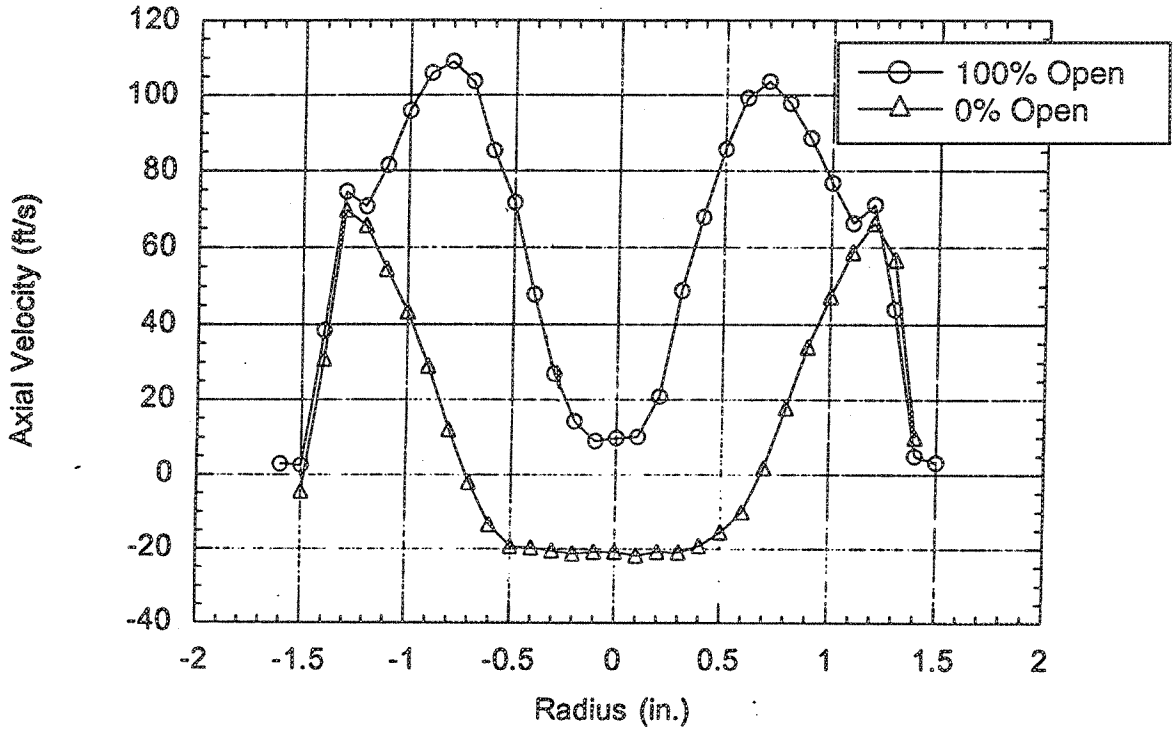

Figure V-38 Effect of Flow Area Variation on Axial Velocity Profile for the Axial Flow High Shear Injector.

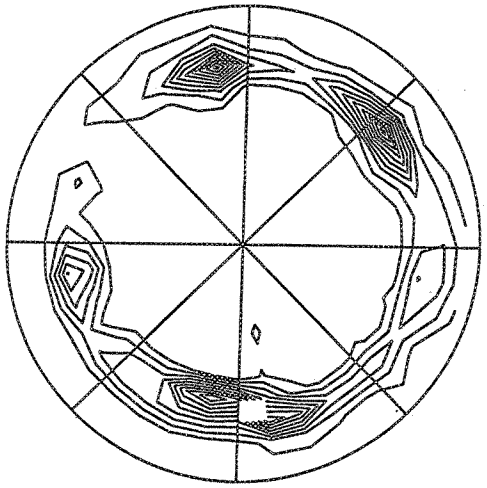

Figure V-39 Spray Distribution for the Axial Flow High Shear Injector. Subsonic Cruise Simulation.

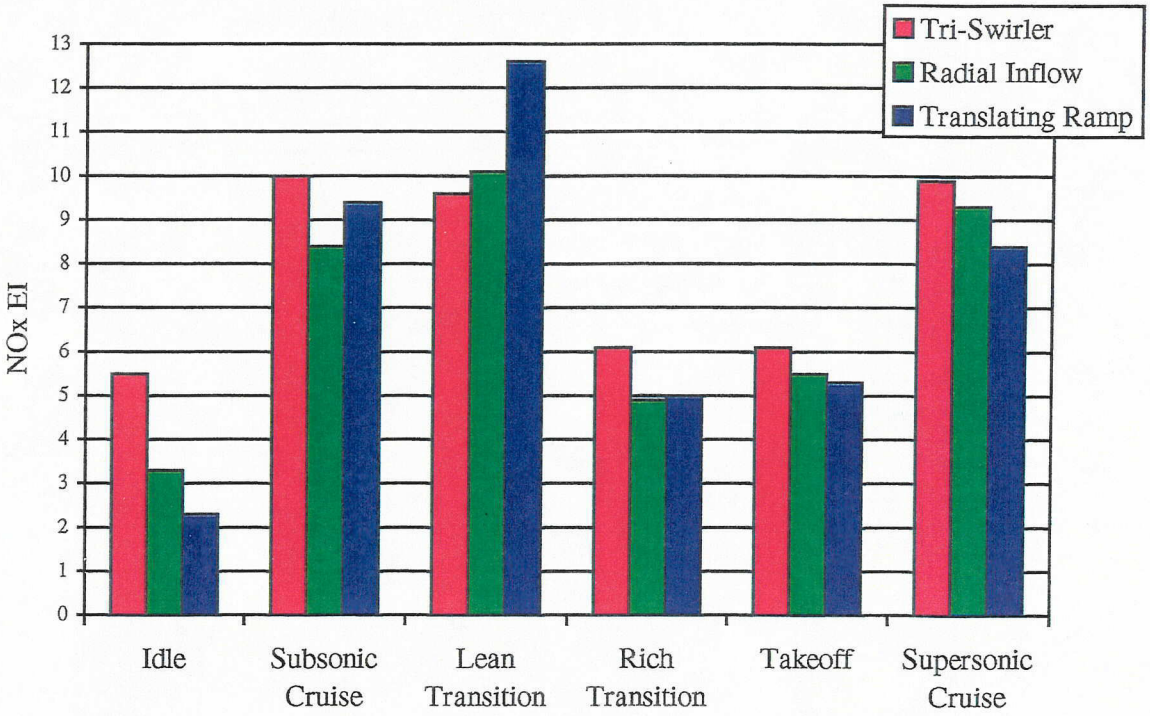

Figure VI-3 NO_x Emissions Results for Variable Geometry Injectors.

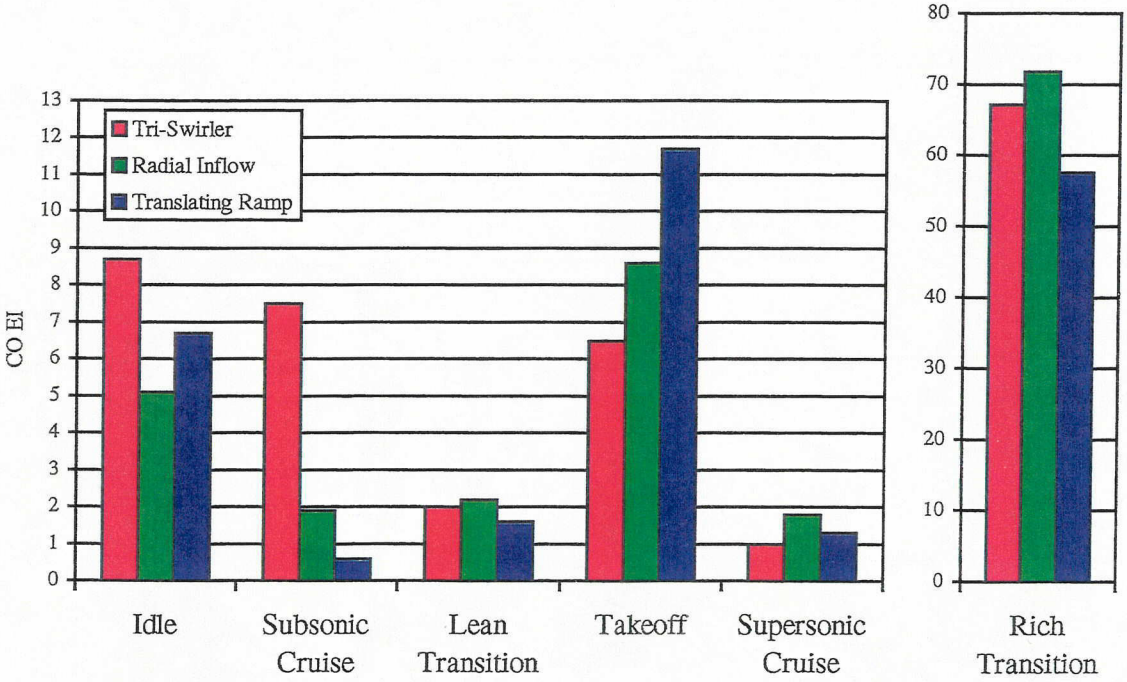

Figure VI-4 Carbon Monoxide Emissions Results for Variable Geometry Injectors.

SECTION VI FIGURES

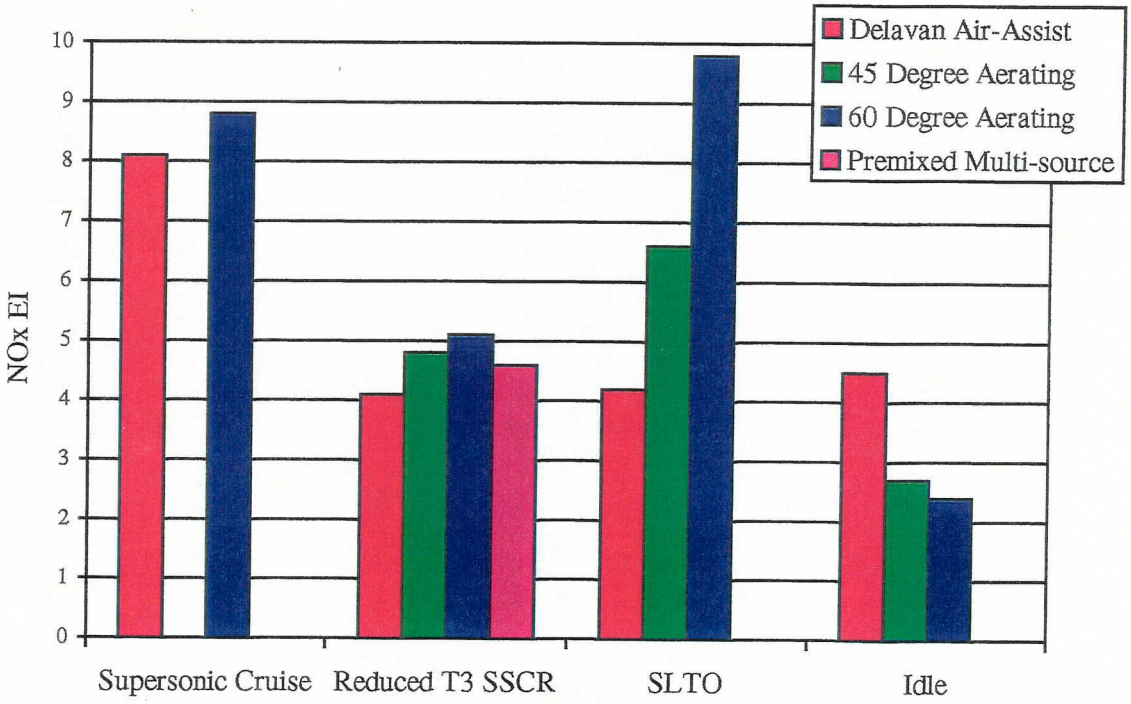

Figure VI-1 NO_x Emissions Results for Baseline Injectors.

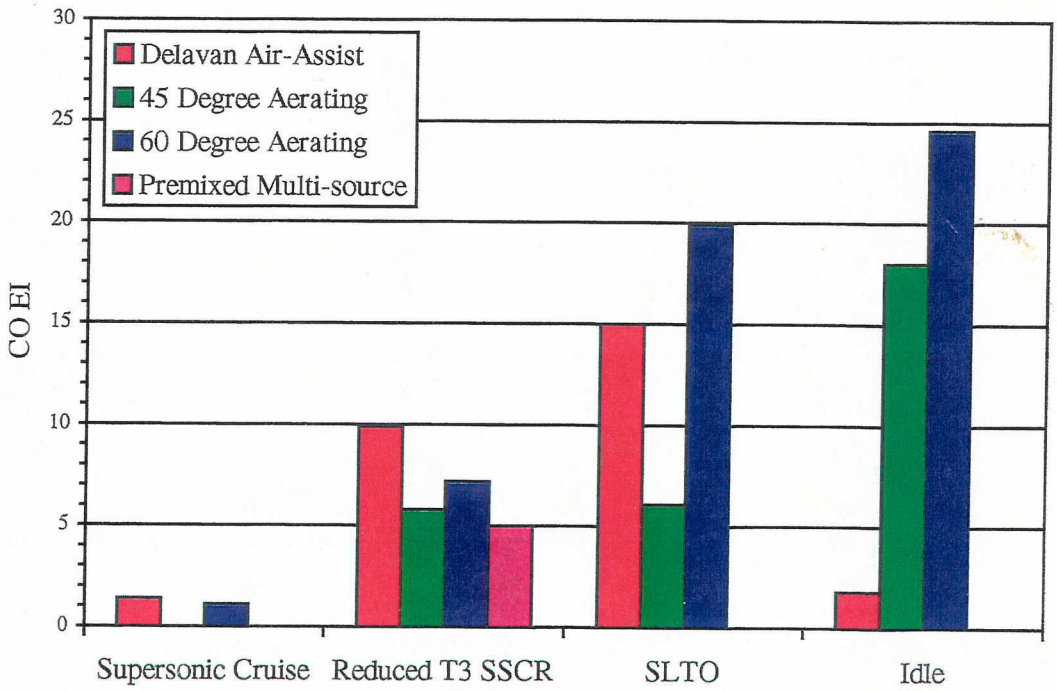

Figure VI-2 Carbon Monoxide Emissions Results for Baseline Injectors.

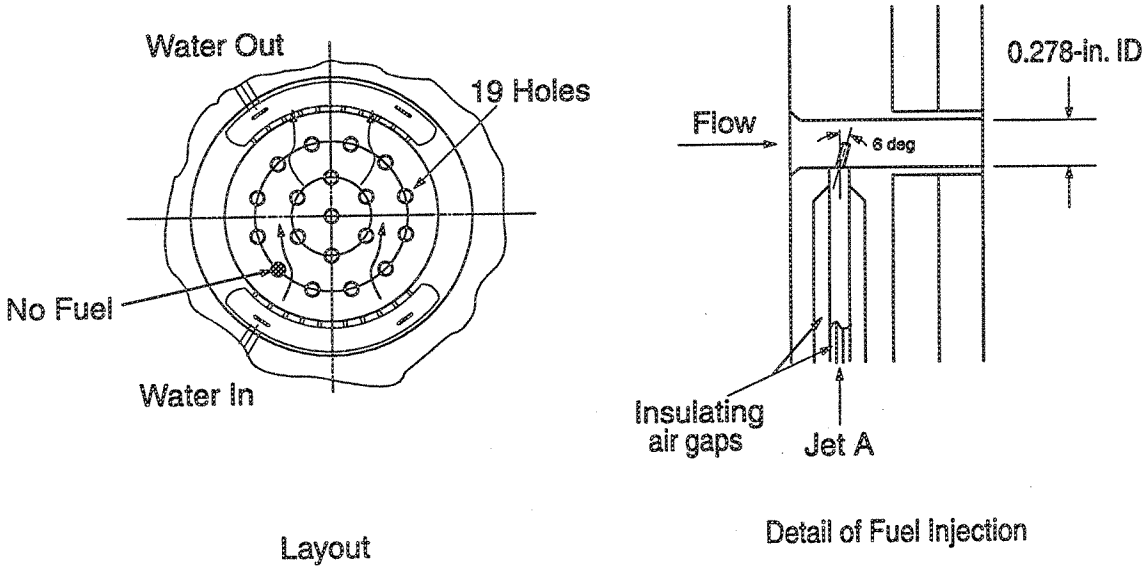

Figure VI-5 Pre-Mixed Multi-Source Fuel Injector Configured for Air Leak Simulation.

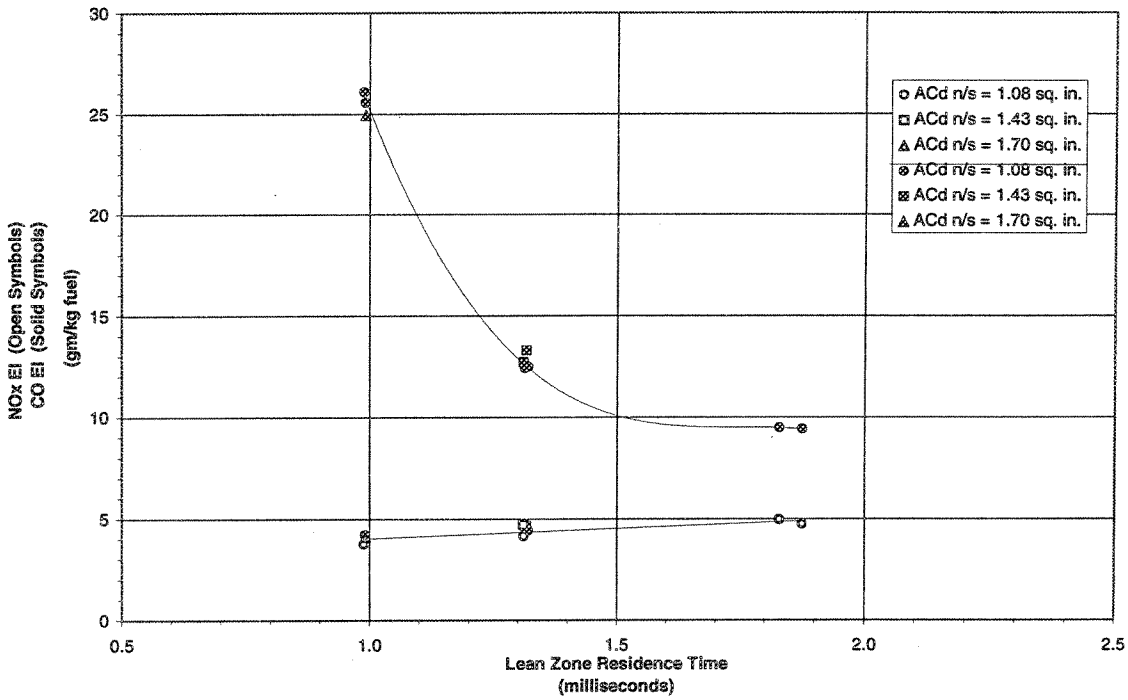

Figure VI-6 Residence Time Effect on Emissions. Tri-Swirler Fuel Injector. De-rated (low P3, T3, f/a) Scaled Supersonic Cruise Simulation (P3 = 76 psia, T3 = 850 F, f/a = 0.028, Φ_{rich} = 1.8)

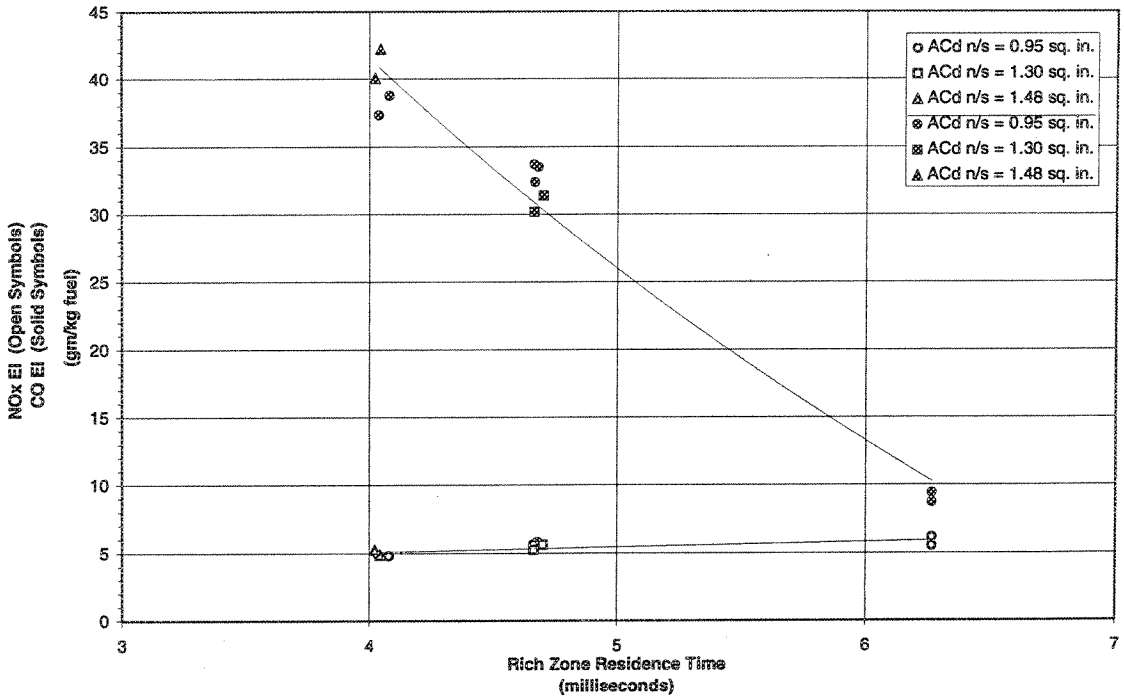

Figure VI-7 Residence Time Effect on Emissions. Tri-Swirler Fuel Injector. Idle Simulation (P3 = 67 psia, T3 = 430 F, f/a = 0.009, Φ_{rich} = 0.6)

APPENDIX A - COMPUTATIONAL FLUID DYNAMICS CALCULATIONS

CFD Research Corporation

3325 Triana Blvd. • Huntsville, Alabama 35805 • Tel.: (205) 536-6576 • FAX: (205) 536-6590

DEFINITION AND EVALUATION OF FUEL/AIR ADMISSION SYSTEMS FOR RICH BURN-QUICK QUENCH COMBUSTORS AND 3-D CFD ANALYSES OF THE FOUR NOZZLE RQL SECTOR RIG

Final Report

By

D. Scott Crocker
Eric J. Fuller
Clifford E. Smith

January 1995

CFDRC Report 4340/1

P. O. 718749

United Technologies

Pratt & Whitney

East Hartford, CT 06108

Technical Monitor: Dr. Robert Lohmann

R&D Services and Software for Computational Fluid Dynamics (CFD)
Branch Office: 2 Lakeview Ave., Suite 200 • Piscataway, New Jersey 08854 • Tel.: (908) 424-9393 FAX: (908) 424-9399

TABLE OF CONTENTS

		Page
1.	INTRODUCTION	1
2.	DEFINITION AND EVALUATION OF CFDRC'S FUEL-AIR ADMISSION SYSTEMS	1
	2.1 Background	1
	2.2 Definition of CFDRC Concepts	2
	2.3 Predicted and Measured ACd for CFDRC Concept 6	6
	2.4 Reacting Flow Analyses of CFDRC Concepts 3 and 6	7
	2.5 Initial Fuel Injection Velocity and Drop Size Sensitivity Study of CFDRC Concepts 3 and 6	7
3.	EVALUATION OF PRATT & WHITNEY FUEL-AIR ADMISSION SYSTEMS	14
	3.1 Cold Flow Analysis of the P&W High Shear Nozzle (HSCT 1)	14
	3.2 Spray Penetration Validation	15
	3.3 Cold Flow Spray Cases for the P&W High Shear Nozzle (HSCT 1)	15
	3.4 Reacting Flow Cases with Fixed Geometry Fuel Nozzles	19
	3.5 Reacting Flow Cases for the P&W High Shear Nozzle (HSCT 1)	21
	3.6 Diagnostic Cases for the P&W High Shear Nozzle (HSCT 1)	24
	3.7 P&W Dual-Swirler Airblast Nozzle	28
	3.8 Three Passage High Shear Nozzle	31
	3.9 Cold Flow Cases for the P&W Constant Flow Split High Shear Nozzle (HSCT 11)	31
	3.10 Reacting Flow Cases for the P&W Constant Flow Split High Shear Nozzle (HSCT 11)	37
4.	3-D CFD ANALYSES OF THE FOUR NOZZLE RQL SECTOR RIG	41
	4.1 Modular Combustor Modeling	41
5.	REFERENCES	44
APPENDIX A.	MONTHLY PROGRESS REPORTS FOR OCTOBER - DECEMBER 1994	A-1

4340/1

1. INTRODUCTION

A Rich-burn/Quick-quench/Lean-burn (RQL) combustor is a candidate concept for low NO_x emissions in a High Speed Civil Transport (HSCT) engine. Low NO_x is achieved by minimizing combustion near stoichiometric conditions. A schematic of an RQL combustor with typical air flow split is shown in Figure 1. At the design point (supersonic cruise) fuel and air are initially burned in the rich zone at a rich equivalence ratio of approximately 1.8.

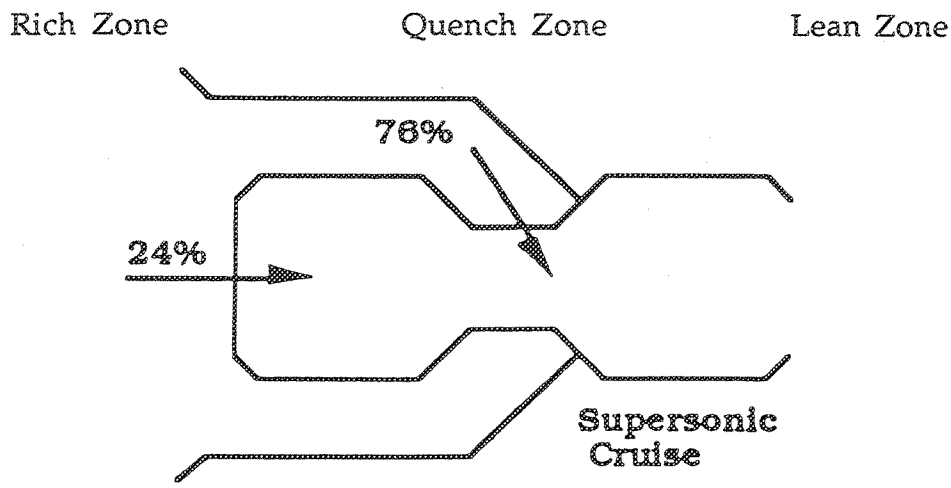

Figure 1. RQL Combustor Schematic

The partially oxidized combustion products are rapidly mixed with quench air to a lean equivalence ratio of about 0.4 in the quench zone and burning is completed in the lean zone.

This report is divided into three major sections, one section dealing with the design of CFDRC's variable geometry fuel-air module, one section dealing with the evaluation of P&W/UTRC fuel-air admissions systems, and the last section dealing with the analysis of the RQL combustor sector rig.

2. DEFINITION AND EVALUATION OF CFDRC'S FUEL-AIR ADMISSION SYSTEMS

2.1 Background

A variable geometry fuel-air admission system has been determined by Pratt & Whitney to be necessary for operation over all engine conditions. The rich zone of the combustor will operate in a lean mode for low power conditions and in a rich mode for high power conditions. The transition from low power (lean) to high power (rich) will occur rapidly to avoid operation near a stoichiometric fuel-air ratio. The fuel-air admission system must have an effective area ranging from 0.61

in^2 to 2.2 in^2 (3.6:1 ratio) to achieve the required equivalence ratio control in the rich zone. The operating conditions for the combustor are shown in Table 1. The design and computational evaluation of several candidate variable geometry fuel-air admission systems is one of the subjects of this report.

2.2 Definition of CFDRC Concepts

Six variable geometry fuel-air admission concepts were proposed and evaluated by CFDRC. (Concepts defined by Pratt & Whitney were also evaluated and are discussed in Section 3.)

The basic premises used for the concept definition were:

a. utilize maximum pressure drop for fuel atomization at all operating conditions. The aim is to avoid taking a large pressure drop upstream of the atomization process for the minimum flow area configuration;
b. mix fuel and variable air flow close to the fuel nozzle injection plane;
c. mechanically reliable/durable variable geometry device;
d. simple fuel system; and
e. use of rich zone air for back-side cooling of dome.

Schematics of concepts 1, 2, 4 and 5 are shown in Figure 2. Each of these concepts were eliminated from consideration after preliminary analyses were completed. Concepts 1 and 2 had inferior mixing for lean cases because the large volume outer swirler air failed to mix effectively with the fuel-air mixture from the dual-spray fuel nozzle. Also, the complexity associated with a duplex (primary/secondary) fuel system was considered unnecessary. CFD analyses showed that concept 4 had a potential problem with flashback for the minimum flow area configuration. Concept 5 was eliminated because of excessive pressure drop caused by the reverse flow configuration.

CFDRC concepts 3 and 6 were selected as most promising after preliminary analyses. Schematics of concepts 3 and 6 are shown in Figure 3. Concept 3 consists of radially inward fuel injection between two radial inflow swirlers. The fuel is injected through discrete holes. Variable geometry is achieved by a translating centerbody that partially blocks the inner swirler. Concept 6 consists of a central fuel injector with two axial swirlers. The fuel is injected radially outward through discrete holes. The variable air enters through a radial inflow swirler that is partially blocked by an axially translating mechanism. A large amount of air from the radial inflow swirler is available (even in the minimum flow area configuration) to cool the face of the translating mechanism. CFDRC concept 6 was eventually selected for fabrication and experimental testing at UTRC.

Table 1.
Design Parameters for Rich/Quench/Lean Combustor Fuel/Air Modules

Power Condition	Inlet Total Pressure psia	Inlet Total Temperature F	Overall Fuel/Air Ratio	Rich Zone Equivalence Ratio	Per Module: Fuel Flow lb/sec	Per Module: Air Flow lb/sec	Per Module: Effective Flow Area ACd sq. in.	Bulkhead Pressure Drop Percent
Ground Idle	67	424	0.0091	0.60	0.026	0.62	0.98	7.5
Subsonic Cruise	92	634	0.0139	0.60	0.046	1.12	1.77	4.7
Lean Transition	227	766	0.0160	0.60	0.123	3.00	2.20	3.9
Rich Transition	227	766	0.0160	1.55	0.123	1.16	0.61	8.1
Supersonic Cruise	207	1250	0.0288	1.80	0.164	1.34	1.05	6.0
Takeoff	264	818	0.0373	1.80	0.272	2.22	1.50	3.6
Subsonic Climb	104	666	0.0402	1.80	0.116	0.94	1.67	3.0

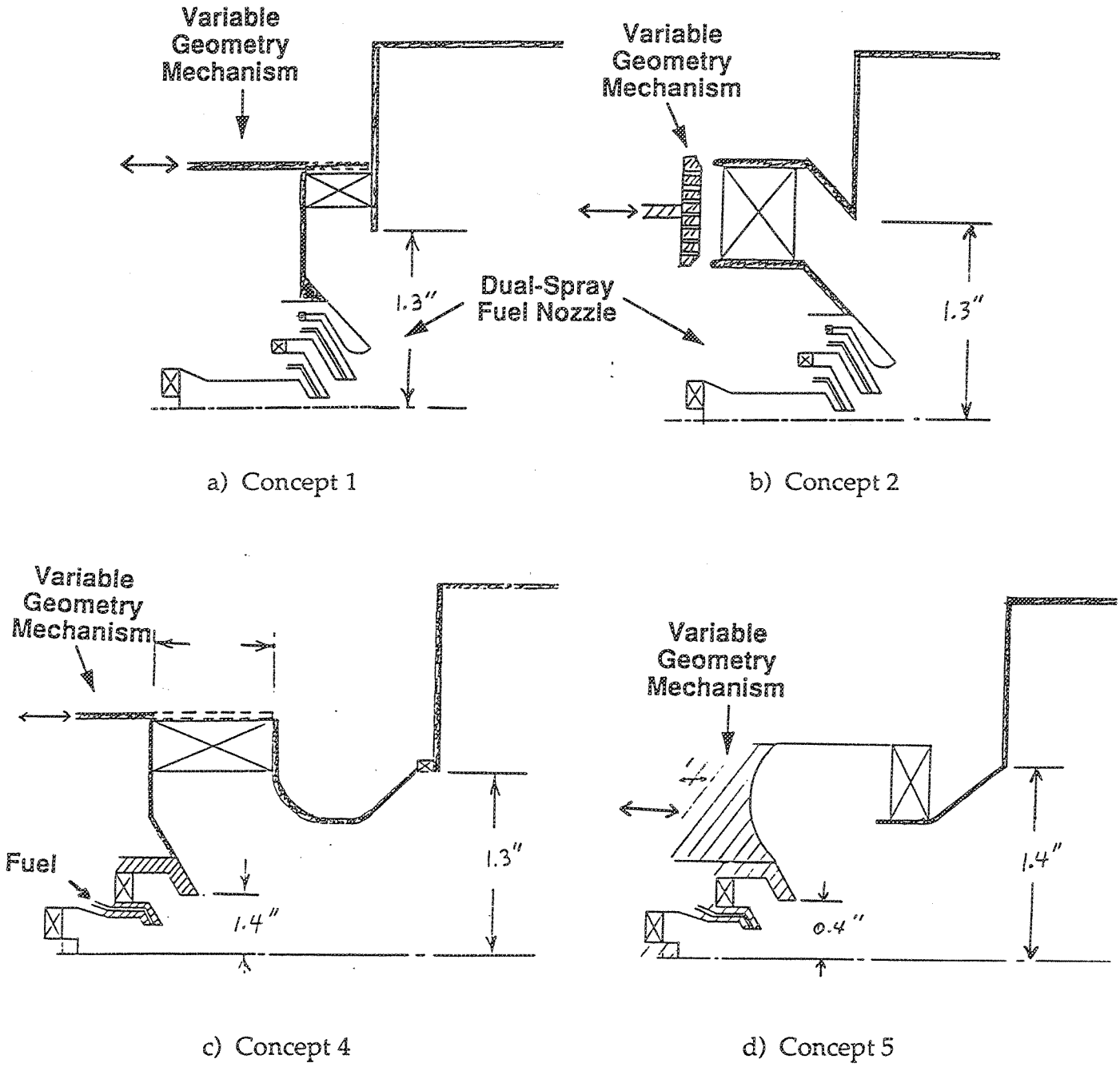

a) Concept 1

b) Concept 2

c) Concept 4

d) Concept 5

Figure 2. Schematic of CFDRC Fuel-Air Admission Concepts 1, 2, 4 and 5

4340/1

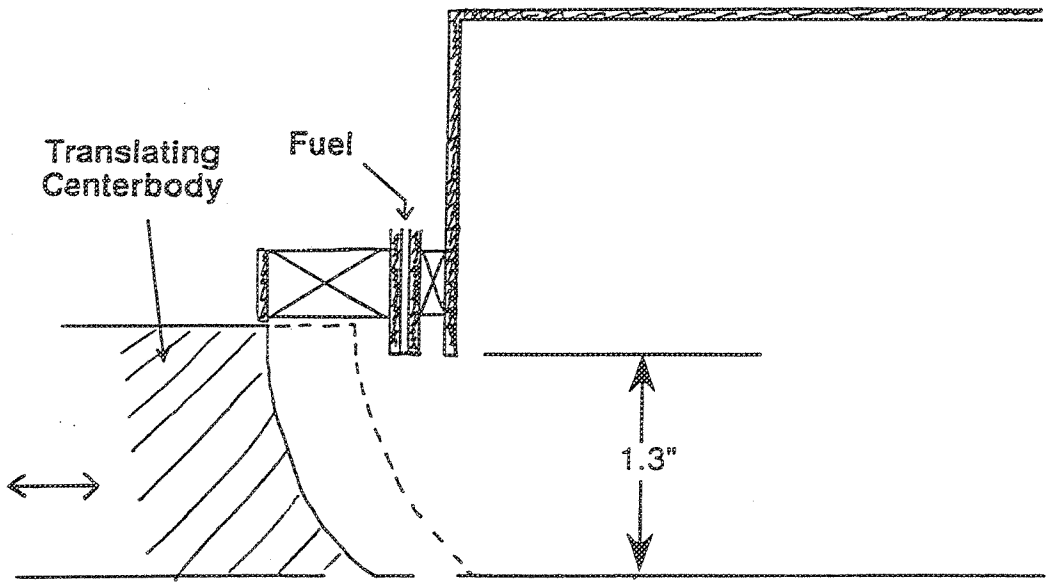

a) Concept 3

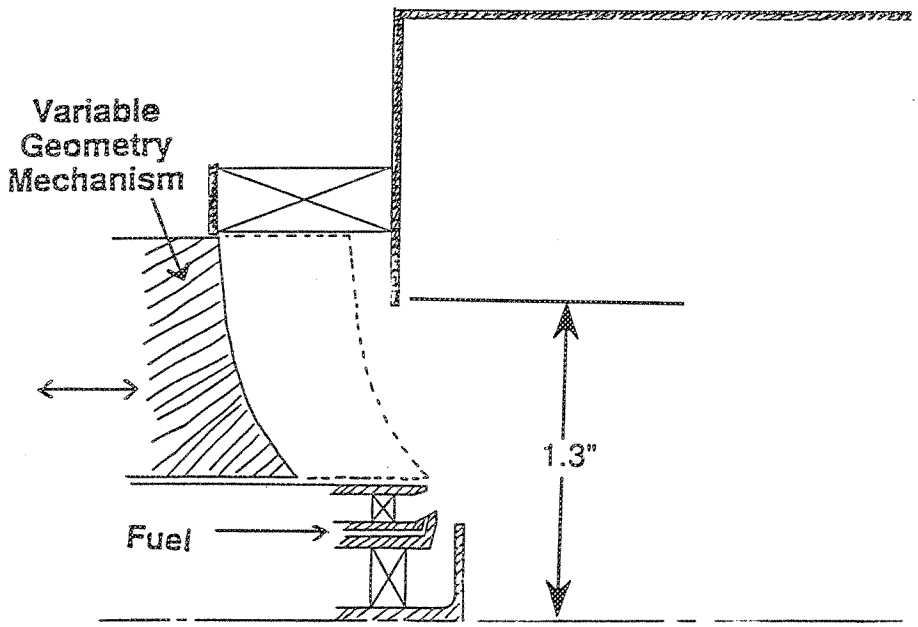

b) Concept 6

Figure 3. Schematic of CFDRC Fuel-Air Admission Concepts 3 and 6

2-D axisymmetric CFD modeling was used to assess the performance of the concepts. A typical grid for concept 6 is shown in Figure 4. The effect of grid resolution on the solutions was evaluated by doubling the number of cells in each direction. The effect on the solution was negligible indicating that the solutions are nearly grid independent.

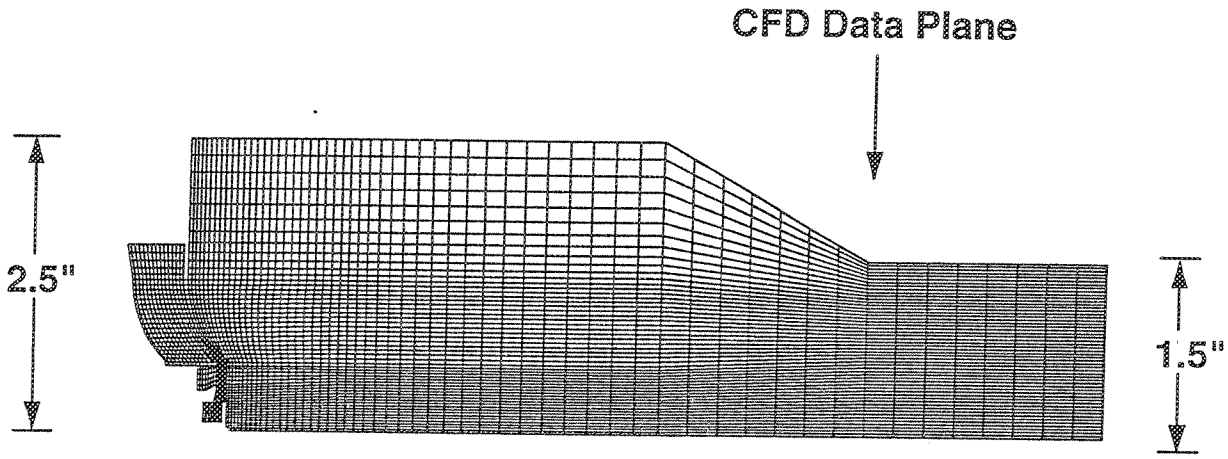

Figure 4. Typical Grid for CFDRC Concept 6

2.3 Predicted and Measured ACd for CFDRC Concept 6

The ACd predicted for CFDRC concepts 3 and 6 ranged from less than 0.6 in^2 when fully closed to just over 2.2 in^2 when fully open. The results for concept 6 compared very well with measurements later taken at UTRC on a prototype model. The measured ACd results are shown in Table 2.

Table 2. CFDRC Concept 6 Measured ACd

% Open	ACd (in^2)
100	2.34
83	2.25
67	2.08
50	1.81
33	1.47
25	1.24
17	0.99
8	0.62
0	0.31

2.4 Reacting Flow Analyses of CFDRC Concepts 3 and 6

Concepts 3 and 6 were analyzed for all seven conditions shown in Table 1. Temperature contours for all seven conditions for concept 3 are shown in Figures 5 and 6. In the idle case (Figure 5a) the fuel penetrates the swirler air very little and remains near the liner. The flame in the subsonic cruise case (Figure 5b) is also located near the liner. The hot region is relatively small indicating low NO_x formation. For the rich cases (Figure 6) the fuel and air mix effectively, especially for the supersonic cruise condition. Temperature contours for concept 6 are shown in Figures 7 and 8. The fuel/air mixing for all seven conditions is reasonably good. The subsonic cruise case (Figure 7b) has a very small hot region near the liner. The supersonic cruise case (Figure 8b) is well mixed after a very short distance in the rich burn section. Off design cases such as idle (Figure 7a) and subsonic climb (Figure 8d) are less well mixed. The fuel was injected as plain jets to improve fuel distribution. Drop sizes were predicted by a correlation from Lefebvre[1] for plain jet atomizers.

Both concept 3 and concept 6 were potential candidates for the variable geometry fuel-air admission system. Analyses indicated good performance for supersonic and subsonic cruise conditions. Adequate performance was also predicted for all other conditions. Backside dome cooling can be easily accommodated by both concepts. A concern for both concepts was that the variable geometry mechanism has moderate exposure to the hot combustor environment. Concept 6 was selected as the best CFDRC concept primarily because the fuel injector part of the system has a small diameter compared to concept 3.

2.5 Initial Fuel Injection Velocity and Drop Size Sensitivity Study of CFDRC Concepts 3 and 6

A total of 20 2-D CFD cases were completed for concepts 3 and 6 to study the sensitivity of initial fuel injection drop size and drop velocity. Temperature contours for selected subsonic cruise (lean) and supersonic cruise (rich) cases are shown in Figures 9 and 10 for CFDRC concept 6. For Figure 9a and 10a, the SMD was determined from a drop size correlation[1] for plain jet atomizers. The initial drop velocity was determined from the fuel pressure drop for a flow number of 50.

Concept 6 subsonic cruise (Figure 9) results show significant sensitivity to both initial drop velocity and drop size. The best case is for an SMD of 29 and fuel injection velocity of 23 ft/sec (Figure 9). Drop size has a large effect on outward radial penetration as shown by comparison of Figure 9c and 9d. Concept 6 supersonic cruise (Figure 10) results indicate a small influence of initial drop velocity. The reduced outward radial penetration degrades fuel/air mixing. Initial drop size variation had a very small effect.

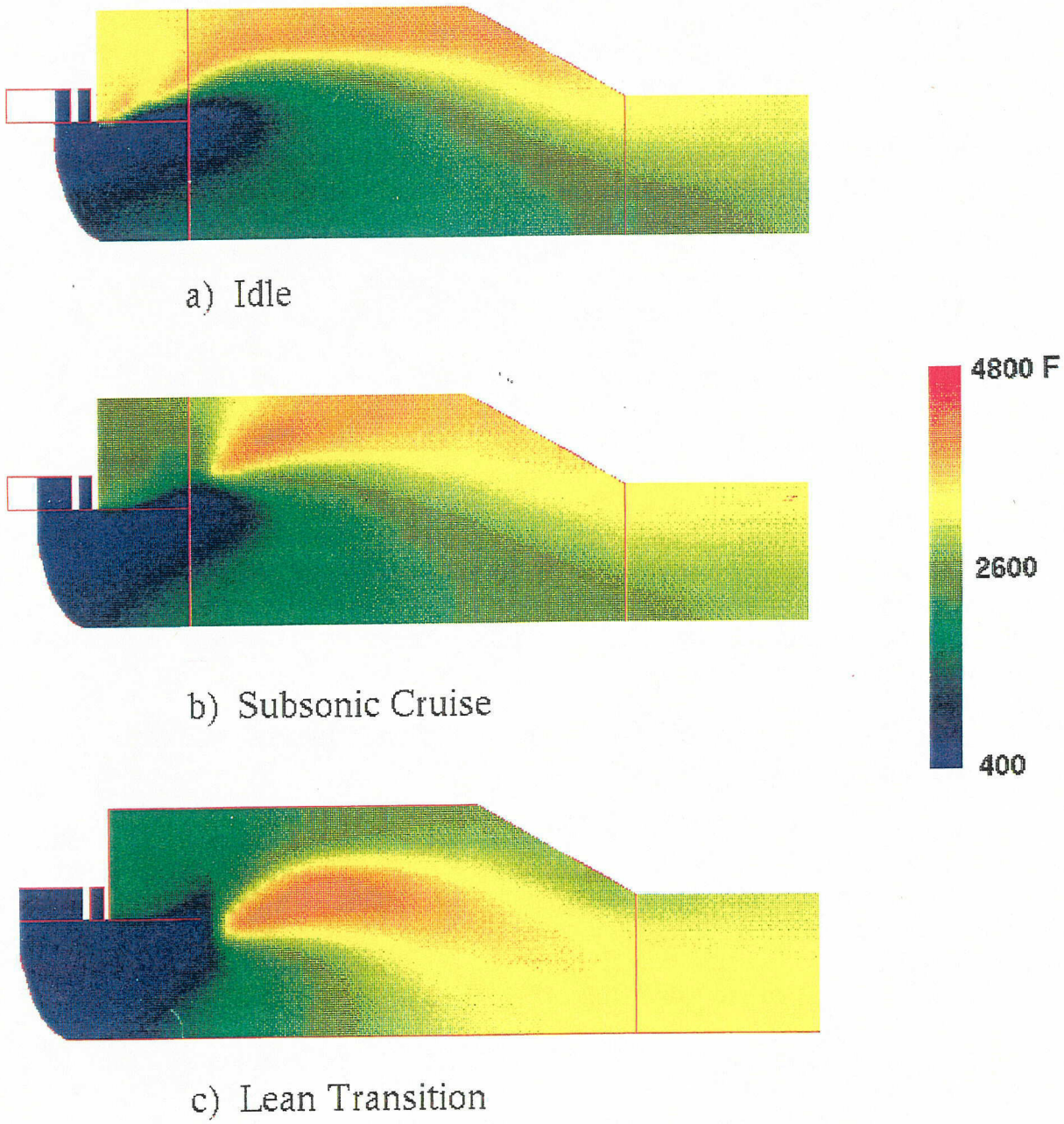

Figure 5. CONCEPT 3 -- Temperature Contours (Lean Cases)

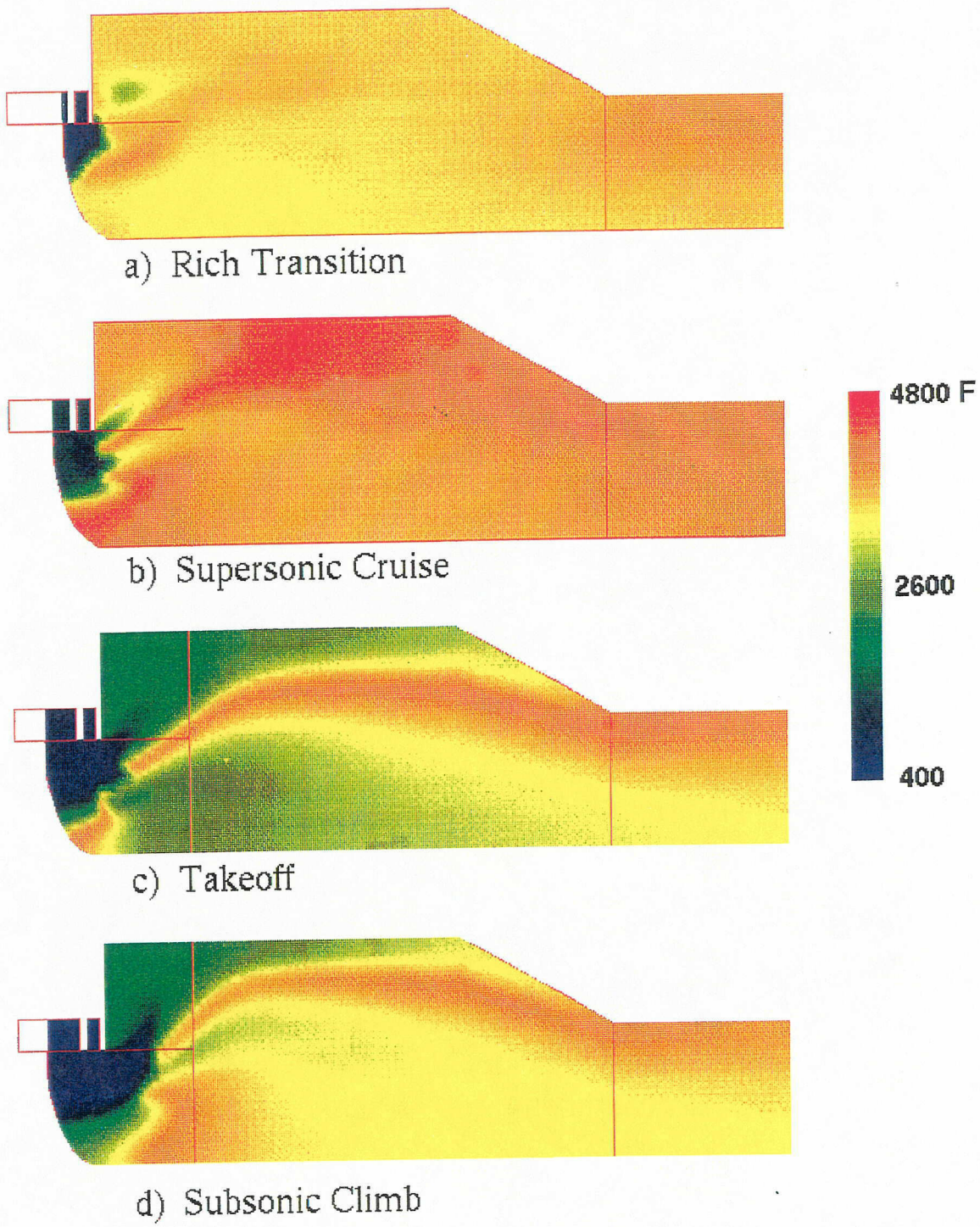

Figure 6. CONCEPT 3 -- Temperature Contours (Rich Cases)

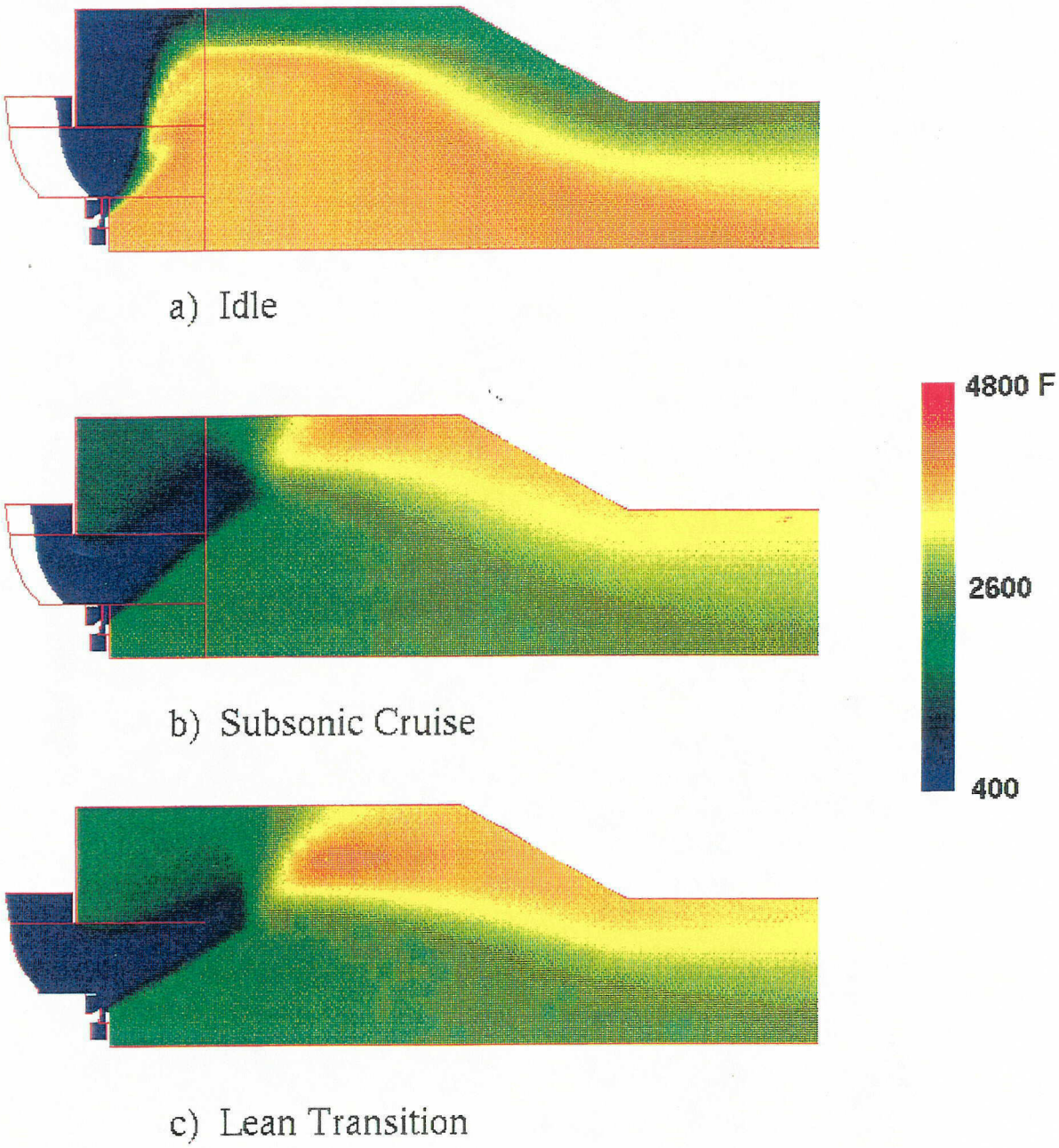

Figure 7. CONCEPT 6 -- Temperature Contours (Lean Cases)

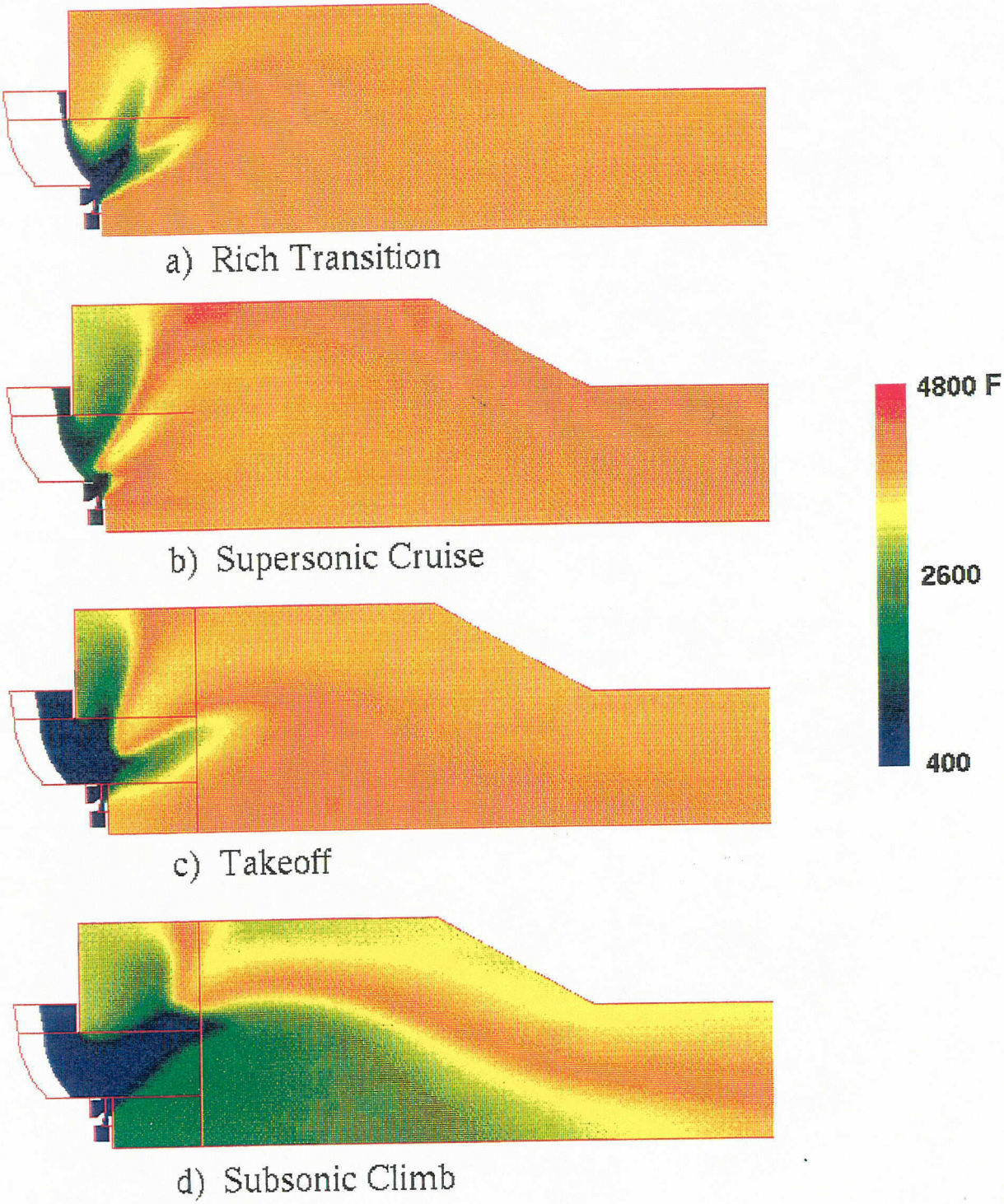

Figure 8. CONCEPT 6 -- Temperature Contours (Rich Cases)

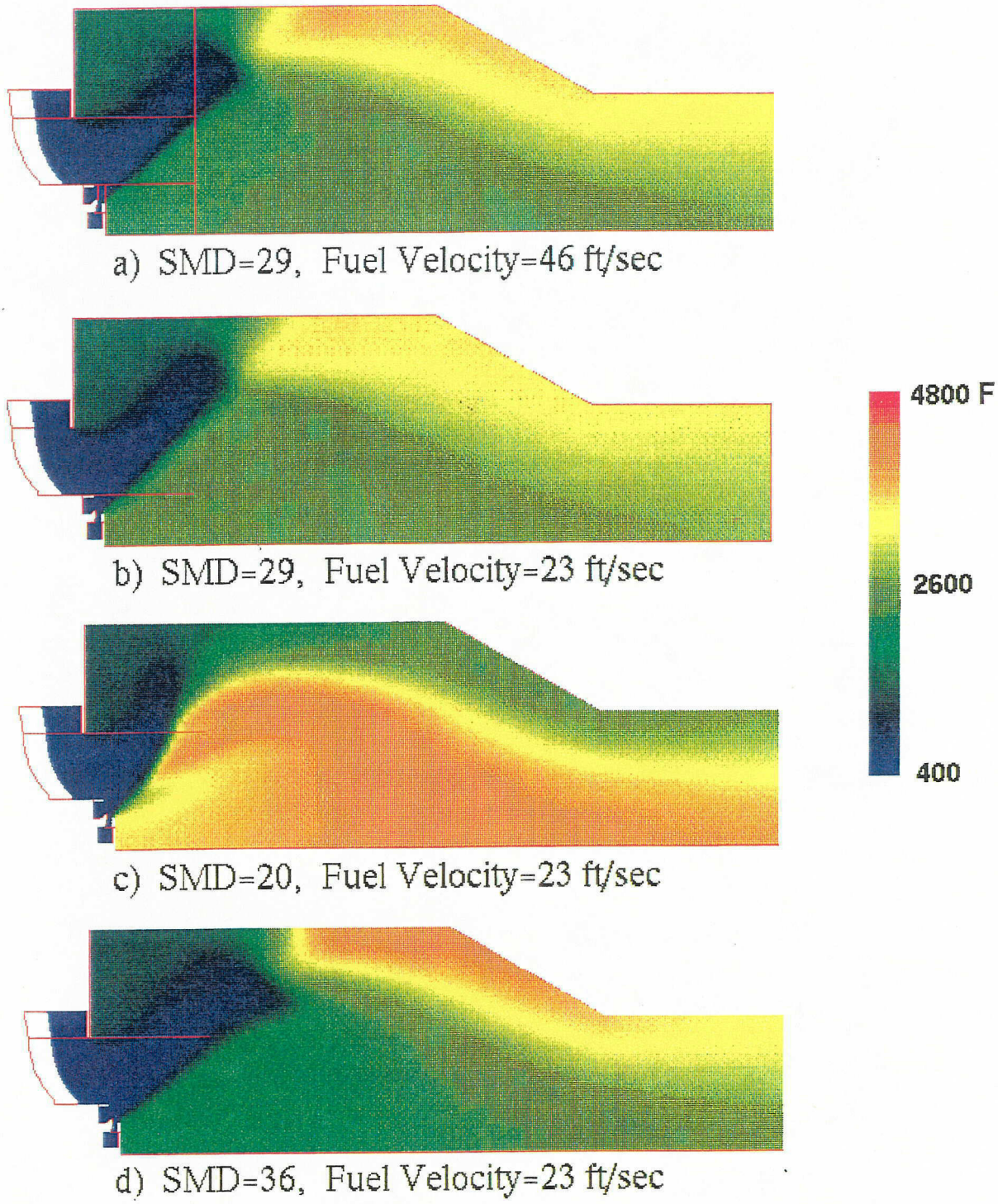

Figure 9. CONCEPT 6 -- Temperature Contours
Subsonic Cruise Cases

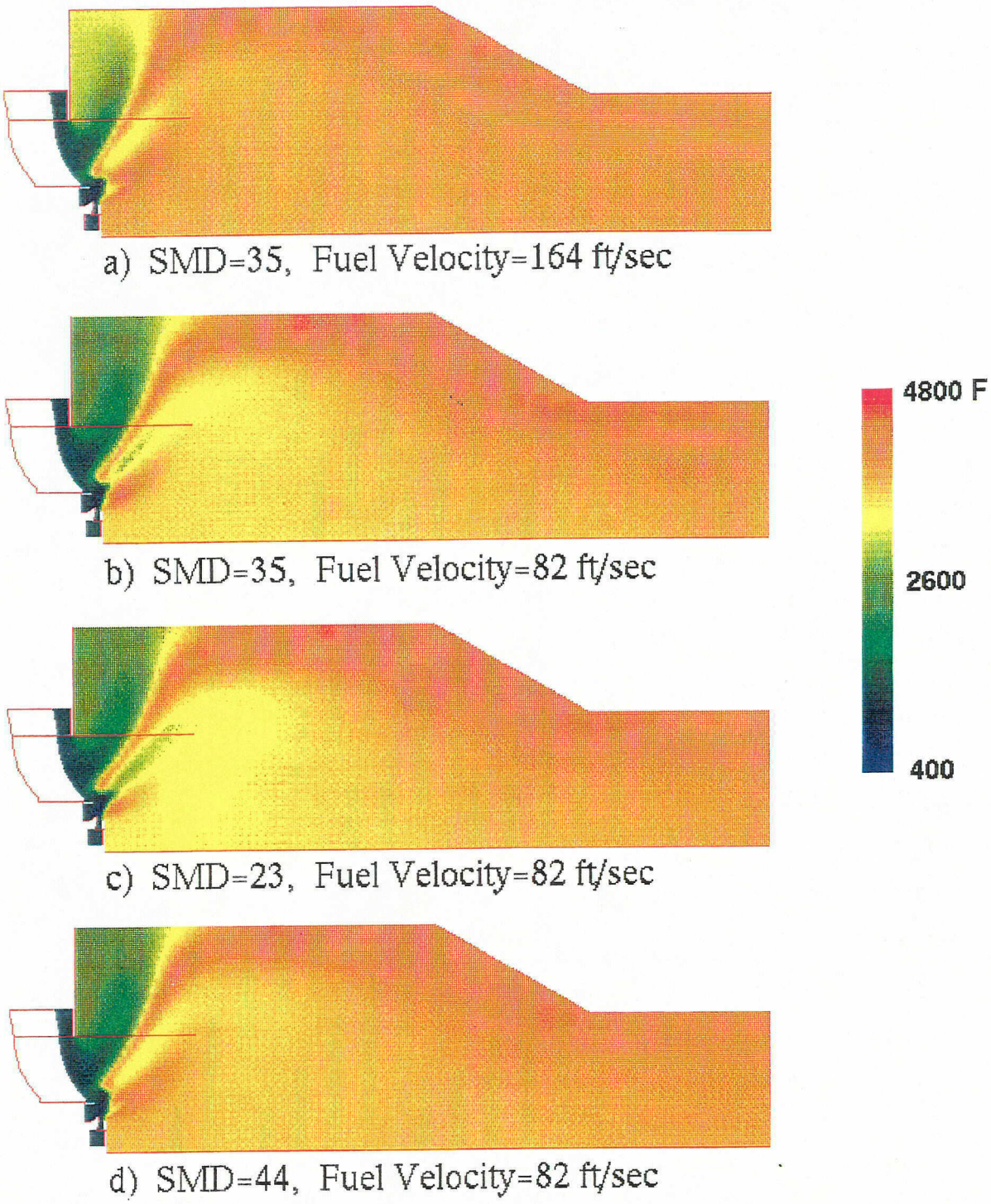

Figure 10 CONCEPT 6 -- Temperature Contours
Supersonic Cruise Cases

Thermal NO_x emission index and the fuel mixture fraction unmixedness are shown for the CFDRC concept 6 cases in Table 3.

Table 3. CFDRC Concept 6 Cases

Power Condition	Fuel Injection				NO_x (EI)	Unmixedness
	Number of Holes	Hole Diameter (in)	Initial Velocity (ft/sec)	Initial SMD (microns)		
Lean Transition	12	0.02	124	30	15.6	0.038
Rich Transition	12	0.02	124	27		0.006
Subsonic Climb	12	0.02	117	40		0.126
Takeoff	12	0.02	274	35		0.028
Idle	12	0.02	26	25	4.0	0.057
Subsonic Cruise*	12	0.02	46	29	6.3	0.029
Subsonic Cruise	12	0.02	23	29	3.5	0.020
Subsonic Cruise	12	0.02	46	20	10.4	0.039
Subsonic Cruise	12	0.02	46	36	6.4	0.046
Subsonic Cruise	12	0.02	23	20	10.4	0.039
Subsonic Cruise	12	0.02	23	36	6.5	0.041
Supersonic Cruise*	12	0.02	165	35		0.023
Supersonic Cruise	12	0.02	82	35		0.046
Supersonic Cruise	12	0.02	165	23		0.036
Supersonic Cruise	12	0.02	165	44		0.009
Supersonic Cruise	12	0.02	82	23		0.049
Supersonic Cruise	12	0.02	82	44		0.038

4340 0294 T2

* Design Case

3. EVALUATION OF PRATT & WHITNEY FUEL-AIR ADMISSION SYSTEMS

3.1 Cold Flow Analysis of the P&W High Shear Nozzle (HSCT 1)

The P&W HSCT 1 high shear nozzle was analyzed using a 2-D CFD model for ambient pressure non-reacting conditions. A pressure drop of 7 inches H_2O, corresponding with experimental conditions was assumed. A 2 inch diameter fuel injector was included in the model. The computed AC_d was 2.38 in^2 with 12.6% of the flow through the outer passage. The experimentally measured AC_d was 2.3 in^2.

A similar case was also run without the 2 inch diameter fuel injector. The total AC_d was 2.48 in^2 indicating only slight blockage by the fuel injector. Cold flow cases with 10% and 100% open area through the inner swirler were compared with laser velocimetry experimental data. Axial and tangential velocities for the numerical and experimental data are shown in Figure 11. The velocity profile agreement is reasonably good. A coanda flow pattern was predicted for the 10% open case. This flow pattern matches the experimental results as shown in Figure 11b. The magnitude of the numerical results is lower than the experimental data, however, the velocities for a coanda flow pattern are a strong function of axial location. The numerical results at x = 0.20″ (rather than x = 0.25″) (x is assumed to be the axial direction) were in very good agreement with the experimental data.

3.2 Spray Penetration Validation

Impingement of fuel jets on the prefilmer is an area of concern for the high shear nozzle. Therefore, some effort was given to validating the predictions of liquid jet penetration in crossflow using CFD-ACE. Comparisons of both 2-D and 3-D predictions were made with experimental data of Hautman & Rosfjord[2]. Experimental and numerical results are shown in Figure 12 for air velocities of 118 and 291 ft/sec. Numerical results are shown for the initial fuel velocity assumed to be 100% or 50% of the actual average fuel injection velocity. The agreement was acceptable, especially for the low liquid jet to air momentum ratio applicable to HSCT 1 conditions.

3.3 Cold Flow Spray Cases for the P&W High Shear Nozzle (HSCT 1)

Several cold flow HSCT 1 spray cases were run to model experimental configurations. Streamline contours and the spray pattern for these cases are shown in Figure 13. A turbulent dispersion model was used to predict the effect of turbulent fluctuations on the spray trajectory. Two fuel injector configurations were modeled: 1) 2 inch diameter with six 0.04 inch holes and 2) 2 inch diameter with eight 0.02 inch holes. The first has a flow number of 100 and the second a flow number of 33, so the fuel injection velocity of the second configuration is three times that of the first configuration. The effect of the higher velocity is evident from comparison of Figure 13a and 13b for lean transition conditions. Penetration of the fuel jets is lowest for the subsonic cruise conditions (Figure 13e and 13f).

4340/1

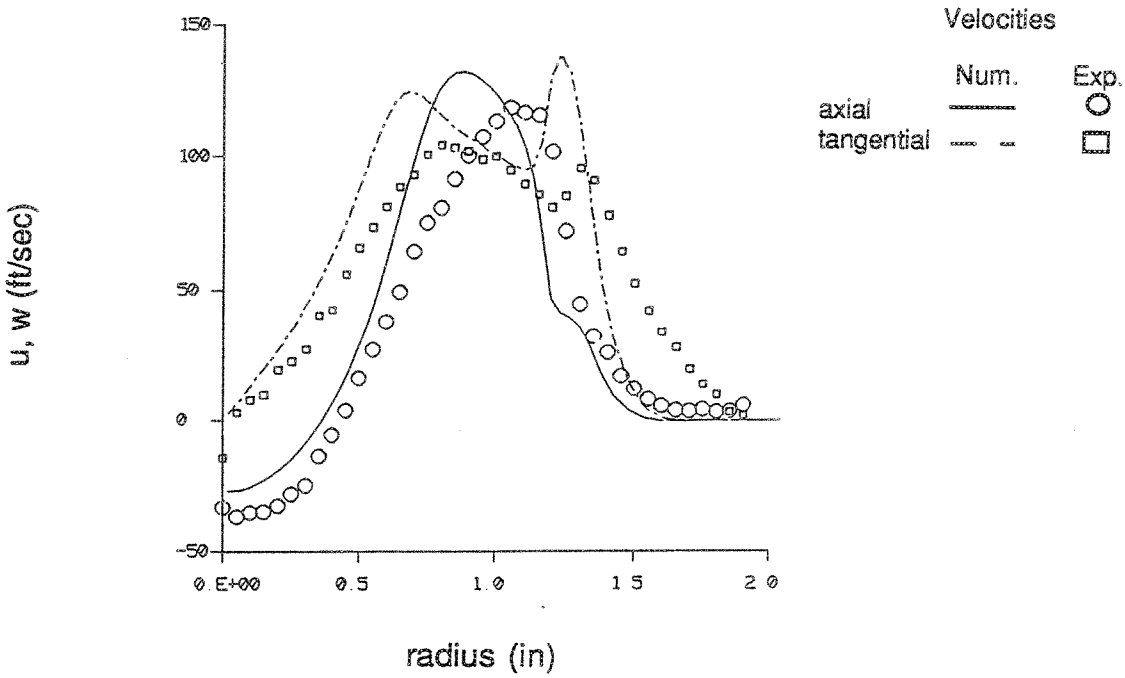

a) 100% open

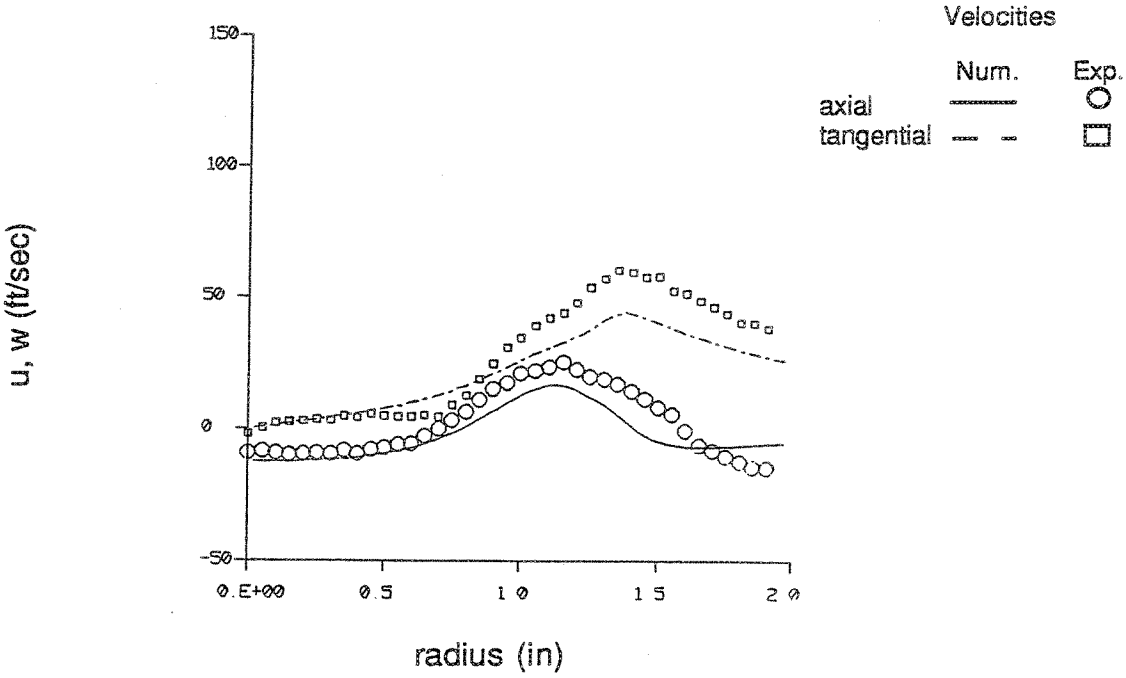

b) 10% open

Figure 11. Comparison of Numerical and Experimental Data for HSCT 2 Cold Flow Case - Pressure Drop = 7 Inches Water; X = 0.25″ Downstream of Nozzle Exit - 2 Inch Diameter Fuel Nozzle

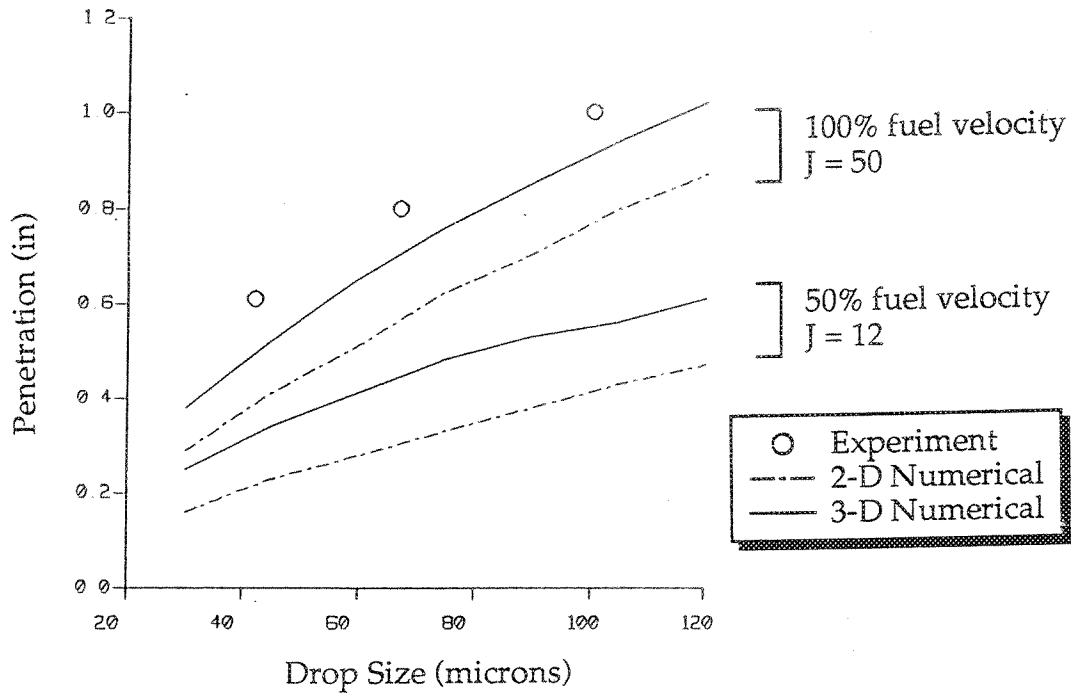

a) Air Velocity = 291 ft/sec

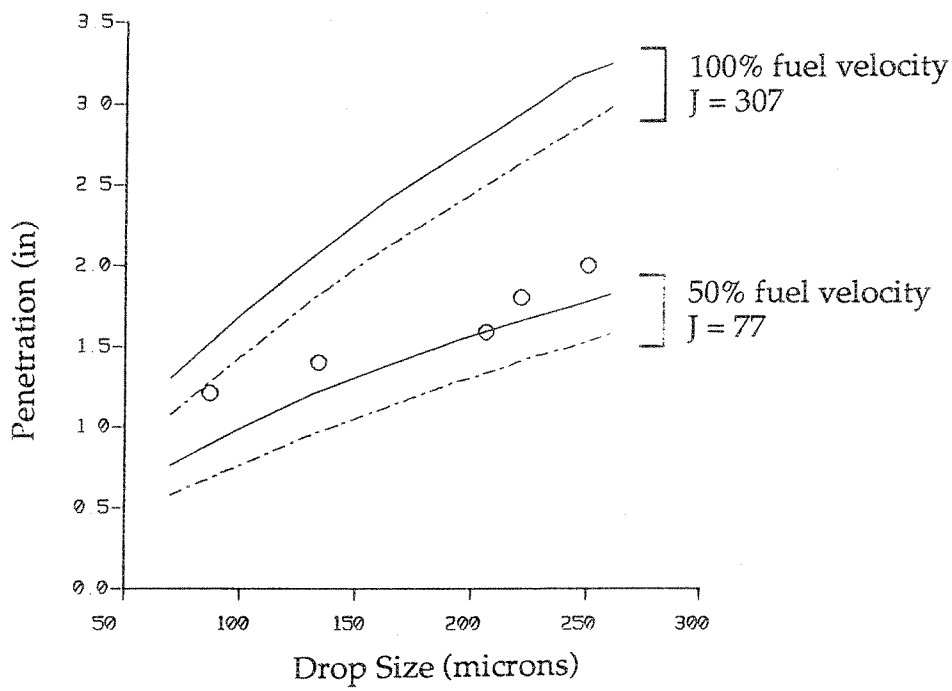

b) Air Velocity = 118 ft/sec

Figure 12. Droplet Penetration - Comparison of Numerical and Experimental[2] Results (x = 0.75 inches)

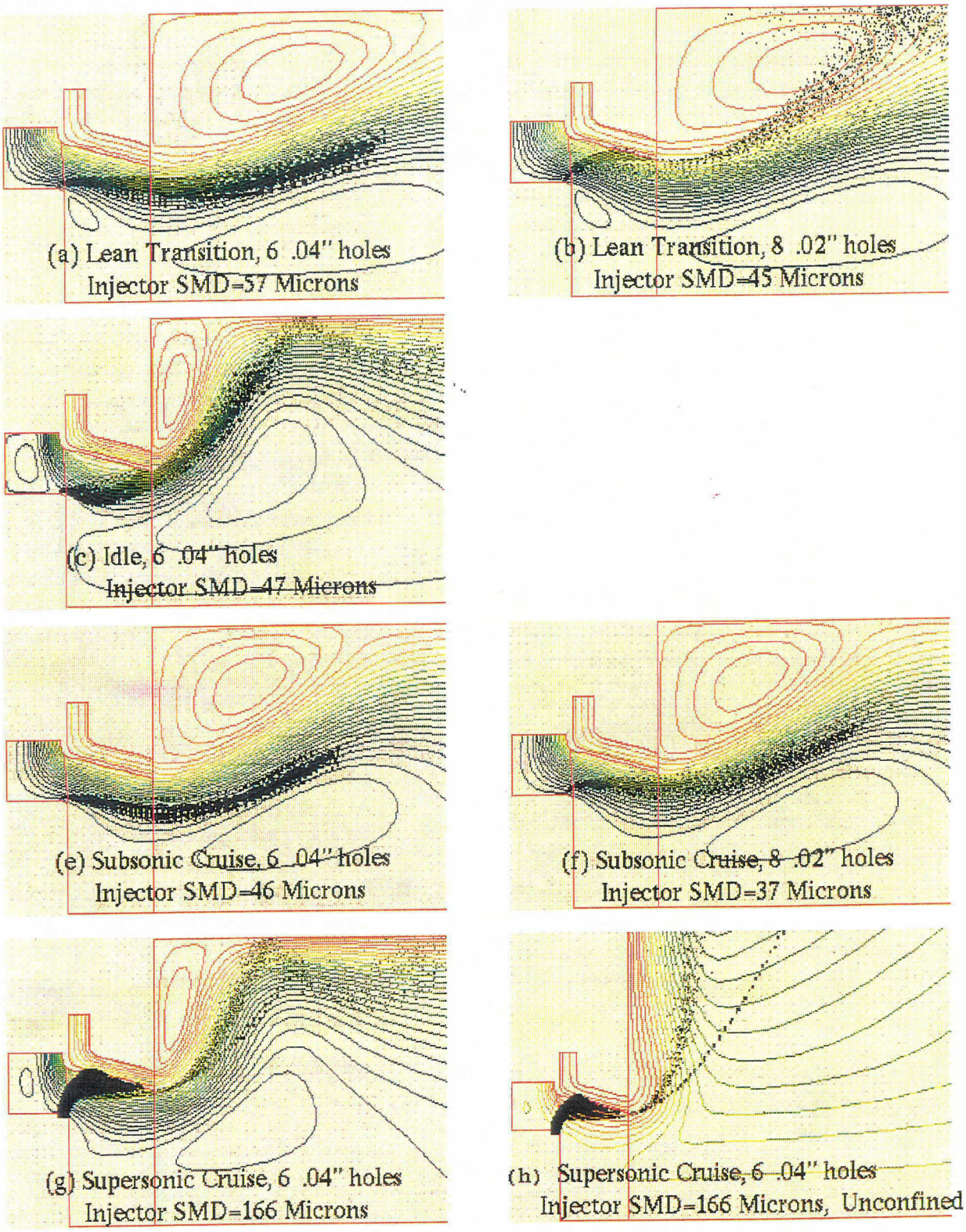

Figure 13 Cold Flow Spray Cases for HSCT1
(Fuel Velocity from 100% delta P)

3.4 Reacting Flow Cases with Fixed Geometry Fuel Nozzles

Two fixed geometry nozzles that were experimentally tested during 1993 in the UTRC cylindrical rig were analyzed. These two nozzles are HSCT AB (an airblast nozzle) and a Delavan air assist nozzle. Results for all of the cases that were run are shown in Table 4. For the HSCT AB nozzle a drop size SMD of 10 microns was assumed based on a correlation for prefilming airblast atomizers.[1] Even with variations in the flow split between the passages (without regard to pressure drop) all of the HSAB cases had excellent mixing. This indicates that the proximity of the fuel injection relative to the air injection is more important than the flow split. For the Delavan air assist nozzle, fuel and air, with a fuel/air ratio of 1.0, were injected at a 45° radial angle. A drop size SMD of 10 microns was assumed.[1] (Note: the fuel nozzle inlet boundary conditions were a rough assumption since fuel nozzle details were not available.) An additional case with SMD of 30 microns was also run. The swirler air was injected with a 45° swirl angle. The nozzle and swirler were recessed 0.5 inches from the dome face. Results for the two Delavan nozzle cases and the supersonic cruise HSCT 1 case are shown in Figure 14. Mixing for the Delavan nozzle is relatively poor (unmixedness = 0.105) compared to the excellent mixing for the HSCT AB nozzle (unmixedness = 0.001). The larger drop size (30 microns) for the Delavan nozzle causes some of the fuel to penetrate through the swirler air resulting in improved fuel distribution.

Table 4. Fixed Geometry Fuel Nozzle Cases

Fuel Nozzle	Power Condition	Flow Split (Inner/Outer)	SMD (microns)	NO_x (EI)	Unmixedness
HSCT AB	Subsonic Cruise	22/78	10	2.8	0.002
HSCT AB	Subsonic Cruise	37/63	10	3.1	0.003
HSCT AB	Supersonic Cruise	37/63	10		0.001
Delavan	Supersonic Cruise	-	10		0.105
Delavan	Supersonic Cruise	-	30		0.019

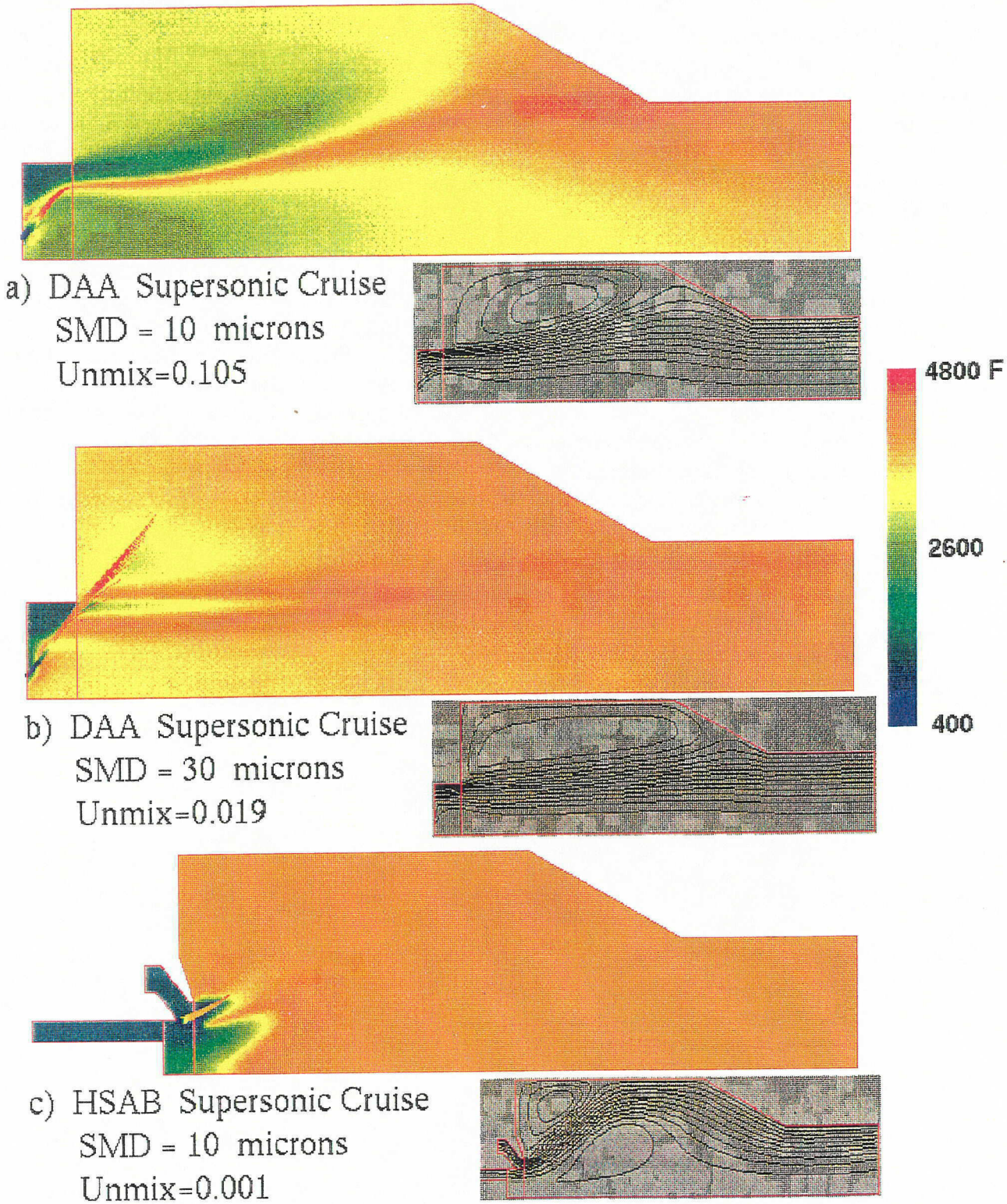

Figure 14 Temperature Contours for (a),(b) Delevan Air Assist Nozzle and (c) Airblast HSAB Nozzle

3.5 Reacting Flow Cases for the P&W High Shear Nozzle (HSCT 1)

Thirteen cases for the high shear nozzle (HSCT 1) were completed. The results are shown in Table 5. Temperature contours for cases with a 2″ diameter fuel injector with size 0.04″ holes are shown in Figure 15. Temperature contours for cases with a 2″ diameter fuel injector with eight 0.02″ holes are shown in Figure 16. The results for the 2.0/12/0.02 (diameter/# holes/hole diameter) nozzle were similar to those for the 2.0/6/0.04 nozzle. Results for the 1.75/8/0.02 nozzle were similar to those for the 2.0/8/0.02 nozzle. Several observations can be made concerning the results:

a. the fuel jets fail to reach the filmer in some cases, especially subsonic cruise;
b. fuel/air mixing is relatively poor even when the fuel jets do hit the filmer, especially for the lean cases (see Figure 5a);
c. surprisingly, the NO_x predicted for the case shown in Figure 4b is slightly lower than for the case shown in Figure 5b. The relatively poor mixing evident in Figure 4b inhibits NO_x production because of the lack of O_2 in the high temperature region; and
d. the fuel nozzle configuration did not affect the supersonic cruise cases since most of the fuel jet hit the filmer in both cases.

Table 5. P&W High Shear Nozzle (HSCT1) Cases

Power Condition	Fuel Injection					NO_x (EI)	Unmixedness
	Inj. Diameter (in)	Number of Holes	Hole Diameter (in)	Initial Velocity (ft/sec)	Initial SMD (microns)		
Lean Transition	2.0	6	0.04	62	59	5.5	0.007
Lean Transition	2.0	8	0.02	186	44	16.7	0.097
Lean Transition	2.0	12	0.02	124	32	12.8	0.031
Lean Transition	1.75	8	0.02	186	44	18.6	0.084
Rich Transition	2.0	6	0.04	62	193		0.035
Subsonic Cruise	2.0	6	0.04	23	41	6.7	0.065
Subsonic Cruise	2.0	8	0.02	69	35	7.7	0.030
Subsonic Cruise	2.0	12	0.02	46	27	6.9	0.067
Subsonic Cruise	1.75	8	0.02	69	35	6.6	0.030
Supersonic Cruise	2.0	6	0.04	82	116		0.037
Supersonic Cruise	2.0	8	0.02	248	84		0.044
Supersonic Cruise	2.0	12	0.02	165	56		0.026
Supersonic Cruise	1.75	8	0.02	248	84		0.037

4340 0394 T1

4340/1

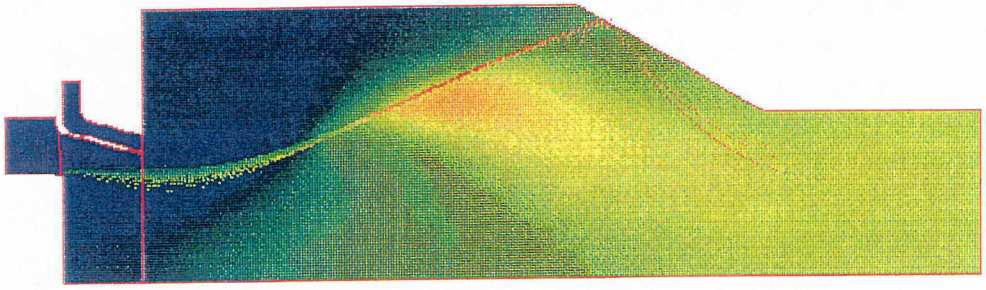

a) Lean Transition – Fuel velocity=61.9 ft/sec
SMD=59 from holes, 10 from filmer

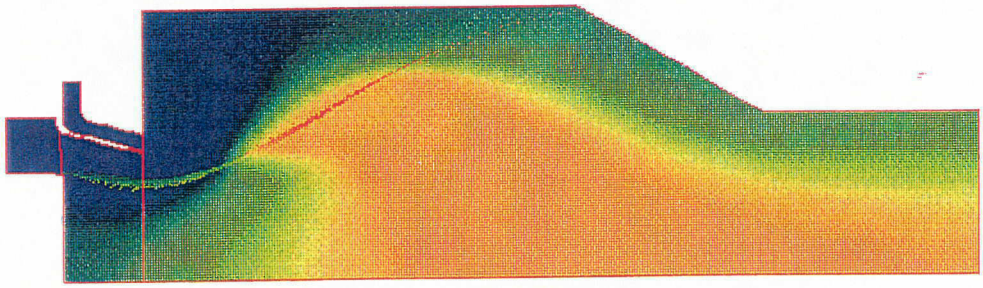

b) Subsonic Cruise – Fuel velocity=23.1 ft/sec
SMD=41 from holes, 10 from filmer

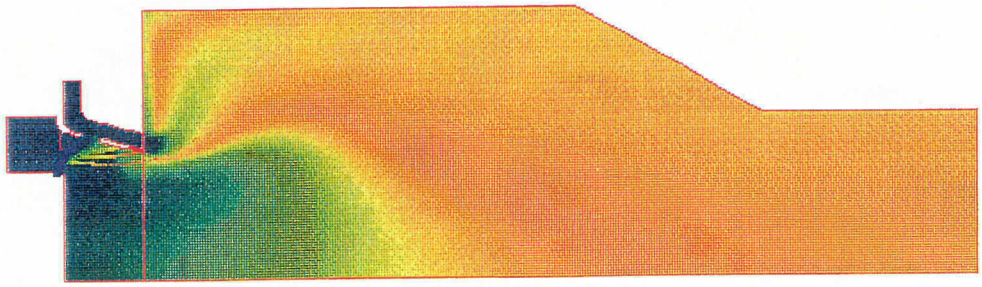

c) Supersonic Cruise – Fuel velocity=82.5 ft/sec
SMD=116 from holes, 10 from filmer

Figure 15 HSCT 1 Temperature Contours –
2" Diam. Fuel Injector with 6 0.04" Holes

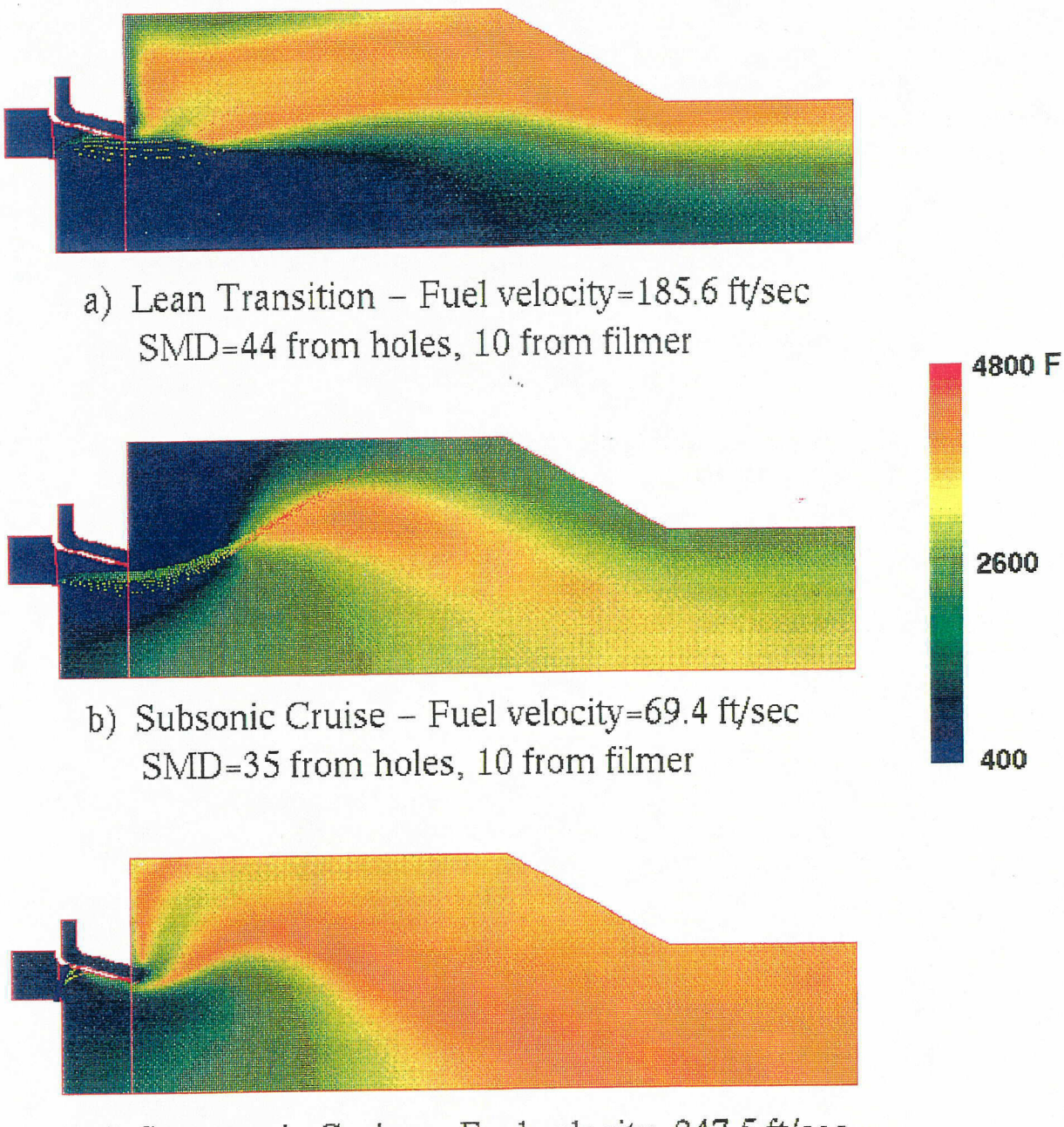

a) Lean Transition – Fuel velocity=185.6 ft/sec
SMD=44 from holes, 10 from filmer

b) Subsonic Cruise – Fuel velocity=69.4 ft/sec
SMD=35 from holes, 10 from filmer

c) Supersonic Cruise – Fuel velocity=247.5 ft/sec
SMD=84 from holes, 10 from filmer

Figure 16 HSCT 1 Temperature Contours –
2" Diam. Fuel Injector with 8 0.02" Holes

3.6 Diagnostic Cases for the P&W High Shear Nozzle (HSCT 1)

Six cases were run to evaluate the effect of flow split, swirl angle, and drop size on fuel-air mixing in the high shear nozzle. All of the cases are for lean transition with the 2 inch diameter nozzle with eight 0.02" holes. NO_x and unmixedness results for the HSCT 1 diagnostic cases and the base case (87/13 split) are shown in Table 6. Temperature contours for three of the cases are shown in Figure 17. Streamlines for the same three cases are shown in Figure 18. Several conclusions can be drawn:

a. the cases with drop sizes of 5 and 25 microns were not significantly different from the 10 micron case. Even at 25 microns the drops follow the streamlines and evaporate quickly;

b. changing the inner/outer flow split to 60/40 from 87/13 improved mixing some, but the result was still poor;

c. reducing the slot angles moved the flame away from the liner, but mixing was worse (Figure 17a). There was only a very small recirculation zone near the fuel injector (Figure 18a);

d. increasing the liner passage swirl improved mixing to some degree (Figure 17b and 17c). A separated flow condition was predicted for all cases with 70° outer passage swirl (Figure 18b). When the outer passage swirl was decreased, the flow streams remained attached (Figure 18c); and

e. an interesting result is that the NO_x was higher for most cases with lower unmixedness. The implication is that for relatively poor overall mixing conditions, NO_x increases with better mixing because more combustion occurs near stoichiometric fuel-air ratio.

Table 6. P&W HSCT 1 Diagnostic Cases
2.0 Inch Nozzle with 8 0.02" holes
Lean Transition

Flow Split (Inner/Outer)	Swirler Angle (Inner/Outer)	Filmer SMD (microns)	NO_x (EI)	Unmixedness
87/13	30/70	10	16.7	0.097
60/41	30/70	10	24.0	0.074
87/13	15/35	10	12.8	0.160
87/13	30/70	25	8.4	0.138
87/13	30/70	5	10.9	0.124
60/40	60/70	10	38.2	0.031
60/40	60/35	10	26.2	0.028

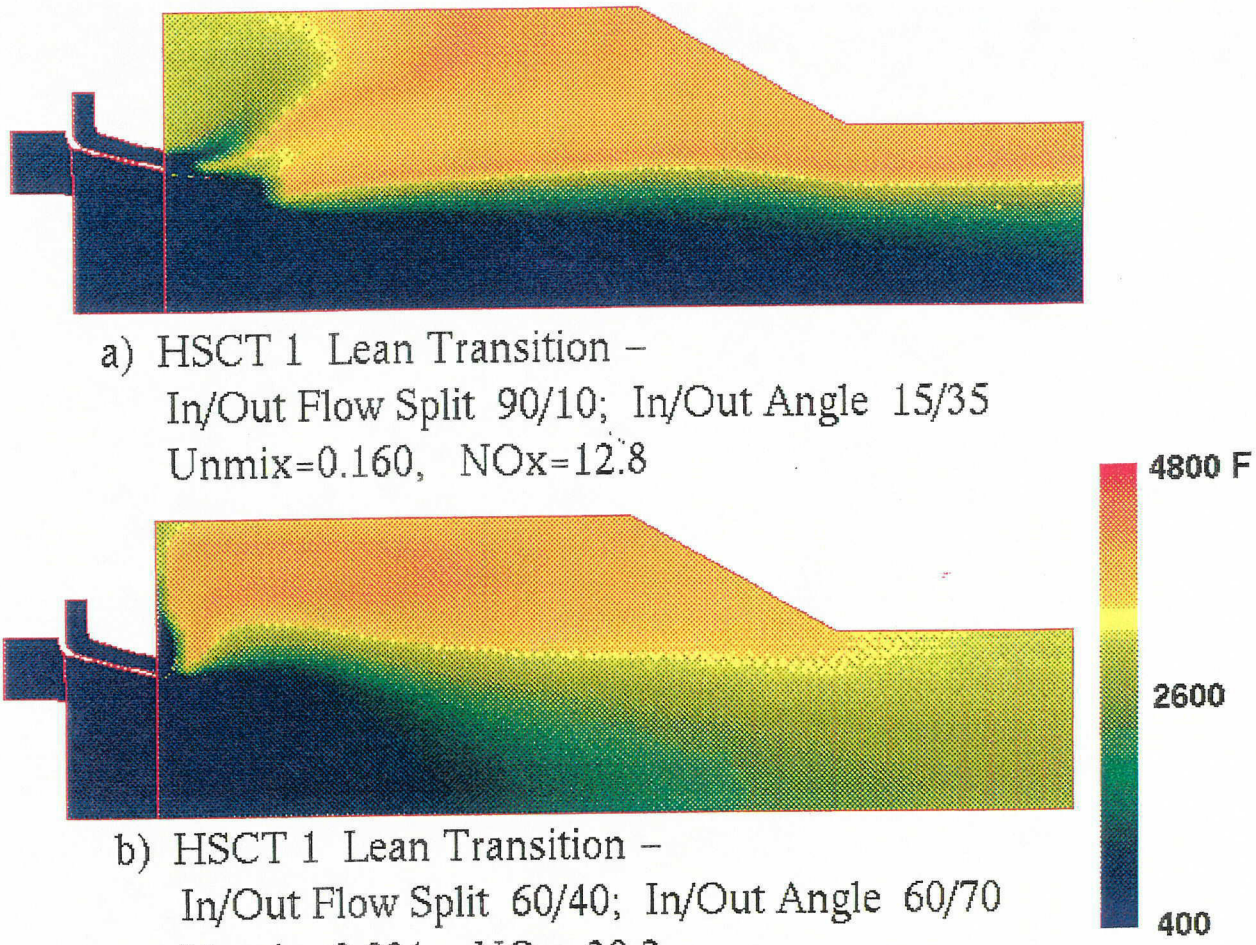

a) HSCT 1 Lean Transition –
In/Out Flow Split 90/10; In/Out Angle 15/35
Unmix=0.160, NOx=12.8

b) HSCT 1 Lean Transition –
In/Out Flow Split 60/40; In/Out Angle 60/70
Unmix=0.031, NOx=38.2

c) HSCT 1 Lean Transition –
In/Out Flow Split 60/40; In/Out Angle 60/35
Unmix=0.028, NOx=26.2

Figure 17 Temperature Contours – Diagnostic Cases

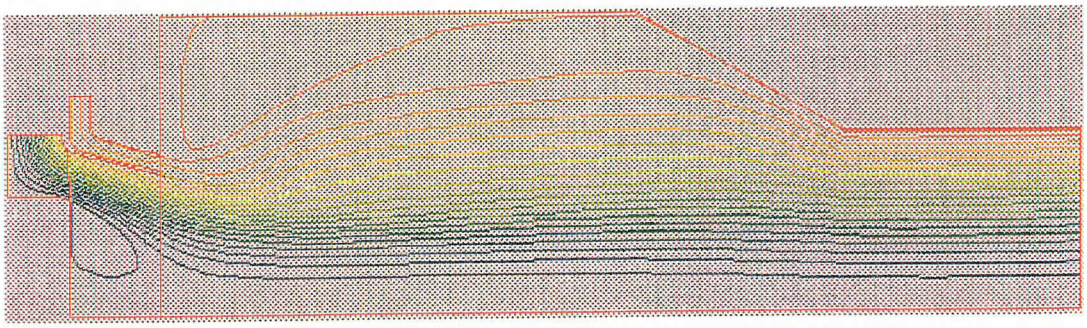

a) HSCT 1 Lean Transition –
In/Out Flow Split 90/10; In/Out Angle 15/35
Unmix=0.160, NOx=12.8

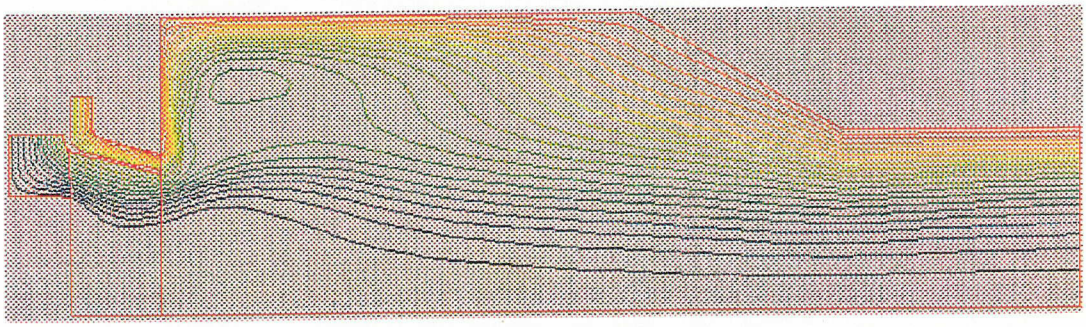

b) HSCT 1 Lean Transition –
In/Out Flow Split 60/40; In/Out Angle 60/70
Unmix=0.031, NOx=38.2

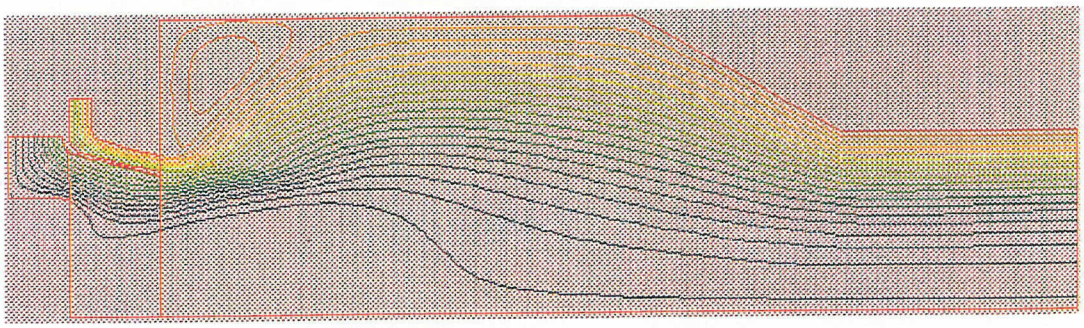

c) HSCT 1 Lean Transition –
In/Out Flow Split 60/40; In/Out Angle 60/35
Unmix=0.028, NOx=26.2

Figure 18 Streamline Contours – Diagnostic Cases

3.7 P&W Dual-Swirler Airblast Nozzle

A cold flow case was run to predict AC_d and flow splits for $\Delta p = 7''$ H_2O. The total AC_d was 1.94 in^2 with 11.6, 13.9, 71.2, and 3.3% of the flow to the inner, mid, outer (variable), and air sweep passages, respectively. The total AC_d of 1.94 in^2 is in good agreement with the measured AC_d of approximately 2 in^2. Five reacting cases were completed with results given in Table 7. Temperature contours for the lean transition, subsonic cruise and supersonic cruise cases are shown in Figure 19. The fuel did not mix completely with the outer swirler air in the lean cases. The subsonic cruise case had relatively low swirl since flow to the outer swirl (which contributes most to the overall swirl) is significantly reduced. Temperature contours for the rich transition and idle cases is shown in Figure 20. Fuel/air mixing for rich transition was very good. For the idle condition the fuel did not ignite until it entered the outer recirculation zone. A converged steady state solution was not obtained for the idle condition because of instability in the flame front location.

Table 7. P&W Dual Swirler Airblast Cases

Power Condition	SMD (microns)	NO_x (EI)	Unmixedness
Lean Transition	10	7.3	0.080
Subsonic Cruise	10	6.3	0.053
Supersonic Cruise	10		0.138
Rich Transition	10		0.003
Idle	18	4.1	0.097

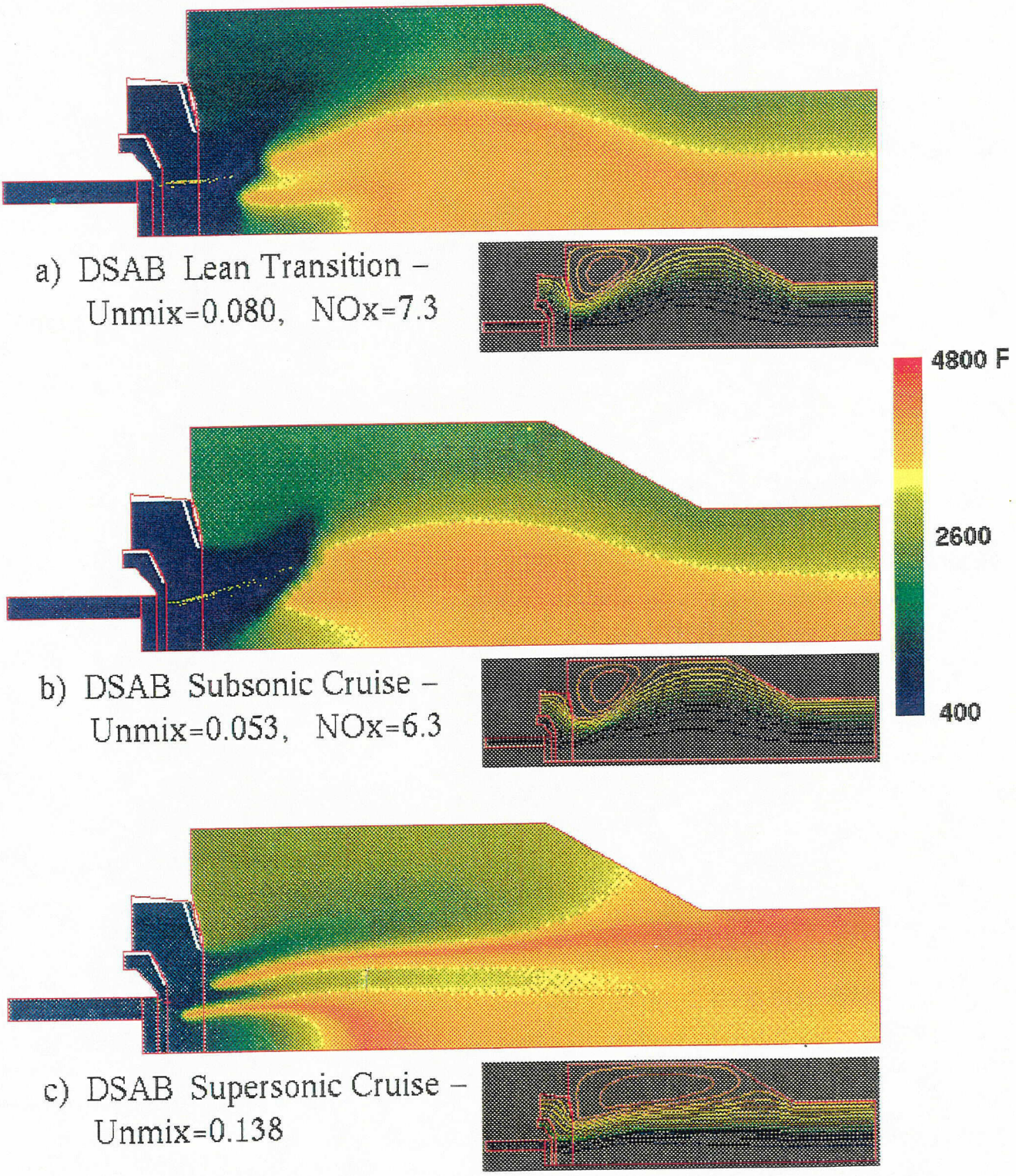

Figure 19 Temperature Contours – P&W Dual Swirler

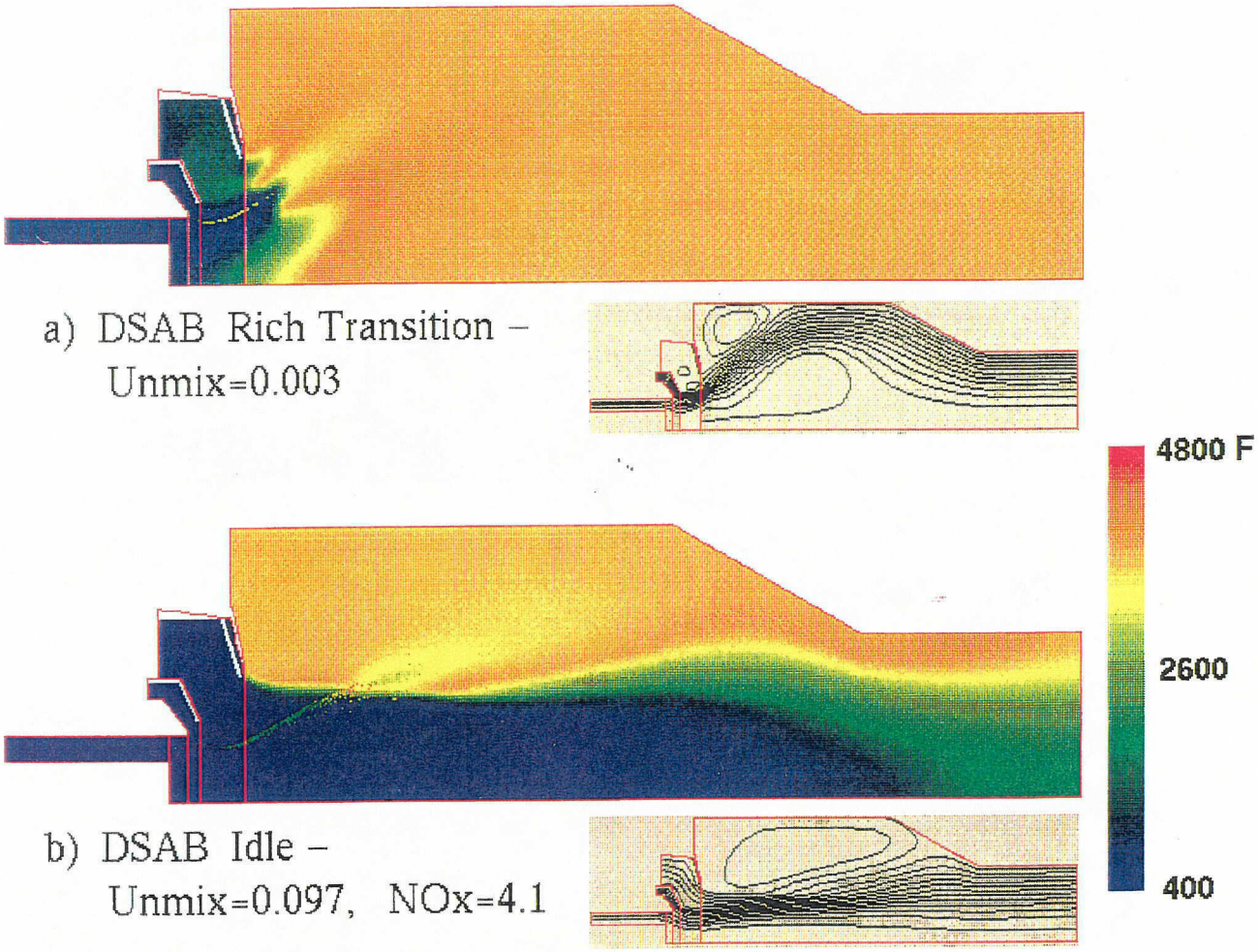

Figure 20 Temperature Contours – P&W Dual Swirler Airblast

3.8 Three Passage High Shear Nozzle

A three passage high shear nozzle was designed (at CFDRC) and analyzed. The intent of this design is to redistribute the air injection such that the fuel is injected more central to the air. A schematic of the three passage high shear nozzle is shown in Figure 21. A single variable geometry device closes both the inner and outer passage simultaneously. The mid passage always remains open. Temperature contours and streamlines for lean transition, subsonic cruise, and supersonic cruise conditions are shown in Figure 22 and for rich transition and idle conditions in Figure 23. All of these cases are for a 1.8 inch diameter fuel nozzle with 8 0.02 inch holes. The fuel easily hits the filmer for all conditions because of reduced airflow with greater swirl in the inner passage and increased filmer length. The fuel-air mixing is also substantially improved compared to the two passage design (HSCT 1). (Compare with Figures 15 and 16).

3.9 Cold Flow Cases for the P&W Constant Flow Split High Shear Nozzle (HSCT 11)

One cold flow ambient pressure case to determine ACd and two cold flow spray cases were run. The total predicted ACd in the full open position was 2.37 in^2. The inner passage ACd was predicted to be 1.72 in^2 and the outer passage 0.65 in^2 for a 72/28 flow split. The two cold flow spray cases were performed for ambient pressure and temperature simulations of subsonic and supersonic conditions. The simulated conditions match the nozzle ACd, air velocity, and fuel/air momentum ratio.

The fuel nozzle was 1.0 inch in diameter and had 12 holes each with a diameter of 0.02 inches. Initial drop sizes[1] were

	Subsonic Cruise	Supersonic Cruise
From Injector Holes	56	240
From Filmer Lip	25	24

Air flux and liquid spray fuel flux at an axial location 0.5 inches downstream of the nozzle exit were compared with experimental results. The results for the subsonic cruise case are shown in Figure 24 and for the supersonic cruise case in Figure 25. Agreement between numerical and experimental results for air flux is very good for both subsonic and supersonic cruise conditions. The fuel flux location is also predicted reasonably well. The numerical peak fuel flux value is higher because 1) the numerical fuel spreading is less than the experiment and 2) the spray capture efficiency is significantly less than 100% for the experimental results. Note that the fuel did not reach the filmer for the numerical subsonic cruise case.

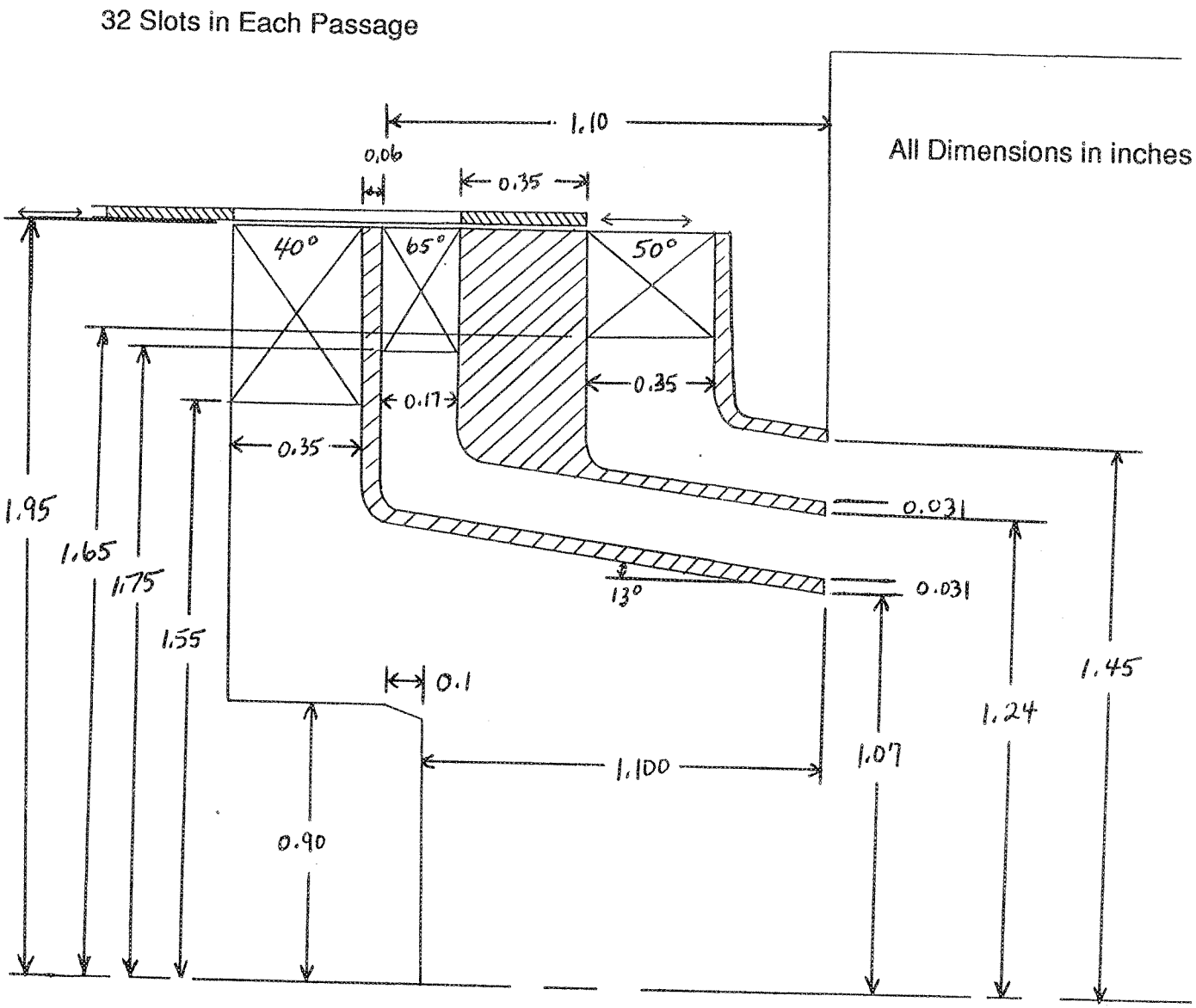

Figure 21. Schematic of Three Passage High Shear Nozzle

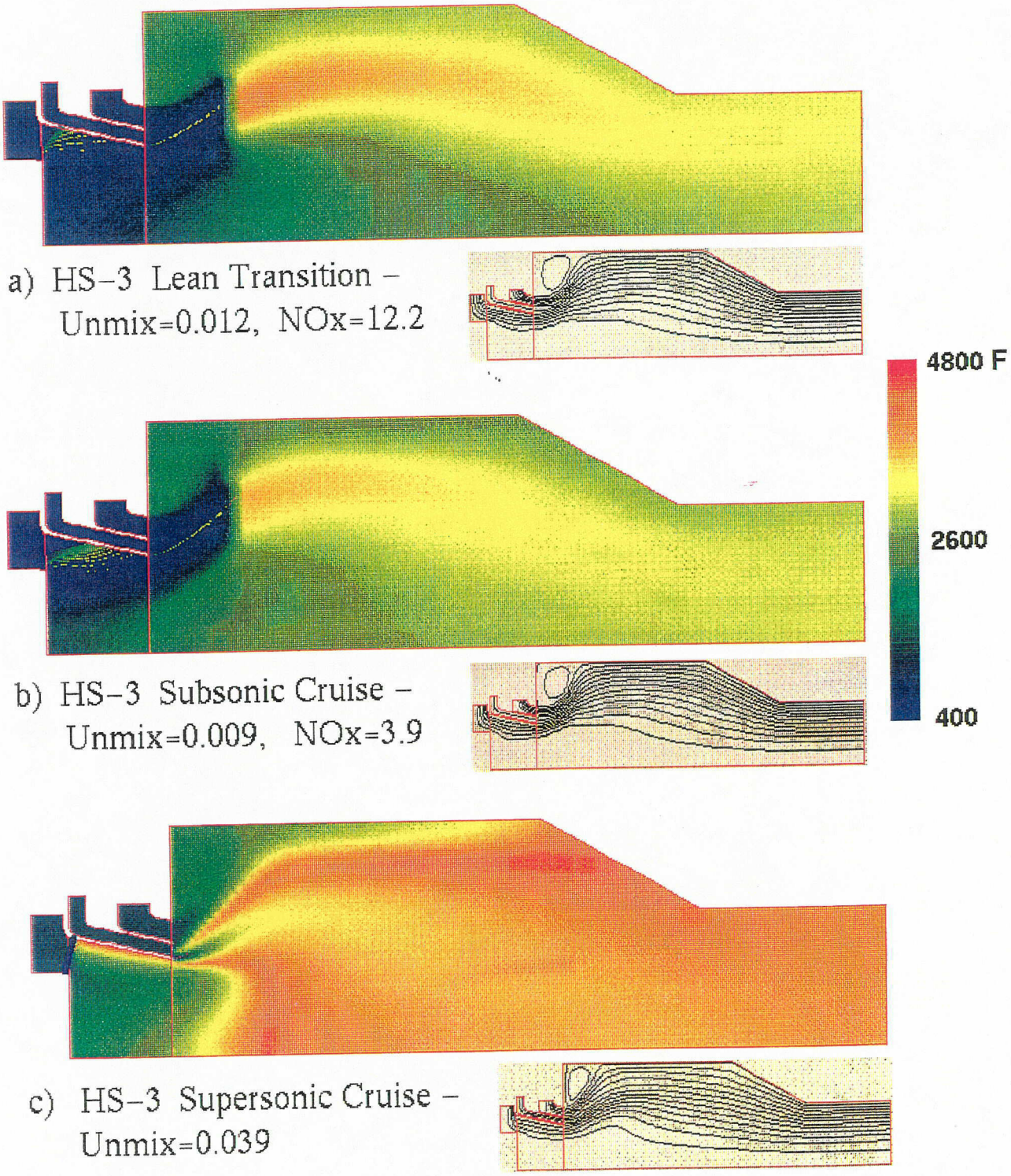

Figure 22 Temperature Contours – Three Passage High Shear Nozzle

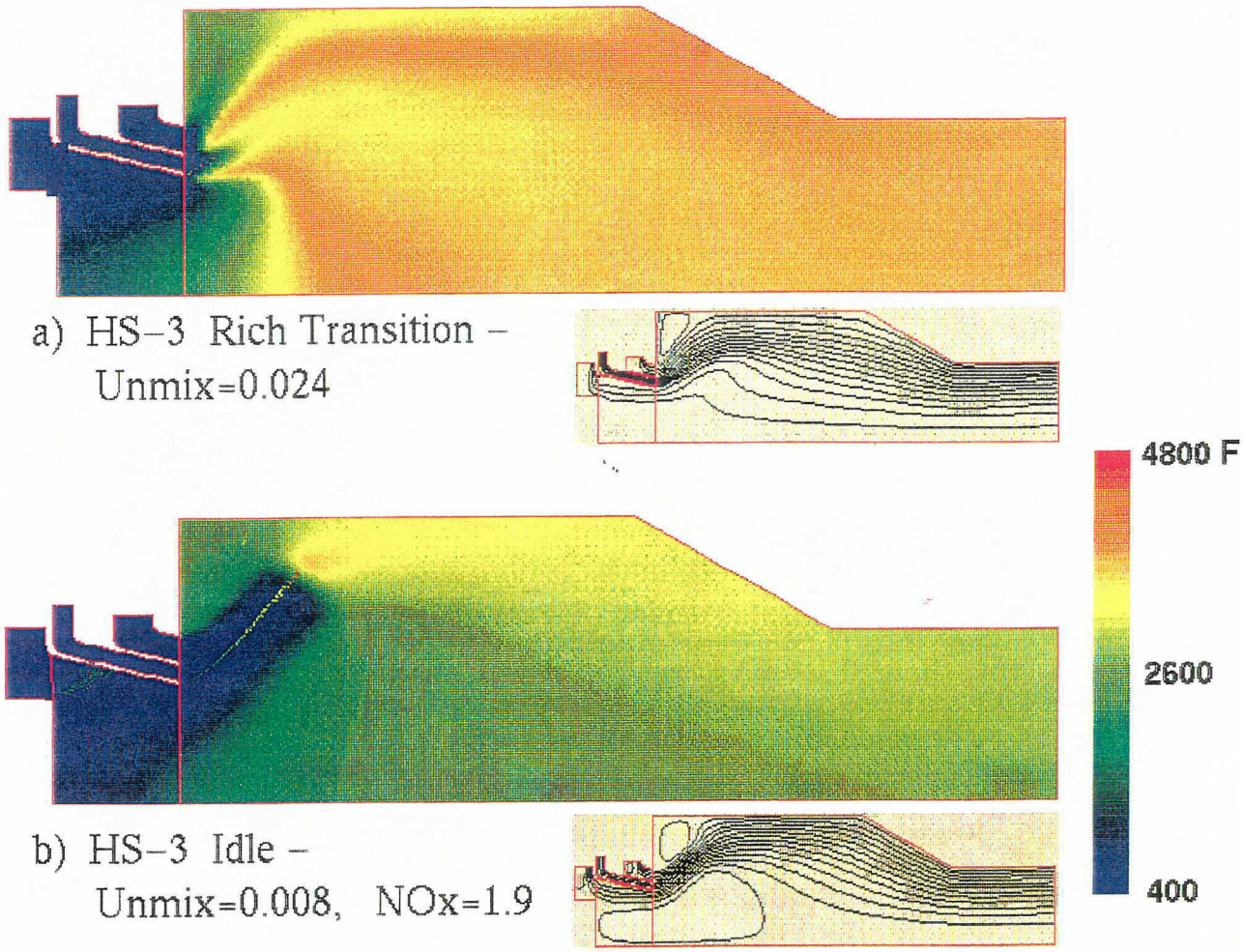

Figure 23 Temperature Contours – Three Passage High Shear Nozzle

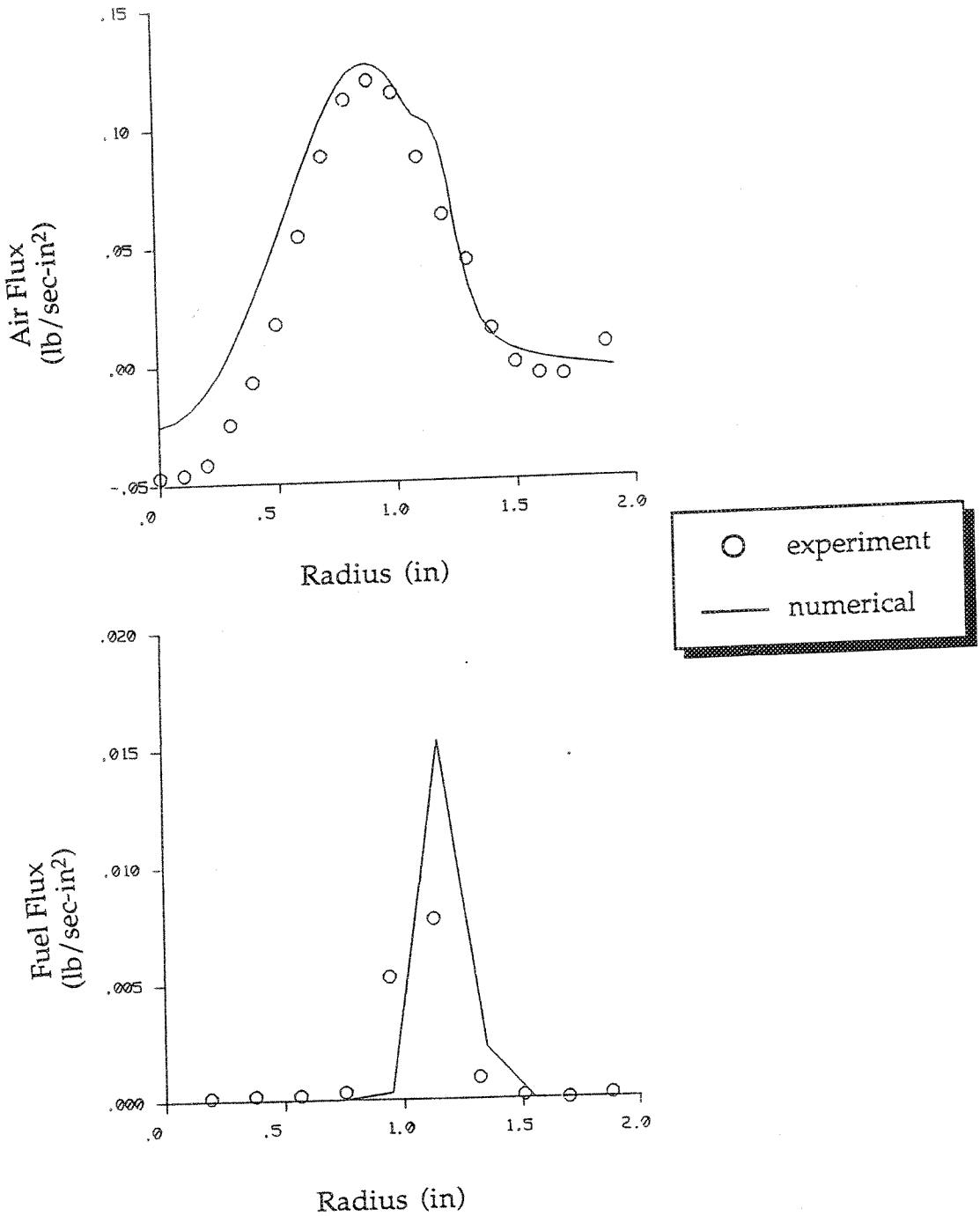

Figure 24. Subsonic Cruise Air Flux and Fuel Flux (Cold Flow Simulation) at x = 0.5 inches for HSCT 11

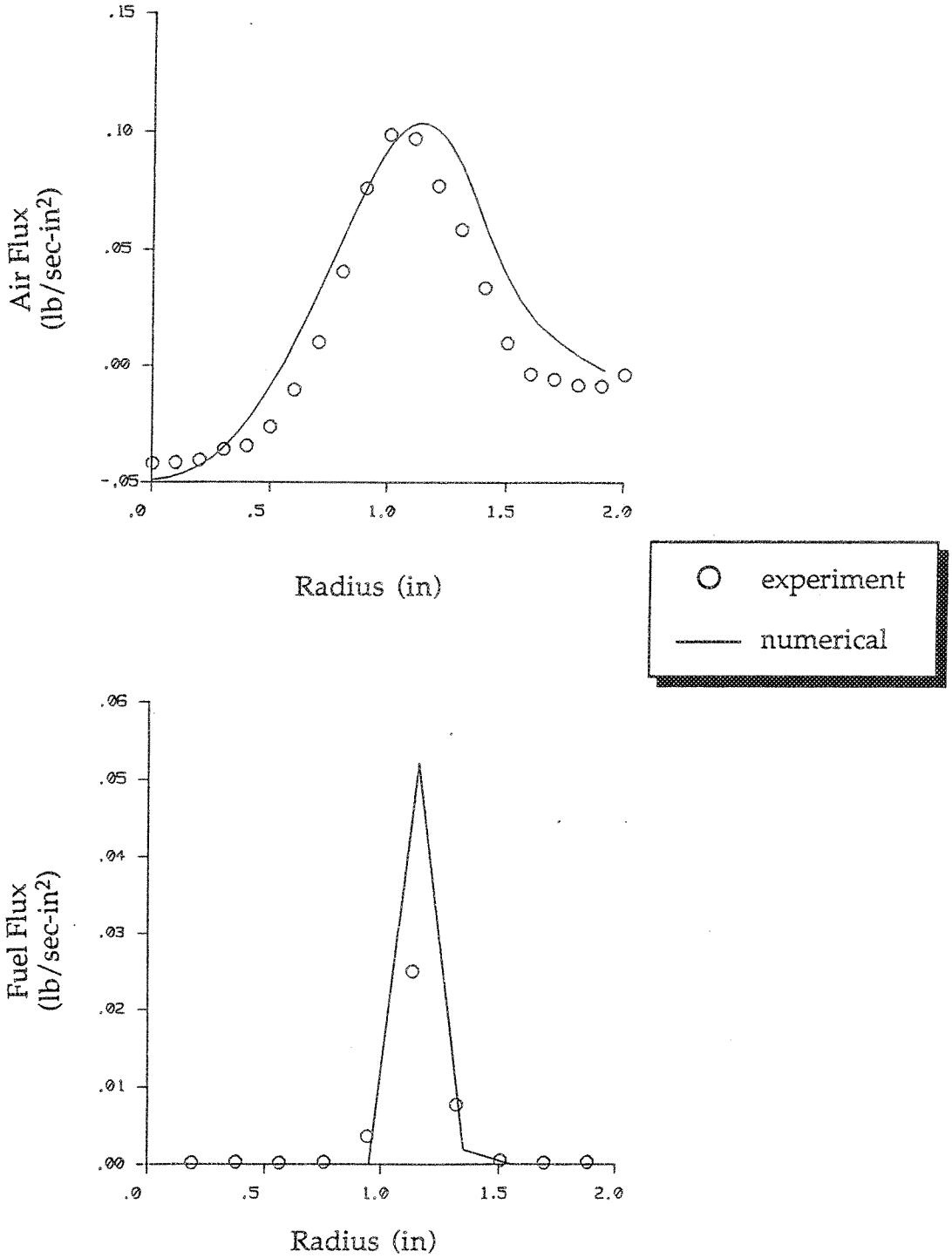

Figure 25. Supersonic Cruise Air Flux and Fuel Flux (Cold Flow Simulation) at x = 0.5 inches for HSCT 11

3.10 Reacting Flow Cases for the P&W Constant Flow Split High Shear Nozzle (HSCT 11)

HSCT 11 reacting flow cases for lean transition, subsonic cruise, supersonic cruise, rich transition and idle operation conditions are shown in Figures 26 and 27. A 1.0 inch diameter fuel nozzle with 12 0.02 inch holes was modeled. Three additional cases with a 1.6 inch diameter fuel nozzle are shown in Figure 28. NO_x EI and unmixedness results for each case are shown in Table 8. The drop size from the filmer is assumed to be 10 microns for each case. A few comments on these results follow:

a. The fuel does not reach the filmer for the initial subsonic cruise case (Figure 26b). A larger fuel injector diameter (Figure 28a) did not significantly improve the fuel penetration. Reducing the number of fuel injection holes with an associated increase in fuel injection velocity (Figure 28b) did result in most of the fuel hitting the filmer.

b. The flame was held only in the outer recirculation zone for all of the subsonic cruise cases. The inner recirculation zone did not hold flame, even for the case (Figure 28b) where most of the fuel hit the filmer.

c. The supersonic cruise and rich transition cases held flame inside the fuel nozzle (Figure 26 and 27a). This was caused by the relatively low velocity near the fuel nozzle. This problem did not occur for the larger 1.6 inch diameter fuel nozzle (Figure 28c).

Table 8. P&W Constant Flow Split High Shear Nozzle (HSCT 11) Cases

Power Condition	Fuel Injection					NO_x (EI)	Unmixedness
	Inj. Diameter (in)	Number of Holes	Hole Diameter (in)	Initial Velocity (ft/sec)	Initial SMD (microns)		
Lean Transition	1.0	12	0.02	124	35	19.0	0.042
Rich Transition	1.0	12	0.02	124	98		0.002
Subsonic Cruise	1.0	12	0.02	46	54	2.4	0.119
Subsonic Cruise	1.6	12	0.02	46	54	2.9	0.106
Subsonic Cruise	1.6	8	0.02	69	55	4.4	0.091
Supersonic Cruise	1.0	12	0.02	165	40		0.024
Supersonic Cruise	1.6	12	0.02	165	40		0.023
Idle	1.0	12	0.02	26	47	8.5	0.019

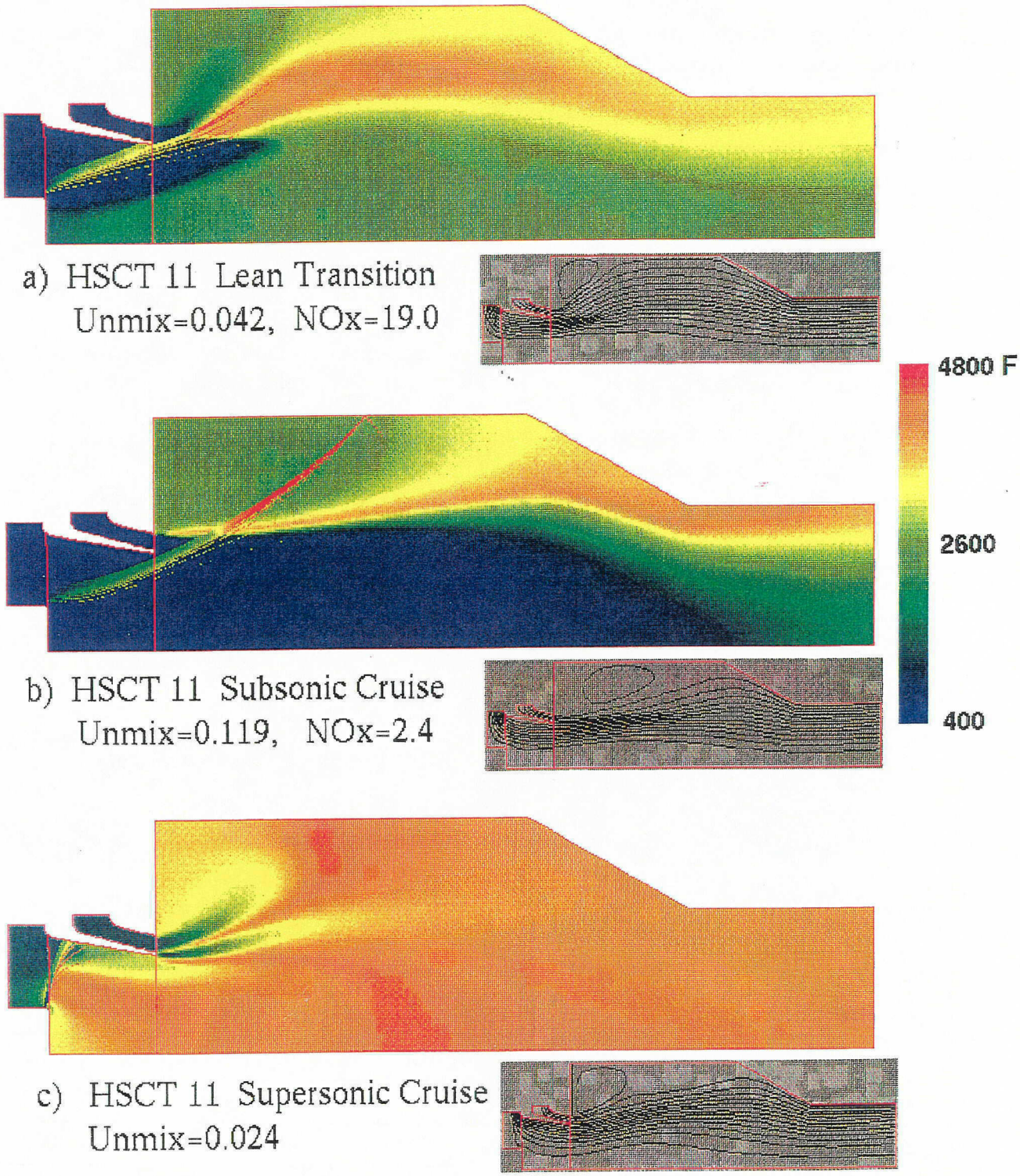

Figure 26 Temperature Contours – HSCT 11, Constant Flow Split Radial Inflow High Shear Nozzle

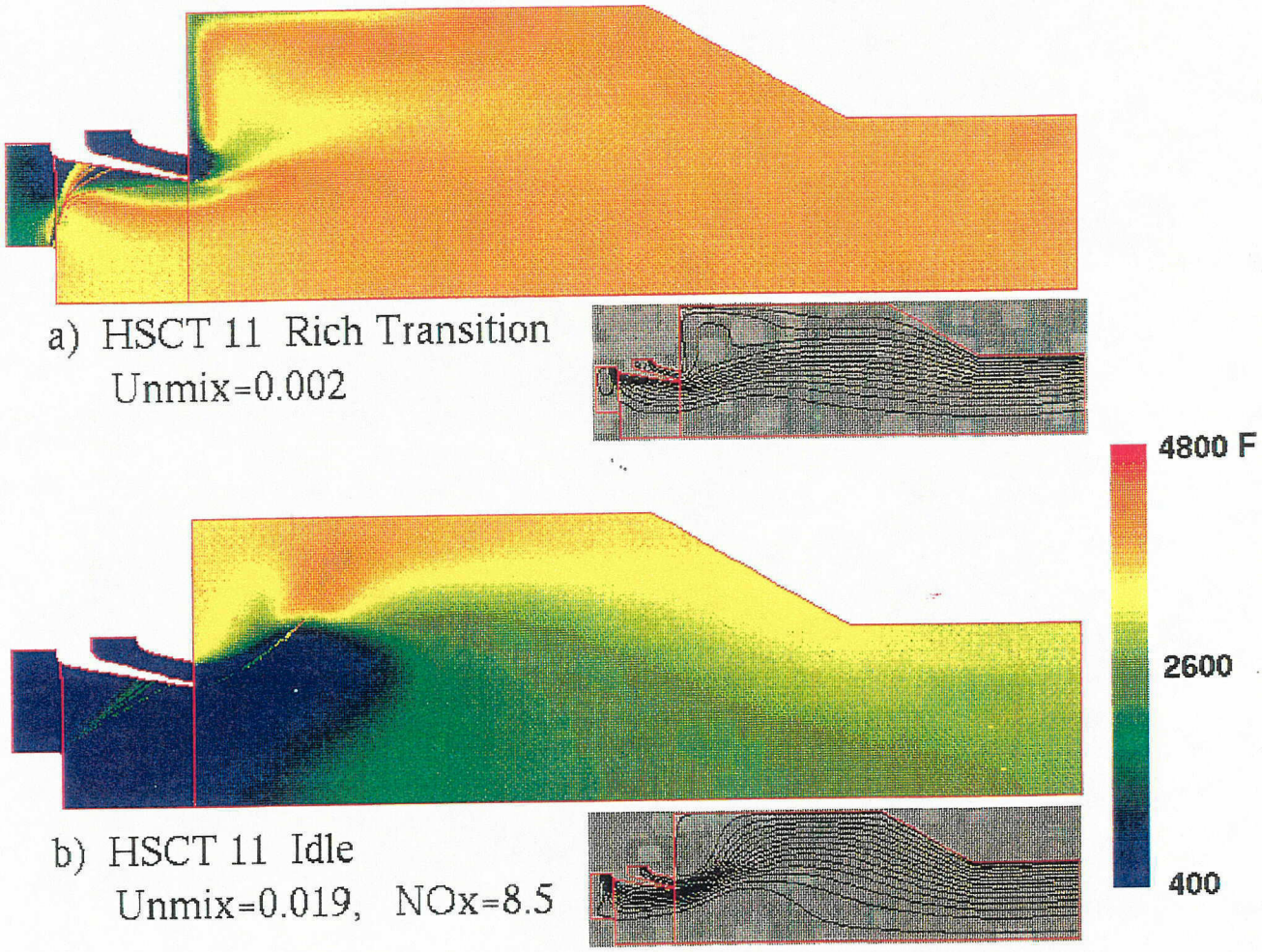

Figure 27 Temperature Contours – HSCT 11, Constant Flow Split Radial Inflow High Shear Nozzle

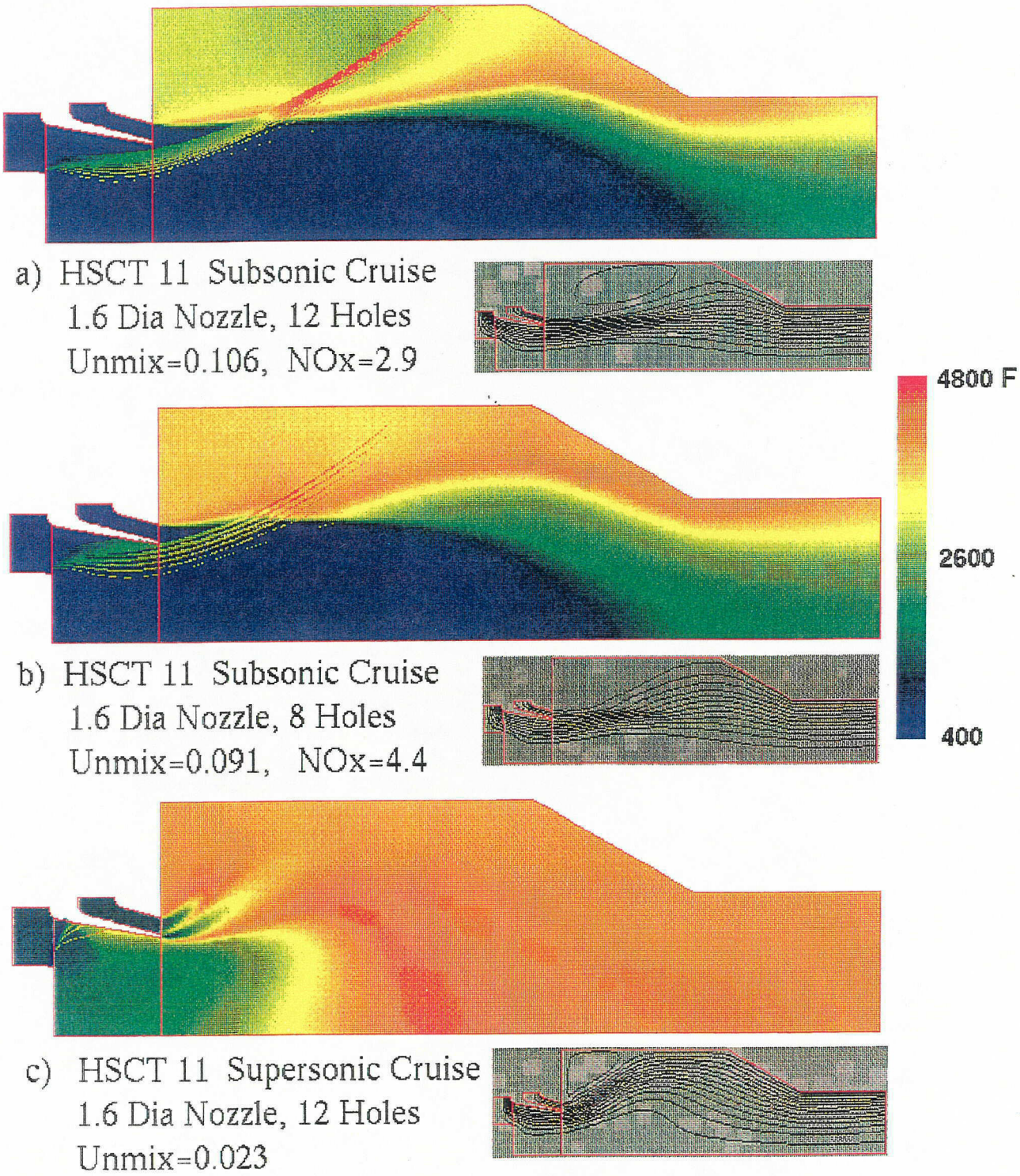

Figure 28 Temperature Contours – HSCT 11, Constant Flow Split Radial Inflow High Shear Nozzle --Modified Fuel Nozzle

4. 3-D CFD ANALYSES OF THE FOUR NOZZLE RQL SECTOR RIG

3-D CFD analysis was performed on 17 test cases as shown in Table 9. The baseline geometry (Case 1), shown in Figure 29, was representative of the P&W four-nozzle RQL sector combustor tested experimentally. The calculation domain extended from the fuel nozzle through the combustor exit. The fuel nozzle boundary conditions were taken from 2-D CFD analysis, while the quench-zone jets were modeled as plenum fed-jets. The CFD-ACE code, developed and commercialized by CFDRC, was used to perform the calculations. The following parametrics were studied:

a. the effect of changing mass flow splits between nozzle and quick-mix orifices;

b. the effect of changing mass flow splits with a fuel nozzle flowing 16% excessive fuel;

c. the effect of changing mass flow splits on a P&W proposed 2-inch configuration;

d. the effect of grid resolution between jet orifices;

e. the effect of dump versus ramp lean burn sections;

f. the effect of unequal number of orifices on I.D. and O.D.;

g. the effect of orifice shape and blockage; and

h. the effect of a 90 degree rich-burn section.

All results were documented in monthly progress reports, included as Appendix A of this final report.

4.1 Modular Combustor Modeling

This effort involved modeling a can geometry for the rich-burn/quick-mix sections, then dumping into an annular lean burn section. The purpose of this CFD analysis was to qualitatively assess if excessive NO_x was formed in the lean burn section, and how well the flow fills the annulus. The test conditions were:

Table 9. NO_x Summary from CFD Analysis

Case	Date	Quench Height	ϕ_{RB}	ϕ_{LB}	NO_x (RB)	NO_x (QM + LB)	NO_x (Tot)	No_x (Probe) $\mathcal{C}_L$	NO_x (Probe) Cyclic Bound	Case Description
1	10/13	3″	1.8	0.43	1.61	5.10	6.71	6.79	6.25	SMD = 10
2	10/19	3″	1.8	0.43	1.02	5.16	6.18	6.65	5.81	SMD = 5
3	10/17	3″	2.0	0.43	0.64	4.87	5.51	6.12	5.11	
4	10/15	3″	2.2	0.43	0.44	6.36	6.80	7.94	6.27	
5	10/22	3″	2.08	0.5	0.44	8.11	8.55	8.40	7.89	
6	10/21	3″	2.32	0.5	0.25	8.48	8.73	9.72	8.12	
7	10/19	3″	2.55	0.5	0.15	9.87	10.02	12.20	9.22	
8	10/18	2″	1.8	0.43	1.02	4.12	5.14	5.02	5.15	
9	10/20	2″	2.0	0.43	0.64	3.87	4.51	4.39	4.59	
10	10/23	2″	2.2	0.43	0.44	3.91	4.35	4.32	4.35	
11	11/26	2″	2.0	0.43	0.54	5.66	6.20	6.35	6.07	Refined Grid Between Holes
12	11/28	2″	2.0	0.43	0.55 (0.89)	5.67 (7.79)	6.22 (8.68)	6.64 (9.15)	5.89 (8.26)	Ramped LB
13	12/5	2″	2.0	0.43	0.56	6.22	6.78	6.65	6.46	3 I.D. Holes and 4 O.D. Holes
14	12/11	2″	2.0	0.43	0.45	7.38	7.83	7.91	7.63	90 degree RB w/ Slots @ 75% Blk
15	12/13	2″	2.0	0.43	0.56	7.10	7.66	7.80	7.44	Slots @ 75% Blk
16	12/15	2″	2.0	0.43	0.57	6.18	6.75	6.96	6.61	Slots @ 50% Blk
17	12/17	2″	2.0	0.43	0.56 (0.90)	5.49 (7.49)	6.05 (8.38)	6.45 (8.82)	5.72 (7.95)	Rounded Slots @ 72% Blk

Note:
1. NO_x Calculations Used Anderson Constants, Extended Zeldovich Mechanism with PDF.
2. Calculation Corrected on 11/14 (NO_x Values Cannot be Directly Compared to Cases 1-10).
3. ( ) NO_x Calculations Used Literature Constants, Extended Zeldovich Mechanism with PDF.

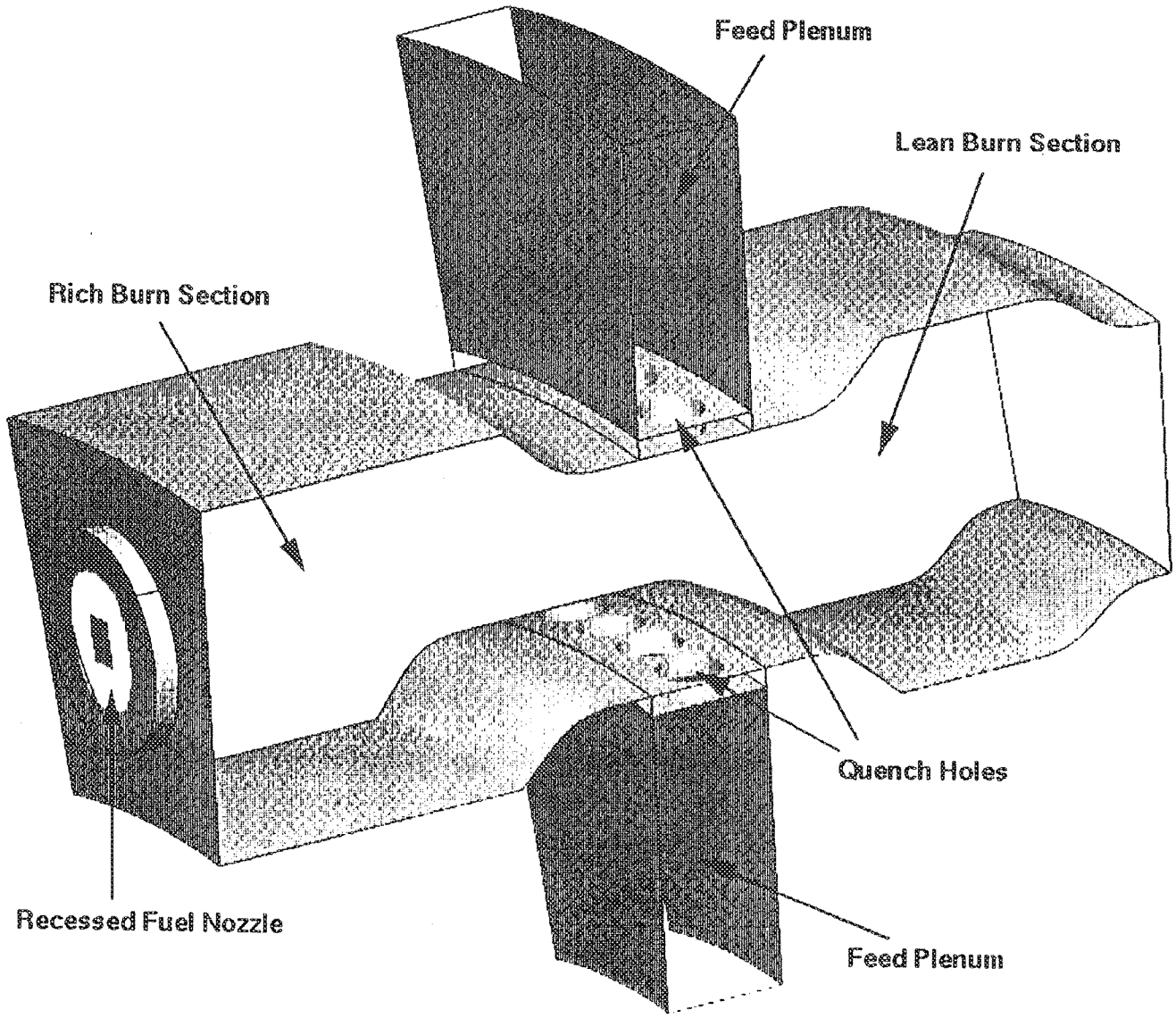

Figure 29. RQL Baseline Geometry with 3" Quench Height

$P = 150$ psia
$T = 1200$ °F
$W = 3.0$ lbm/s
$\phi_{RB} = 1.8$
$\phi_{LB} = 0.43$

The can geometry duplicated UTRC's can geometry (i.e., 5-inch diameter rich burn section, 3-inch diameter quench zone and 8 circular orifices).

CFD analysis was first performed on the can geometry as shown in Figure 30. Figure 30 depicts the temperature contours at the can exit. Although only a 90° sector was computed, the full 360° field is shown. One can see that the quench jets are underpenetrated. The flow conditions at the exit of the can were used as the inlet boundary conditions to the annulus. Note that the flow field is comprised of eight nearly identical sectors indicating that the CFD cyclic planes are behaving properly.

CFD analysis was then performed on the annulus geometry, as depicted in Figures 31 through 35. The temperature and NO_x contours in Figures 31 and 32, respectively, indicate that the rich mixture exiting the can does not significantly spread laterally. The temperature and velocity contours shown in Figures 33, 34, and 35 also illustrate the low circumferential and radial mixing rates. NO_x EI was calculated to be approximately 3.5 at the exit of the can, and a total NO_x EI was found to be nearly 13.5 at the annulus exit.

5. REFERENCES

1. Lefebvre, A.H., Gas Turbine Combustion, New York: Hemisphere Publishing Corp., 1983.

2. Hautman, D.J., and Rosfjord, T.J., "Transverse Liquid Injection Studies," AIAA.

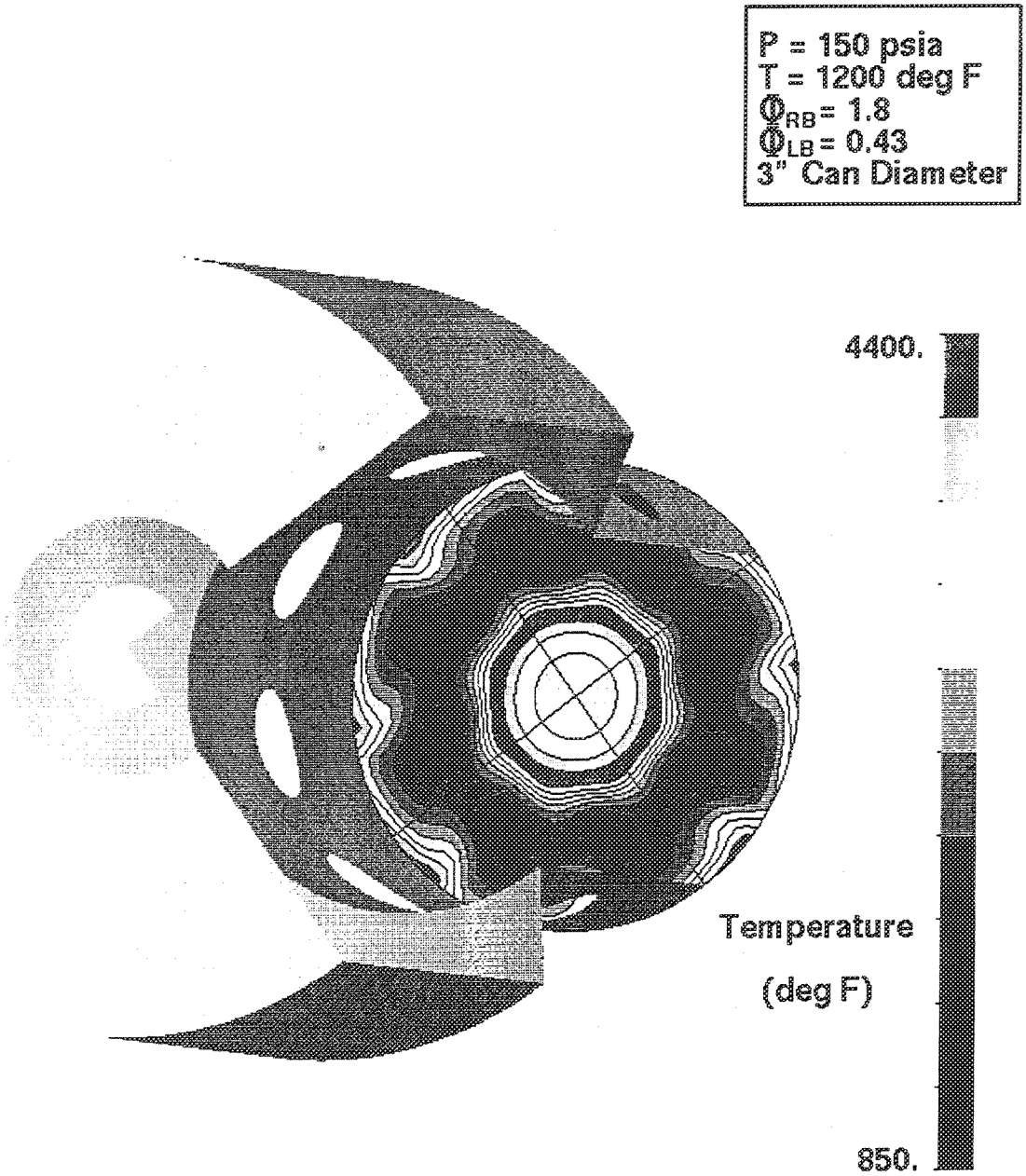

Figure 30. Temperature Contours at Can Exit

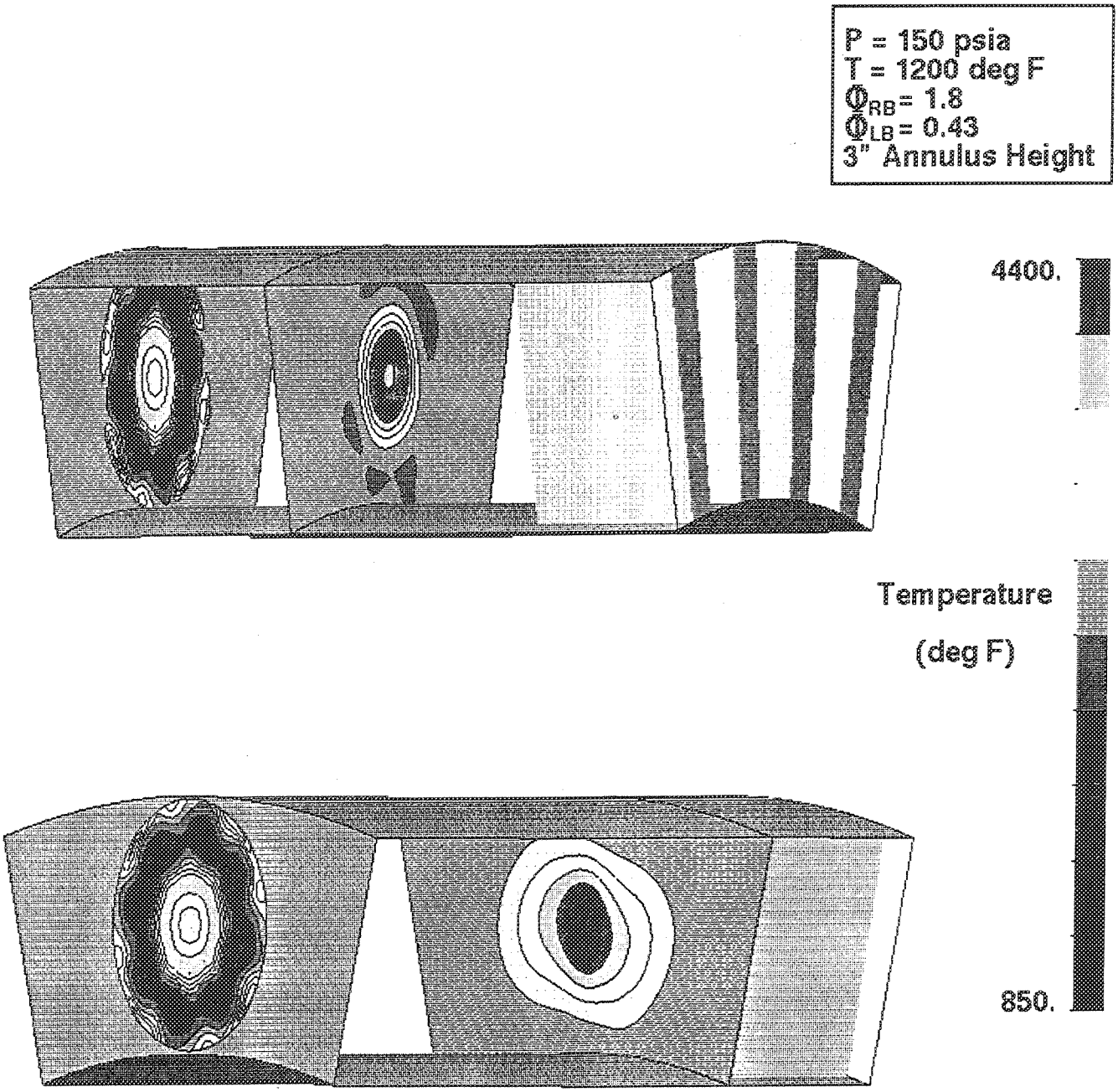

Figure 31. Temperature Contours in Annulus Indicate Little Lateral Mixing

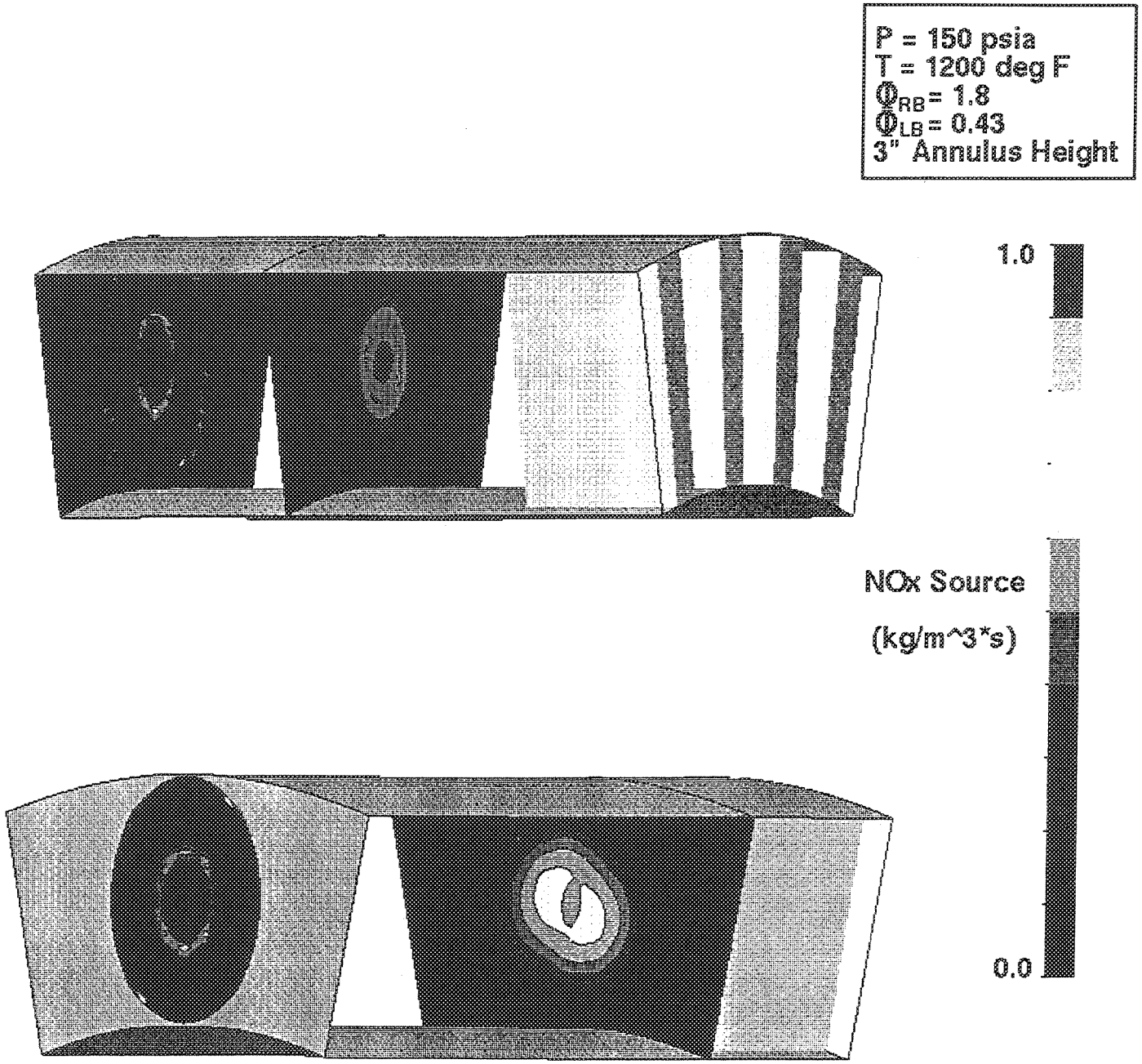

Figure 32. NO_x Source Through the Annulus

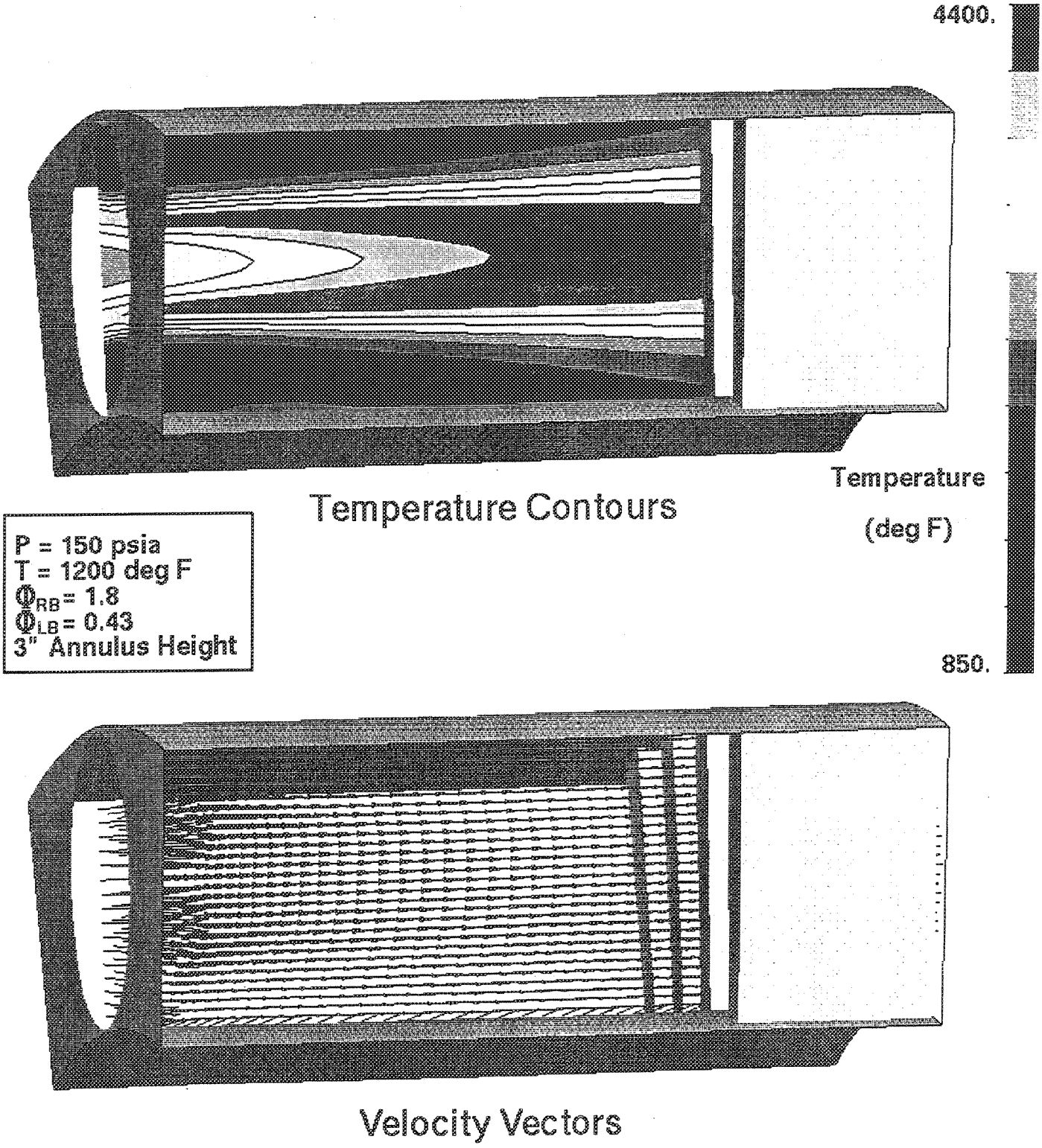

Figure 33. Velocity Vectors and Temperature Contours along the Can Centerline

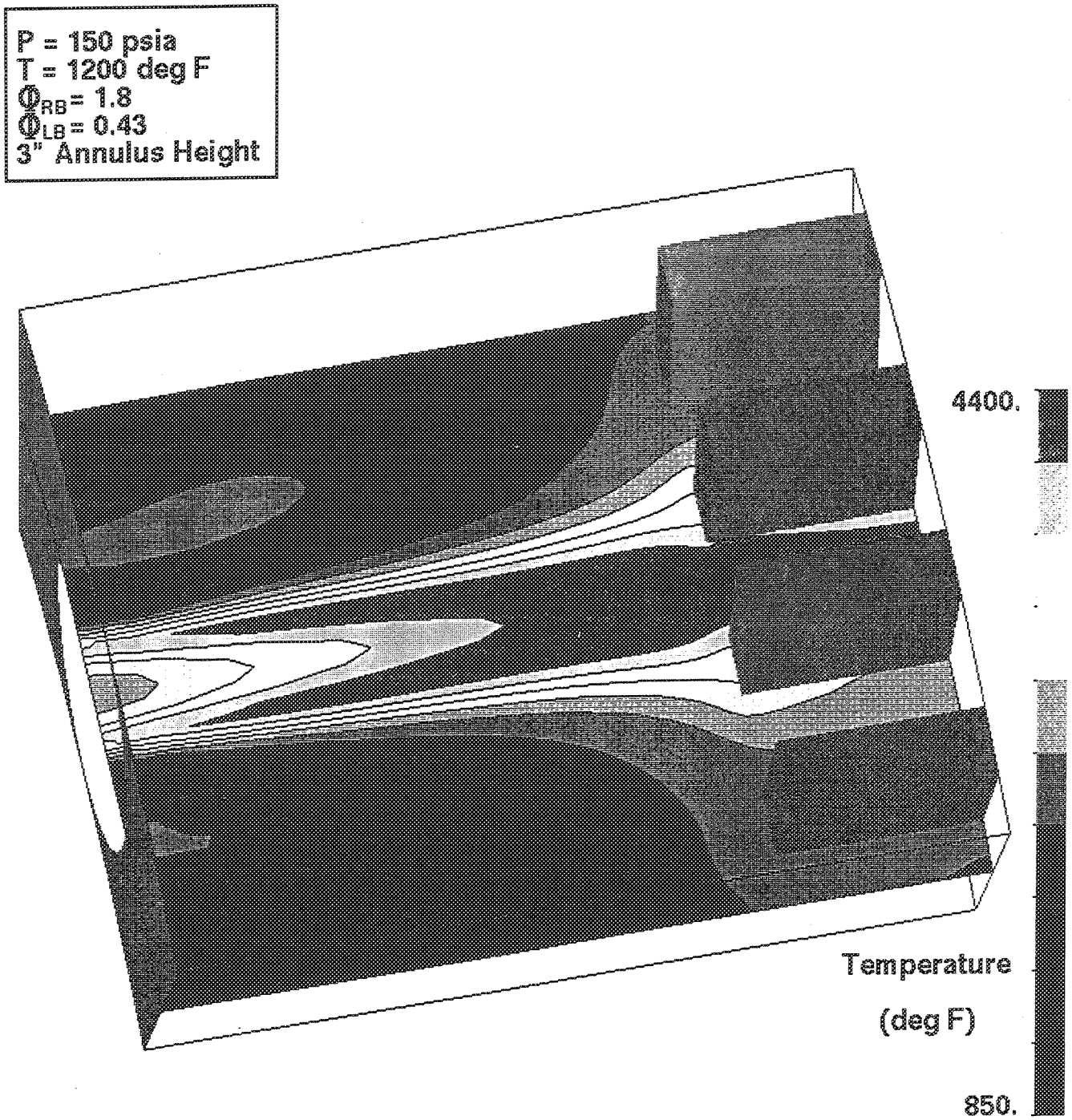

Figure 34. Temperature along the Annulus Mid-Line

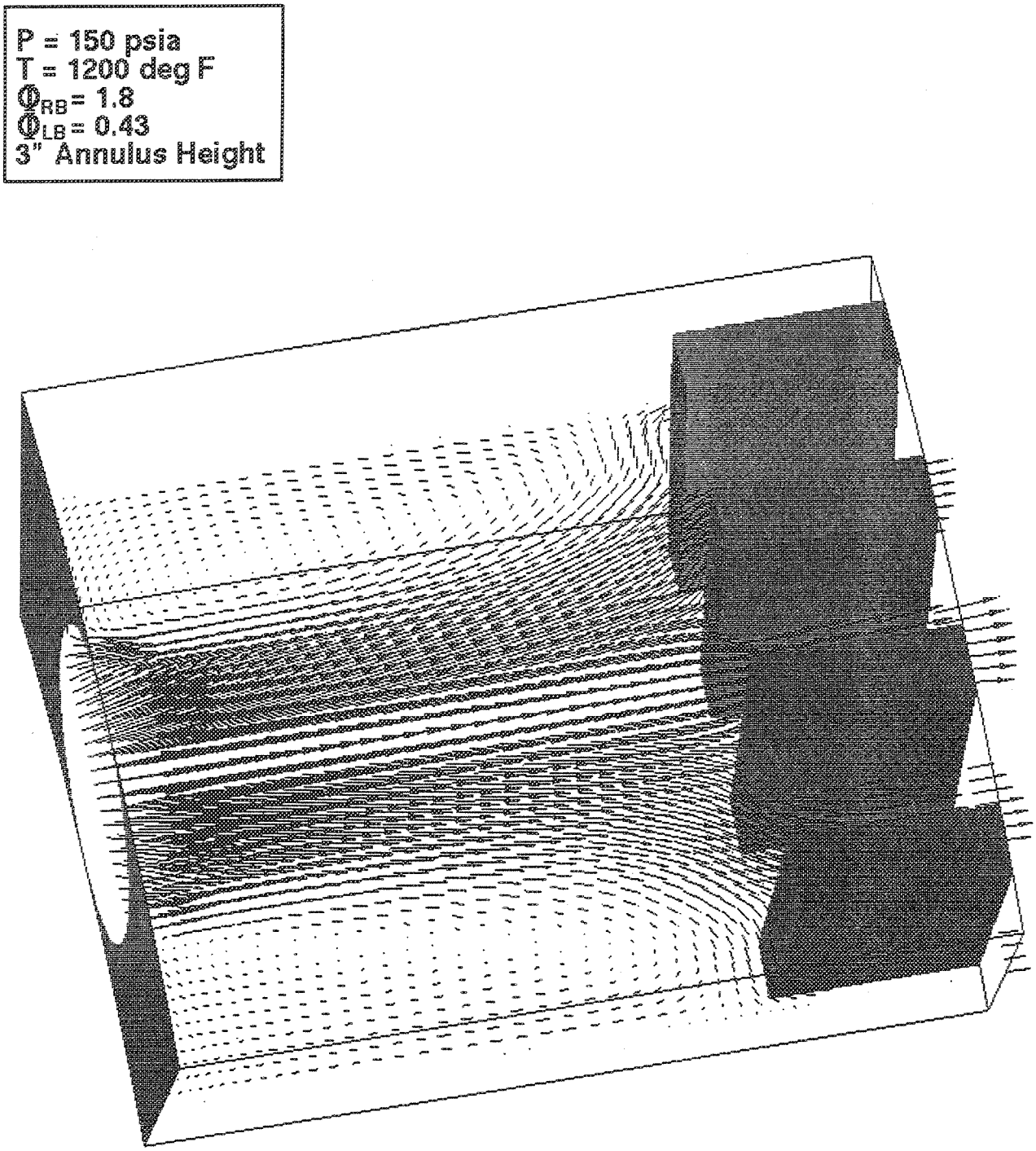

Figure 35. Velocity Vectors along the Annulus Mid-Line

REPORT DOCUMENTATION PAGE

Form Approved
OMB No. 0704-0188

Public reporting burden for this collection of information is estimated to average 1 hour per response, including the time for reviewing instructions, searching existing data sources, gathering and maintaining the data needed, and completing and reviewing the collection of information. Send comments regarding this burden estimate or any other aspect of this collection of information, including suggestions for reducing this burden, to Washington Headquarters Services, Directorate for Information Operations and Reports, 1215 Jefferson Davis Highway, Suite 1204, Arlington, VA 22202-4302, and to the Office of Management and Budget, Paperwork Reduction Project (0704-0188), Washington, DC 20503.

1. AGENCY USE ONLY (*Leave blank*)

2. REPORT DATE
February 2005

3. REPORT TYPE AND DATES COVERED
Final Contractor Report

4. TITLE AND SUBTITLE
Large Engine Technology Program: Task 22—Variable Geometry Concepts for Rich-Quench-Lean Combustors

5. FUNDING NUMBERS
WBS–22–714–09–46
NAS3–26618

6. AUTHOR(S)
J.M. Cohen, F.C. Padget, D. Kwoka, Q. Wang, and R.P. Lohmann

7. PERFORMING ORGANIZATION NAME(S) AND ADDRESS(ES)
United Technologies Research Center
411 Silver Lane
East Hartford, Connecticut 06108

8. PERFORMING ORGANIZATION REPORT NUMBER
E–14788

9. SPONSORING/MONITORING AGENCY NAME(S) AND ADDRESS(ES)
National Aeronautics and Space Administration
Washington, DC 20546–0001

10. SPONSORING/MONITORING AGENCY REPORT NUMBER
NASA CR—2005-213328

11. SUPPLEMENTARY NOTES
This research was originally published internally as HSR062 in November 1997. J.M. Cohen and F.C. Padget, United Technologies Research Center, East Hartford, Connecticut 06108; and D. Kwoka, Q. Wang, and R.P. Lohmann, Pratt & Whitney, West Palm Beach, Florida 33478. Project Manager, Robert R. Tacina. Responsible person, Diane Chapman, Ultra-Efficient Engine Technology Program Office, NASA Glenn Research Center, organization code PA, 216–433–2309.

12a. DISTRIBUTION/AVAILABILITY STATEMENT
Unclassified - Unlimited
Subject Categories: 01, 02, 05, and 07 Distribution: Nonstandard
Available electronically at http://gltrs.grc.nasa.gov
This publication is available from the NASA Center for AeroSpace Information, 301–621–0390.

12b. DISTRIBUTION CODE

13. ABSTRACT ***(Maximum 200 words)***
The objective of the task reported herein was to define, evaluate, and optimize variable geometry concepts suitable for use with a Rich-Quench-Lean (RQL) combustor. The specific intent was to identify approaches that would satisfy High Speed Civil Transport (HSCT) cycle operational requirements with regard to fuel-air ratio turndown capability, ignition, and stability margin without compromising the stringent emissions, performance, and reliability goals that this combustor would have to achieve. Four potential configurations were identified and three of these were refined and tested in a high-pressure modular RQL combustor rig. The tools used in the evolution of these concepts included models built with rapid fabrication techniques that were tested for airflow characteristics to confirm sizing and airflow management capability, spray patternation, and atomization characterization tests of these models and studies that were supported by Computational Fluid Dynamics analyses. Combustion tests were performed with each of the concepts at supersonic cruise conditions and at other critical conditions in the flight envelope, including the transition points of the variable geometry system, to identify performance, emissions, and operability impacts. Based upon the cold flow characterization, emissions results, acoustic behavior observed during the tests and consideration of mechanical, reliability, and implementation issues, the tri-swirler configuration was selected as the best variable geometry concept for incorporation in the RQL combustor evolution efforts for the HSCT.

14. SUBJECT TERMS
High speed civil transport; Rich-Quench-Lean combustor; Injectors; Swirlers

15. NUMBER OF PAGES
129

16. PRICE CODE

17. SECURITY CLASSIFICATION OF REPORT	18. SECURITY CLASSIFICATION OF THIS PAGE	19. SECURITY CLASSIFICATION OF ABSTRACT	20. LIMITATION OF ABSTRACT
Unclassified	Unclassified	Unclassified	